Impact of Baz/PAR-3 phosphorylation by aPKC on cell polarity

DISSERTATION ZUR ERLANGUNG DES DOKTORGRADES DER NATURWISSENSCHAFTEN (DR.RER. NAT.) DER FAKULTÄT FÜR BIOLOGIE UND VORKLINISCHE MEDIZIN DER UNIVERSITÄT REGENSBURG

vorgelegt von

Sabine Ursula Katharina Feicht

aus

Burglengenfeld

im Jahr 2017

Das Promotionsgesuch wurde eingereicht am:

10.03.2017

Die Arbeit wurde angeleitet von:

Junior Prof. Dr. med. vet. Dr. rer. nat. Michael Krahn

Unterschrift:

Table of contents

1 Zusammenfassung

Die apikal-basale Zellpolarisierung und die Bildung von Zell-Zell Verbindungen sind fundamentale Mechanismen in der epithelialen Entwicklung, um Abgrenzungen festzulegen sowie einen gerichteten Transport und die mechanische Integrität des Gewebes sicherzustellen. Hierbei ist der PAR-Komplex, welcher aus den multimodularen Gerüstproteinen Bazooka (Baz, PAR-3 in Säugern) und PAR-6, sowie der atypischen Proteinkinase C (aPKC) besteht, von wesentlicher Bedeutung. Die Proteine in diesem Komplex agieren in einer spezifischen Hierarchie, bei der Baz die Schlüsselrolle in der korrekten subzellulären Lokalisation anderer apikaler Marker spielt. Später in der epithelialen Entwicklung wirken das Gerüstprotein Baz mit dem Transmembranprotein Crb redundant zusammen, um die apikale Region der epithelialen Zelle zu bestimmen und die Bildung apikaler Zellverbindungen durch die Rekrutierung von aPKC zu dirigieren. Demgegenüber wird die Formierung des aktiven PAR Komplexes auch durch die basolaterale Kinase PAR-1 ausbalanciert. Allerdings ist die genaue Positionierung von Baz durch aPKC an die apikalen Zellverbindungen noch nicht gänzlich verstanden.

In der vorliegenden Studie wurde eine genaue Untersuchung der Interaktion zwischen aPKC und Baz/PAR-3 vorgenommen. aPKC kann mit der PDZ2-3 Domäne und dem aPKC-Binde Motiv von Baz interagieren. Weiterhin konnten fünf Serine/Threonine in Baz_{PDZ2-3} und entsprechend sieben Serine/Threonine im Säugerhomolog $PAR\text{-}3_{PDZ2-3}$ identifiziert werden, welche von aPKC phosphoryliert werden. Eine veränderte Baz-PDZ Phosphorylierung beeinträchtigt die Akkumulation von Baz/aPKC an die apikalen Zellverbindungen und stört die AJ-Bildung während der späten Zellularisierung/frühen Gastrulation in der *Drosophila* Epidermis. Diese Defekte können durch eine ektopische Crb-Expression oder durch aktiviertes aPKC sowie durch Inhibierung von PAR-1 gerettet werden. Folglich ist die PDZ-Phosphorylierung von Baz durch aPKC essentiell für die Rekruitierung und Aktivierung von aPKC in Abwesenheit von Crb, um entsprechend die basolaterale PAR-1-Aktivität zu regulieren und dadurch eine korrekte apikal-basale Polarisierung sowie AJ-Bildung der epithelialen Zelle zu gewährleisten.

Da PAR-6 ein putatives PDZ-Binde Motiv (PBM) aufweist, stellte sich die Frage, ob dieses Motiv wichtig für die PAR-6 Lokalisierung und Funktion ist. Experimente in dieser Studie geben einen ersten Hinweis darauf, dass das PDZ-Binde Motiv eine gewisse Rolle bei der richtigen Funktionalität von PAR-6 spielt.

2 Summary

The apical-basal polarization and the formation of cell-cell junctions are important key steps in the development of epithelia to ensure barrier formation, directed transport and mechanical integrity of the tissue. In this context the PAR complex, which consists of the multi modular scaffold proteins Bazooka (Baz, PAR-3 in mammals), PAR-6 and the atypical protein kinase C (aPKC), is of essential significance. The proteins in this complex operate in a specific hierarchy, in which Baz plays a key role in the proper subcellular localization of other apical markers. Later in epithelial development, the scaffolding protein Baz and the transmembrane protein Crumbs (Crb) function to some extent redundantly to determine the apical domain of epithelial cells and further direct the formation of apical junctions by recruiting aPKC. On the other hand, the formation of the active PAR complex is counterbalanced by the basolateral kinase PAR-1. However, it is still not entirely understood, how aPKC functions in positioning Baz at the apical junctions.

In this study the interaction between aPKC and Baz/PAR-3 was characterized in more detail. aPKC can interact with the PDZ2-3 domain and the aPKC-binding motif of Baz. Furthermore, five serines/threonines within the Baz_{PDZ2-3} region and seven serines/threonines of the mammalian homolog PAR-3_{PDZ2-3}, respectively, could be identified to be phosphorylated by aPKC. Impaired Baz PDZ-phosphorylation disrupts apical junctional accumulation of Baz/aPKC and AJ formation during late cellularization/early gastrulation in the *Drosophila* epidermis. These defects can be rescued by ectopic expression of Crb or activated aPKC as well as by inhibition of PAR-1. Thus PDZ-phosphorylation of Baz by aPKC is essential to recruit and activate aPKC in the absence of Crb in order to restrict basolateral PAR-1 activity to ensure correct apical-basal polarization and AJ formation of epithelial cells.

As PAR-6 has a supposed PDZ-binding motif (PBM), we questioned if this PBM is important for PAR-6 localization and function. Experiments made in this study give a first hint to a certain role of the PDZ-binding motif in the correct function of PAR-6.

3 Introduction

3.1 Cell polarity

Cell polarity is a fundamental mechanism from single cells to multicellular organisms in order to establish and maintain epithelial barrier formation, directed three-dimensional growth and movement as well as communication between tissues over long distances like between neurons. The prerequisite of polarity consists in a difference of architecture, composition and function within a cell. Hence a polarized cell comprises an asymmetric distribution of cell components, which is achieved by defined spatial and temporal localization and interactions of key polarity proteins and other molecules like lipids in a complex network. The mechanisms controlling these complex interactions are fundamentally important for the establishment and maintenance of epithelial tissues up to complex body plans and are therefore highly conserved throughout evolution.

Cell polarity can be classified into four general concepts according to their orientation and temporal appearance: the transient polarity like in directed migrating cells, the planar polarity during tissue formation, the anterior-posterior polarity in one-cell embryos in oocytes of the worm *Caenorhabditis elegans* and the fruit fly *Drosophila melanogaster* and finally the apical-basal polarity found in epithelial cells (Figure 1) (Chen and Zhang, 2013).

Initial cues for a cell to start polarization can be either from internal or external origin. For example a contact to another cell or the extracellular matrix can lead an epithelial cell to form junctions with other cells in order to start the formation of an epithelial tissue (Nelson, 2003).

Model organisms like the fruit fly *Drosophila melanogaster* are commonly used in many aspects of cell and developmental biology to understand fundamental mechanisms of cell polarity in order to gain deeper insight in processes, such as differentiation, proliferation and morphogenesis. This understanding of complex cellular processes in detail forms the basis of the development of drugs or therapies against many diseases including cancer.

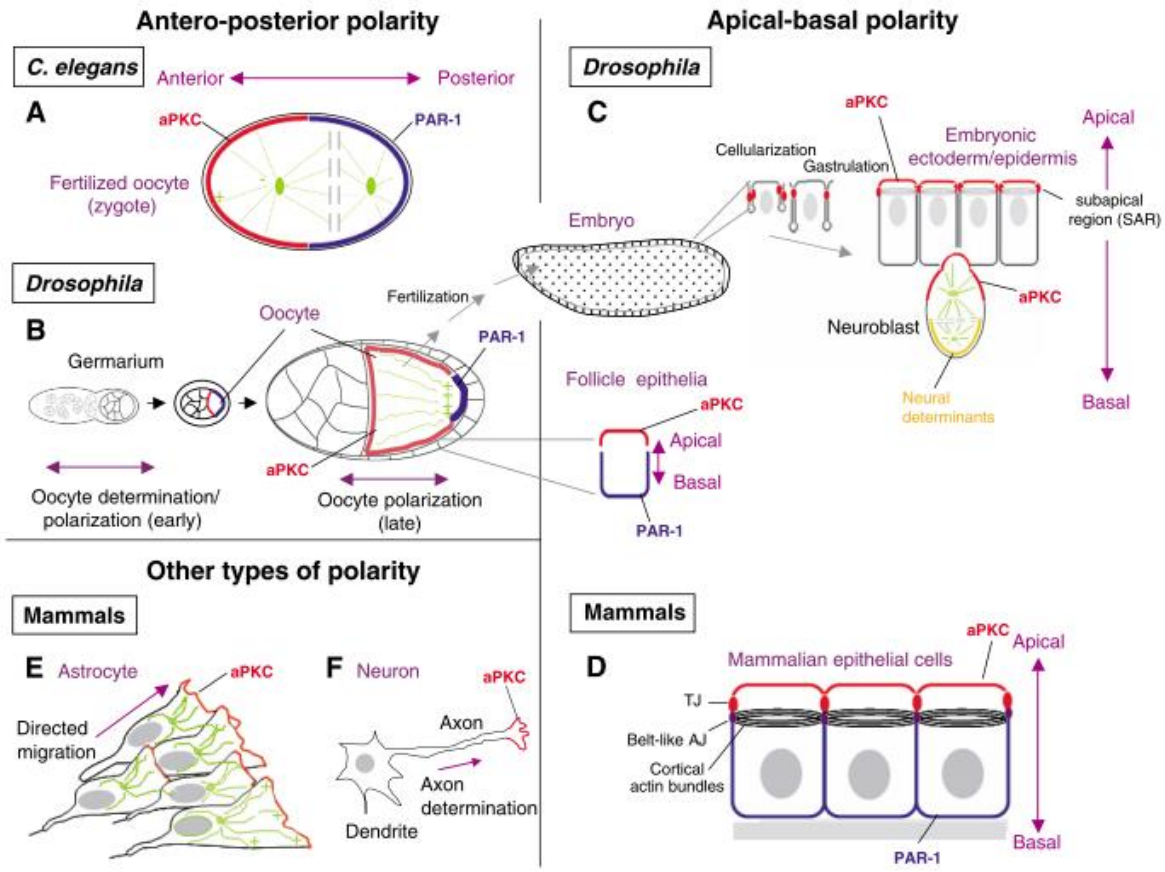

Figure 1 General types of cell polarity

The four general concepts of cell polarity are shown in various tissues: the anterior-posterior polarity in one-cell embryos in oocytes of the worm *C. elegans* (A) and the fly *Drosophila* (B), the apical-basal polarity in *Drosophila* epithelial cells (C) and in mammalian cultured epithelial cells (D), transient polarity during directed migrating cells in mammalian primary-cultured astrocytes to the front (E) and the planar cell polarity in a mammalian primary-cultured neuron that specifies one of the immature neurites as an axon (from Suzuki and Ohno 2006).

3.2 Epithelial cell polarity in the model organisms *Drosophila melanogaster*

One of the most important and thereby easily accessible model organisms for studying cell polarity *in vivo* is the epithelial tissue with its apical-basal polarization in *Drosophila melanogaster*. Epithelial cells play key roles throughout evolution by forming physiological and mechanical barriers and controlling tissue architecture (Rodriguez-Boulan and Nelson, 1989).

In multicellular organisms, epithelial cells are organized as a layer that subdivides the body into morphologically and physiologically different compartments. The epithelial tissue functions as a diffusion barrier between the inside and outside of the organism, thereby allowing vectorial transport from one side to the other (Chen and Zhang, 2013).

The polarity of epithelial cells is achieved by the presence of distinct apical, lateral and basal domains. The apical region faces the external environment or a lumen, the lateral membrane contacts neighboring cells, whereas the basal domain attaches the interstitial space of the body and the extracellular matrix (ECM) (Chen and Zhang, 2013). As the lateral and the basal domains are excluded from the external environment in contrast to the apical domain, they are often summarized as the basolateral domain. The specific function of these domains results from different protein and lipid compositions. Several protein complexes and lipids act in a coordinated interaction to produce together a cell polarity axis and develop cell-cell junctions in epithelial cells. Moreover the establishment and maintainance of epithelial polarity includes besides cell junctions also cytoskeletal cues and membrane trafficking (Harris and Pfeifer, 2004; Harris and Pfeifer, 2005).

The formation of special cell-cell contact zones is a very important step to establish membrane domains and guarantee close adhesion, which provides barrier function and interaction among the cells in an epithelium. Epithelial cells possess an adhesive belt surrounding the cell just below the apical domain, called the *zonula adherens* (ZA), where adherens junctions between neighboring cells are formed. Apical to the ZA a specialized plasma membrane microdomain in vertebrates, called the tight junction (TJ), is formed (Feigin and Muthuswamy, 2009; Flores-Benitez and Knust, 2016). The TJs are composed of different protein complexes and are responsible for intercellular sealing (Tsukita et al., 2001). Although the assembly and also the regulation of epithelial cell architecture and function are highly conserved, the *Drosophila* epithelium exhibits in contrast to vertebrate TJ the so-called subapical region (SAR) apical to the ZA. Nevertheless the *Drosophila* SAR includes protein complexes that correspond to tight junction proteins in vertebrates and thereby are highly conserved throughout evolution. Additionally *Drosophila* epithelial cells possess another complex basal to the ZA, the so-called septate junction (SJ), which covers large parts of the lateral domain and acts as the functional equivalent to the

vertebrate TJ by forming a paracellular diffusion barrier (Figure 2) (Knust and Bossinger, 2002). Transmembrane proteins, containing extracellular domains within these junctions, mediate interactions between adjacent cells in order to enable interplay with signaling molecules and cytoskeletal proteins (Feigin and Muthuswamy, 2009).

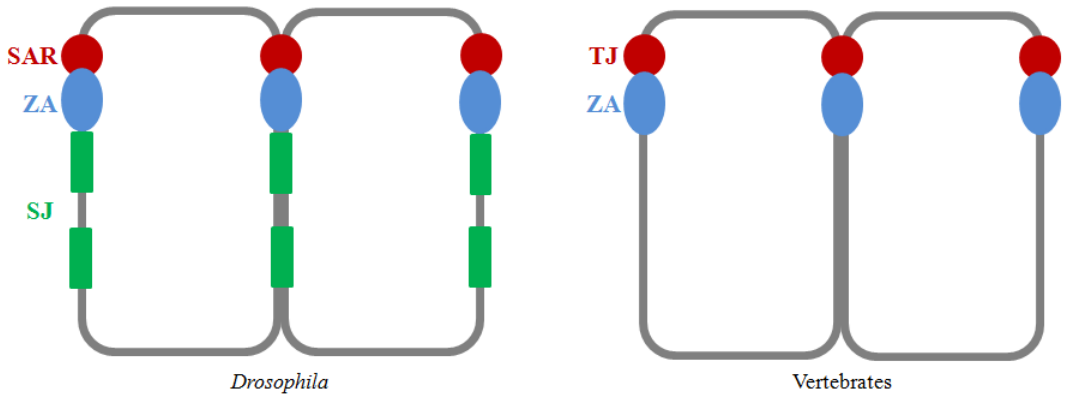

Figure 2 The organization of epithelial cells in comparison between Drosophila and vertebrates

Comparison between epithelial cells of *Drosophila* (left) and vertebrates (right) shows for both the ZA (blue), surrounding the cells just below the apical domain. In vertebrates TJs (red) apical to the ZA are formed, whereas *Drosophila* epithelial cells possess the SAR (red) including protein complexes comparable to TJ proteins in vertebrates. Additionally *Drosophila* epithelial cells possess SJ (green) basal to the ZA (adapted from Knust and Bossinger, 2002).

The initial cues to start epithelial differentiation comprise cell-cell contacts and cell-extracellular matrix contacts, which are mainly mediated by transmembrane adhesion molecules and receptors of the cadherin superfamily and the integrin family, respectively (Drubin et al., 1996; Yeaman et al., 1999; Tepass et al., 2000; Giancotti et al., 1999; Wodarz, 2002). The development of epithelial cells starts with the formation of cadherin-containing cell contacts, the spot adherens junctions (AJ) along the lateral plasma membrane between neighboring cells (Tepass and Hartenstein, 1994; Wodarz, 2002). As the TJs are not emerged at this developmental stage, several components of the TJs colocalize with AJ components. Afterwards AJs comigrate to the apicolateral region thereby establishing the ZA, whereas simultaneously residual components of both AJ and TJ start to arrange and establish the TJ domain (Wodarz, 2002). The establishment of the TJ requires the proper arrangement of the ZA, which in turn is achieved by the transmembrane protein E-

cadherin and its associated cytoplasmic proteins α-catenin and β-catenin (Armadillo (Arm) in *Drosophila*) and furthermore by the formation of special protein complexes apical and basal to the ZA itself (Feigin and Muthuswamy, 2009; Knust and Bossinger, 2002).

In the *Drosophila* SAR as well as in the vertebrate TJs a highly conserved protein complex can be found, namely the PAR complex, consisting of the PDZ-domain containing protein PAR-3 (Bazooka (Baz) in *Drosophila*), the atypical protein kinase C (aPKC) and PAR-6, together with Cdc42. Moreover a second very important conserved complex located slightly apical to the AJs is the Crumbs (Crb)/PALS1 (protein associated with Lin7; Stardust (Sdt) in *Drosophila*)/PATJ (PALS1-associated TJ protein)/Lin7 complex. Crb is a transmembrane protein which binds to the MAGUK (membrane associated guanylate kinase) protein Stardust.

Moreover transmembrane proteins like occludin and members of the claudin family, which span the membrane four times, are localized at the TJ domain as well as the single-span transmembrane proteins JAM (junctional adhesion molecule) (Ebnet et al., 2001). These transmembrane proteins interact directly with cytoplasmic, PDZ domain containing proteins, like the zonula occludens (ZO) proteins 1-3, Baz/PAR-3 and Sdt/PALS1, which function as scaffolds to recruit other cytoskeletal and signaling molecules (Tsukita et al., 2001; Shin et al., 2006; Flores-Benitez and Knust, 2016).

Basally to the ZA, another important protein complex is located at the basolateral membrane domain, called the Discs large/Scribble/Lethal (2) giant larvae complex, which consists of the multi-PDZ and leucine rich-repeat protein Scribble (Scrib), the MAGUK protein Discs large (Dlg) and the WD-40 repeats containing Lethal (2) giant larvae (Lgl) (Feigin and Muthuswamy, 2009). Several additional polarity regulating proteins are located at the basolateral membrane domain, namely the serine-threonine kinase MARK1/2 (PAR-1), the adaptor protein 14-3-3 (PAR-5) and the multifunctional protein kinase LKB1 (PAR-4).

Although most constituents are highly conserved, the *Drosophila* epithelial cells show some differences in the arrangement of the lateral domain. In the *Drosophila* SAR, the Crb/Sdt/PATJ complex localizes slightly apical to the PAR complex and the Dlg/Scrib/Lgl complex is localized to the special SJs.

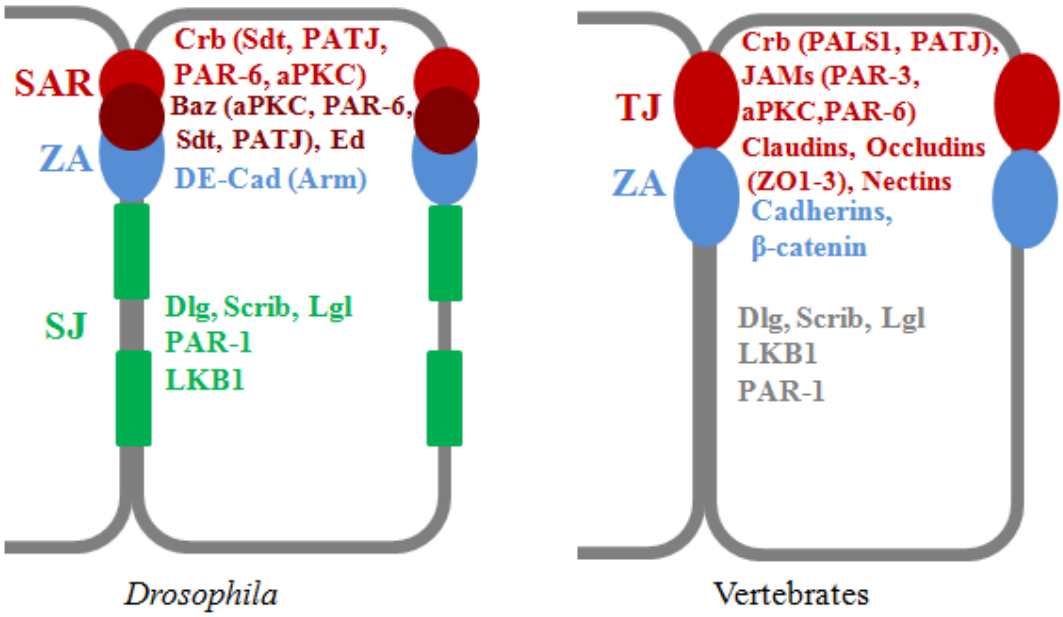

Figure 3 Localization of protein complexes in Drosophila and vertebrate epithelial cells

Comparison of the distribution of important protein complexes along the apical to basal axis between epithelial cells of *Drosophila* (left) and vertebrates (right). In vertebrates, TJ (red) apical to the ZA are formed, whereas *Drosophila* epithelial cells possess a SAR (red) whereby most of the constituents are highly conserved. Different to the vertebrate TJs the Crb/Sdt/PATJ complex (light red) localizes slightly apical to the PAR-3/PAR-6/aPKC complex (dark red) in the *Drosophila* SAR. The Dlg/Scrib/Lgl complex is localized to the special SJ (green). All complexes are working in a dynamic and spatial interaction (adapted from Knust and Bossinger, 2002).

3.3 The PAR complex

One of the key regulators of apical-basal polarity in epithelial cells is the PAR complex. The PAR complex, consisting of the multi modular scaffold proteins Bazooka (Baz, PAR-3 in mammals), PAR-6 and the atypical protein kinase C (aPKC), contribute to the initial establishment of epithelial cell polarity and it controls the localization of additional complexes functioning further downstream in the regulation of epithelial development (Figure 4). The name "PAR" derives its origin from genetic screens in *C. elegans* zygotes for genes that establish anterior-posterior polarity and stands for "partitioning-defectiveness of zygotes after mutation of the genes" (Kemphues et al., 1988). The PAR complex was initially found to regulate polarity in early stages of *C. elegans* and *Drosophila* embryos (Tabuse et al.,

1998), as well as in the asymmetric cell division of *Drosophila* neuroblasts (Wodarz et al., 1999) and also in mammalian epithelial cells and the axon-dendrite polarity of neurons (Figure 1) (Plant et al., 2003; Lin et al., 2000).

The proteins in this complex operate in a specific hierarchy, in which Baz/PAR-3 plays a key role in the proper subcellular localization of other apical markers (Johnson and Wodarz, 2003). At the onset of epithelial polarization Baz/PAR-3 can associate via PDZ-PDZ domain interaction with the hetero-dimer PAR-6/aPKC (Hung and Kemphues, 1999; Lin et al., 2000; Chen and Zhang, 2013). The PDZ (Post-synaptic-density protein 95 - Discs large - Zonula Occludentes 1) domain is a highly conserved protein-protein interaction module which can occur from single to multiple copies in many cytoplasmic as well as membrane adaptor proteins (Lee and Zheng, 2010). This domain can either interact with proteins via other PDZ domains or with specific carboxy-terminal motifs, the so-called PDZ-binding motif (PBM). The specific peptide sequence of PBMs is usually located at the very C-terminus of the target protein, nevertheless also internal PBMs have been reported (Javier and Rice, 2011).

The scaffold protein PAR-6 can interact with aPKC through their N-terminal PB1 (phagocyte oxidase/Bem1) domains (Terasawa et al., 2001; Suzuki et al., 2001; Suzuki et al., 2003). Additionally PAR-6 can interact with the small GTPase Cdc42 via its Semi-CRIB (N-terminal Cdc42/Rac interactive binding) motif (Burbelo et al., 1995). This binding of Cdc42 activates the kinase activity of associated aPKC (Garrard et al., 2003; Joberty et al., 2000; Lin et al., 2000; Peterson et al., 2004). Cdc42 is a member of the family of Ras-like GTPases and is involved in many pathways connected to cell polarity. Nevertheless it is not jet completely investigated how Cdc42 interacts in detail with the PAR complex. Subsequently activated aPKC can phosphorylate Baz/PAR-3, which in turn dissociates from the PAR-6/aPKC heterodimer (Nagai-Tamai et al., 2002; Horikoshi et al., 2009; Morais-de-Sá et al., 2010).

At a later point in development, Baz/PAR-3 directly binds the scaffolding protein Stardust (Sdt)/PALS-1, which becomes expressed during early gastrulation (Krahn et al., 2010a; Chen and Zhang, 2013). Thereby, the transmembrane protein Crumbs (Crb) is stabilized at the apical junctions by its adaptor Sdt. Upon maturation of epithelia, the scaffolding protein Baz/PAR-3 and the transmembrane protein Crb

function to some extent redundantly to determine the apical domain of epithelial cells (Tanentzapf and Tepass, 2003) and further direct the formation of apical junctions by recruiting aPKC.

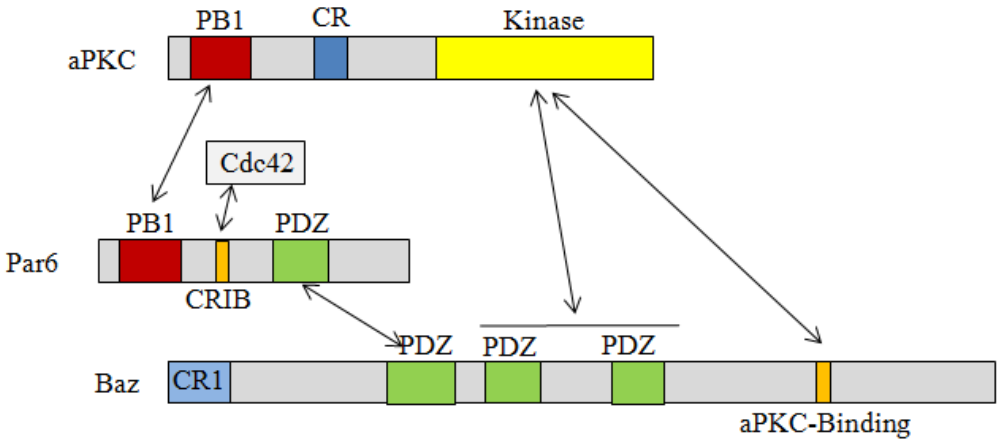

Figure 4 The PAR complex

PAR-6 can interact with aPKC through their N-terminal PB1domains, whereas the first PDZ domain of Baz can interact with the PDZ domain of PAR-6 and the aPKC-binding domain of Baz with the kinase domain of aPKC. Interaction of PAR-6 with the small GTPase Cdc42 via its Semi-CRIB motif activates the kinase activity of associated aPKC, which in turn leads to phosphorylation of Baz in the PDZ2-3 region and the aPKC-binding domain (adapted from Chen and Zhang, 2013; Johnson and Wodarz, 2003; n.t.s.).

On the other hand, the activity of the PAR complex is counterbalanced by basolateral polarity proteins in order to achieve and maintain distinct cortical domains. aPKC can phosphorylate and thereby inactivate the kinase PAR-1 to prevent it from associating with apical regions (Benton and St. Johnston, 2003a; Chen and Zhang, 2013). On the other way round PAR-1 is able to phosphorylate Baz/PAR-3 at two conserved serines (at position 151 and 1085 in Baz; figure 5) in *Drosophila* and mammalian epithelial cells and the basal cortex of *Drosophila* neural stem cells, thereby preventing dimerization of Baz/PAR-3 and providing a movement of Baz/PAR-3 to a more apical position via binding to 14-3-3 proteins (PAR-5 in *Drosophila*) (Benton and St. Johnston, 2003a; Hurd et al., 2003; Krahn et al., 2009; McKinley and Harris, 2012). In the beginning of *Drosophila* epithelial development PAR-1 and Baz show a partial overlap during early cellularization (McKinley and Harris, 2012). However already in late cellularization/early gastrulation PAR-1 and

Baz start to segregate to establish a clear apical (Baz) and basal (PAR-1) localization (McKinley and Harris, 2012).

Moreover Lgl can physically interact with the heterodimer aPKC/PAR-6. Thereby Lgl is phosphorylated by aPKC in order to stay at the basolateral membrane (Betschinger et al., 2003; Plant et al., 2003; Chen and Zhang, 2013).

3.4 Bazooka/PAR-3

The name "Bazooka" has its origin from the big holes observed in the cuticle of *Drosophila baz* mutant embryos and was first identified in a screen for embryonic defects (Wieschaus et al., 1984) as a gene product essential for the polarization of the *Drosophila* embryonic ectoderm (Kuchinke et al., 1998). The PDZ-domain-containing scaffold protein Baz is highly conserved in evolution and has a homolog in worm and mammalian called PAR-3. The *Drosophila baz* encodes for a large protein with 1464 amino acids whereas the human homologue *par-3* has 1319 amino acids. Both show high similarities and possess corresponding domains (Figure 5).

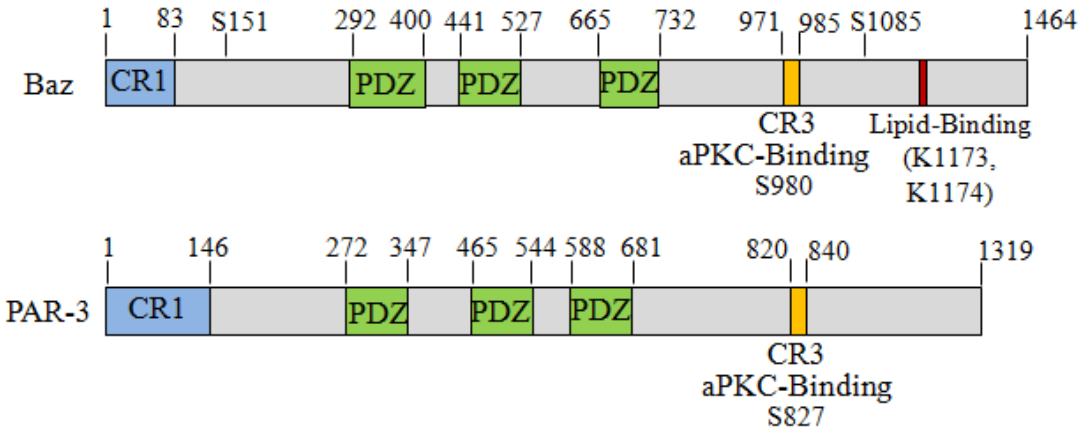

Figure 5 Stucture of Drosophila Baz and human PAR-3

Drosophila Baz and its homologe PAR-3 show high similarities. Both possess an N-terminal conserved region, three PDZ domains and an aPKC-binding motif in the CR3 (data according to NCBI databases, n.t.s.).

Baz/PAR-3 contains a conserved N-terminal domain (NTD) or CR1 (conserved region 1), which is able to self-associate (Benton and St. Johnston, 2003a). The CR1 self-association leads to an oligomerization of Baz/PAR-3 molecules in order to establish a molecular basis for an enrichment of the PAR complex and their binding partners (Chen and Zhang, 2013; Benton and St. Johnston, 2003b; Mizuno et al., 2003; Feng et al., 2007).

Baz/PAR-3 displays three highly conserved PDZ domains, whereby the first PDZ domain interacts with the PDZ domain of PAR-6 (Lin et al., 2000; Suzuki et al., 2001) and moreover with several cell adhesion molecules like nectin, p75 and members of the transmembrane protein families JAM (junctional adhesion molecule) (Chan et al., 2006; Ebnet et al., 2003; Itoh et al., 2001; Chen and Zhang, 2013). Baz can interact with aPKC via its PDZ domains 2 and 3 (Wodarz et al., 2000; Rolls et al., 2003). Moreover the Baz/PAR-3 PDZ domains 2 and 3 are described to bind to lipid membranes in order to achieve a localization at the TJs and PDZ 3 interacts with the C-terminal PDZ binding motif (PBM) of the lipid Phosphatase PTEN (Yu and Harris, 2012; Wu et al., 2007; Chen and Zhang, 2013), which has been reported to promote apical polarity in *Drosophila* (Chartier et al., 2011) and mammalian system (Martin-Belmonte al., 2007).

The C-terminal half of Baz/PAR-3 possesses another interaction domain with aPKC, a short conserved aPKC-binding motif, also annotated as conserved region 3 (CR3), whereby in detail a serine at position 980 for *Drosophila* Baz and a serine at position 827 in human PAR-3, respectively, are phosphorylated by aPKC (Horikoshi et al., 2009; Izumi et al., 1998; Lin et al., 2000; Morais-de-Sá et al., 2010; Nagai-Tamai et al., 2002). The CR3 of Bazooka starts at position 971 and spans over 14 amino acids, whereas for the vertebrate homologe PAR-3 the CR3 of twenty amino acids, starting at position 820, is reported to interact with the kinase domain of aPKC (Izumi et al., 1998; Tabuse et al., 1998). Sdt binds to Baz at a region which includes the aPKC-binding motif. Therefore a phosphorylation of Baz by aPKC at the serine 980 weakens the interaction of Baz with Sdt, which in turn enables the formation of the Crb-Sdt complex (Krahn et al., 2010a). Baz also exhibits a lipid-binding domain which consists of two lysines at position 1173 and 1174 (Figure 5). Furthermore the C-terminal part of Baz/PAR-3 contains three conserved regions, called 4N1/2/3, which show no recognizable domain composition (Chen and Zhang, 2013).

Moreover Baz/PAR-3 binding partners include phosphoinositols (Krahn et al., 2010b), the Rho-kinase (Simões et al., 2010) and AJ proteins Armadillo (Arm in *Drosophila*; ß-catenin in vertebrates) and Echinoid (Ed) (Wei et al., 2005), which bind to the central PDZ domain region.

3.5 The serine/theronine kinase aPKC

The atypical protein kinase C (aPKC) is a very important component of the PAR complex, as it represents prominently an evolutionary conserved regulator in cellular polarity by phosphorylation of many important polarity proteins including PAR-3, PAR-1, Crb, Lgl, GSK-3ß, MARCKS and LIN5/NuMA (Chen and Zhang, 2013). PAR-6 operates as a regulatory subunit of aPKC, thereby controlling its position and regulating its kinase activity (Tepass, 2012; Atwood et al., 2007; Graybill, 2012). This is achieved by a PAR-6 mediated interaction with active, thereby GTP-loaded, Cdc42, which derestrict inhibition of aPKC kinase activity (David et al., 2010; Atwood et al., 2007). The PAR-6/aPKC heterodimer initially needs to form a complex with Baz/PAR-3 to be recruited to the apical membrane (Harris and Pfeier, 2005; Tepass, 2012). Nevertheless the interaction between the PAR-6/aPKC heterodimer and Baz is weakened by phosphorylation of Baz by aPKC, which in turn allows the interaction between Baz and Sdt in order to achieve the Crb/Sdt/PATJ complex formation (Krahn et al., 2010a). Additionally Baz/PAR-3 is able to act as an inhibitor of the PAR-6/aPKC heterodimer activity, which leads to stabilization of actomyosin networks through a reduced phosphorylation of cytoskeletal regulators by aPKC (Soriano et al., 2016).

Moreover aPKC is also responsible for the regulation of basolateral polarity proteins, particularly by phosphorylation of the basolateral proteins Lgl and PAR-1. This phosphorylation prevents the accumulation of these basolateral proteins at the more apical part of the cell (Betschinger et al., 2003; Hurov et al., 2004; Kusakabe and Nishida, 2004; Plant et al., 2003; Yamanaka et al., 2003; Suzuki et al., 2004). Besides, aPKC is also able to autophosphorylate although the effects are not known at the moment (Tepass, 2012).

The regulation of protein function by aPKC is achieved by the phosphorylation of hydroxyl groups of serine or threonine amino acid residues within a special phosphorylation site on the particular protein. Thereby members of the PKC kinase family, like aPKC possess a consensus phosphorylation site motif, which is conserved from *Drosophila* to mammals, consisting of amino acid sequences like R/K-X-X-S/T, R/K-X-X-X-S/T, or S/T-X-R-X whereby X indicates any amino acid (Pearson and Kemp, 1991).

3.6 The adaptor protein PAR-6

The regulatory adapter protein of the PAR complex, PAR-6, is composed of a N-terminally positioned PB1 domain, which enables PAR-6 to interact with aPKC in order to form the functionally PAR-6/aPKC heterodimer (Terasawa et al., 2001; Suzuki et al., 2001; Suzuki et al., 2003), a semi CRIB domain, which can associate with the small GTPase Cdc42 (Burbelo et al., 1995; Garrard et al., 2003; Joberty et al., 2000; Lin et al., 2000; Peterson et al., 2004), and a PDZ domain for interaction with Baz/PAR-3 (Hung and Kemphues, 1999) (Figure 4).

PAR-6 regulates the kinase activity of aPKC in many different cell types of diverse species (Suzuki and Ohno, 2006; Atwood et al., 2007; Tepass, 2012; Graybill, 2012) and furthermore controls the positioning of the PAR-6/aPKC heterodimer to the apical region. The apical positioning is strengthened by the interaction of PAR-6 with the Crb/Sdt/PATJ complex, which thereby weakens the PAR-6-Baz interaction (Morais-de-Sá et al., 2010; Walter and Pichaud, 2010). PAR-6 directly binds the N-terminal region of Sdt and PATJ as well as the PDZ domain of *Drosophila* PATJ with its N-terminus (Nam and Choi, 2003; Wang et al., 2004; Bulgakova et al., 2008). Additionally PAR-6 can interact with the C-terminus of Crb (Wang et al., 2004). Thus PAR-6 functions as a mediator between the two important apical protein complexes in a polarized cell, the PAR and the Crb complex. Moreover in mammalian epithelial cells the dominant human homologue of Crb, CRB3, can recruit PAR-6 to the apical region in unpolarized cells (Hurd et al., 2003).

3.7 The Crb complex

The Crb complex consists of Crb, Sdt/PALS-1, PATJ and Lin7 and is highly conserved from fly to human. The apical polarity protein Crb regulates the apical-basal polarity and integrity in many different tissues among various species together with its intracellular adaptor protein Sdt/PALS-1 (Tepass and Knust, 1993; Tepass et al., 1990; Bulgakova and Knust, 2009).

The transmembrane protein Crb consists of a large extracellular domain and a short intracellular domain (Tepass et al., 1990; Wodarz et al., 1993). Instead of *Drosophila*, humans possess three Crb genes, CRB1, CRB2 and CRB3. CRB3, which is further subdivided into two isoforms, is broadly expressed in simple epithelial cells in mammals and lacks most of the extracellular domain, but shows in one isoform the highly conserved intracellular tail like in other species (Fan et al., 2007; Shin et al., 2006). Crb can physically interact with its C-terminal ERLI motif with the single PDZ domain of Sdt thereby initiate the formation of the Crb/Sdt complex (Bachmann et al., 2001; Hong et al., 2001). Sdt, which encodes a membrane-associated guanylate kinase (MAGUK) without kinase domain activity (Tepass, 2012), possesses an N-terminal conserved region containing ECR1 and ECR2, which can interact with PAR-6 (Bachmann et al., 2001; Hong et al., 2001; Tepass, 2012). Furthermore Sdt contains two L27 domains with can bind to PATJ and Lin7, respectively (Bachmann et al., 2004; Bulgakova et al., 2008). PATJ and Lin7 comprise an N-terminal L27 domain itself and additionally four PDZ domains in case of PATJ and two PDZ domains in case of Lin7.

Crb is not expressed in all epithelia in *Drosophila*, like for example in the intestinal epithelia (Tepass et al., 1990). In some cases, Crb is not required to maintain epithelial polarity, like in late embryonic epidermis or in larval imaginal disc epithelia and functions to some extent redundantly with other apical polarity regulators like Baz (Campbell et al., 2009; Pellikka et al., 2002; Tanentzapf and Tepass, 2003).

3.8 The embryonic development of *Drosophila melanogaster*

The ectodermal epidermis of *Drosophila* embryos is a good model for studying fundamental processes of cell polarity. The development of *Drosophila* embryos was subdivided into stages in 1975 by Mary Brownes and revised by Volker Hartenstein and José Campos-Ortega, which became a general reference in *Drosophila* research (Brownes, 1975; Campos-Ortega and Hartenstein, 1997) (Table 1).

The ectodermal epidermis is established at first by dividing the zygotic nuclei of a fertilized *Drosophila* egg for thirteen times at the blastoderm stage. The syncytium is established out of 128 nuclei by the first seven synchronous zygotic divisions (Campos-Ortega and Hartenstein, 1997). The following divisions producing pole cells at the posterior pole and continuing to divide until the number of syncytial blastoderm nuclei reaches approximately 5000 (Campos-Ortega and Hartenstein, 1997). Subsequently cellularization takes place to form the somatic cells by multiple invaginations of the plasma membrane around each nucleus, thereby forming definite epithelial cells (Figure 1 C) (Suzuki and Ohno, 2006). This cellular blastoderm stage, before gastrulation occurs is also called stage 5 (Table 1) (Campos-Ortega and Hartenstein, 1997). The transition from late cellularization to early gastrulation is called stage 6 and is a timepoint of special interest for this work as here the PAR complex is recruited to the forming apical junctions. Gastrulation, which causes the formation of germ layers, occurs by the gradual invagination of a consistent midventral cell area, which forms a tubular structure inside the embryo (Campos-Ortega and Hartenstein, 1997). This time span extends over stage 5 until stage 7. In stage 7 the germ band starts to elongate, which proceeds during stage 8 until stage 11 (Campos-Ortega and Hartenstein, 1997). The expression of components of the Crb complex starts also during embryonic stage 8 and therefore is another special point in embryonic epithelial cell polarity development in this study.

Table 1 Time table of Drosophila embryonic development (from http://flymove.uni-muenster.de/stages/StgTabelle.html)

	Stage	Time	Developmental events
	1- 4	0:00 - 2:10 h	Cleavage
	5	2:10 - 2:50 h	Blastoderm
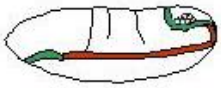	6 - 7	2:50 - 3:10 h	Gastrulation
	8 - 11	3:10 - 7:20 h	Germ band elongation
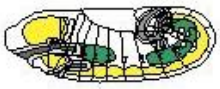	12 - 13	7:20 - 10:20 h	Germ band retraction
	14 - 15	10:20 - 13:00 h	Head involution and dorsal closure
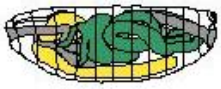	16 - 17	13:00 - 22:00 h	Differentiation

From stage 9 onwards the germ band elongation enters its slow phase and ventral and procephalic neuroblasts start to segregate, which are first divide in stage 10 (Campos-Ortega and Hartenstein, 1997). The epidermal segmentation of the embryo becomes visible in stage 11 and the germ band retraction occurs during stage 12 and 13 (Campos-Ortega and Hartenstein, 1997). The dorsal closure and the head involution take place in stage 14 to 15 and in stage 16 and 17 the embryo finally differentiates (Brownes, 1975; Campos-Ortega and Hartenstein, 1997).

3.9 Research objectives

Cell polarity is a fundamental mechanism in nature and affects various species in different conditions. Therefore it is fundamentally important to understand how cell polarity is achieved and how polarity proteins work together in specific complexes in order to create a basis of the development of drugs or therapies against many diseases including cancer.

Until now, many aspects of the important polarity determinants Baz/PAR-3 and its interaction in the PAR complex and with other polarity complexes are investigated, although there are still many open questions remained.

Thus the main address of this work was to gain knowledge about the interaction and function of phosphorylation events of Baz/PAR-3 by the kinase aPKC. In detailed structure and function analysis the two regions of Baz which are involved in aPKC binding were investigated. Moreover new phosphorylation sites of Baz and its human homologue PAR-3 for aPKC were identified which were analyzed for Baz in studies *in vivo* in the fly.

Moreover we had a closer look on the third member of the Par complex, PAR-6. As PAR-6 has a supposed PDZ-binding motif (PBM), a short peptide at the very C-terminus, we questioned if this PB motif is important for PAR-6 binding and functionality. To clarify this issue, we performed a lethality test as well as immunostainings, were we compared PAR-6 wildtype flies with PAR-6ΔPBM flies, which are lacking the supposed PBM.

4 Material & Methods

4.1 Material

4.1.1 Reagents

Table 2 Reagents

reagents	application	company
[γ-32]ATP	kinase assay	Hartmann Analytic
Acrylamide-Solution (30%) - Mix 29:1 Mol. Biology grade	SDS-PAGE	Diagonal/AppliChem
Adenosine-5'-(γ-thio)-triphosphate (ATPγS)	kinase assay	Abcam
Agarose	agarose gelelectrophoresis	Roth
Albumine, Bovin Serum (BSA)	blocking buffer, *Drosophila* embryo staining	Roth
Ammonium peroxodisulfate (APS)	SDS-PAGE	Thermo Scientific
Ampicillin	selection of *E.coli*	Roth
Aprotinin	protease inhibition	Roth
Bradford Rothi® Quant	protein concentration measurement	Roth
Bromphenol blue	loading dye	BIO-RAD
Cantharidine	protease inhibition	Sigma-Aldrich
Chloramphenicol	selection of *E.coli*	Roth
Chloramphenicol	selection of *E.coli*	Roth
Coomassie Brilliant Blue (CBB)	proteinpurification	Thermo Scientific

1, 4-Dithiothreitol (DTT)	SDS-PAGE	Roth
4',6-Diamidino-2-phenylindole dihydrochloride (DAPI)	immunohistology	Roth
dNTPs (dATP, dGTP, dCTP, dTTP)	PCR	Thermo Scientific
Ethidiumbromide	agarose gelelectrophoresis	Sigma-Aldrich
Ethylendiamintetraacetate (EDTA)	buffer P1/S1	Sigma- Aldrich
Fetal Bovine Serum (FBS)	cell culture	gibco®
Formaldehyde 37%, v/v	fixation of *Drosophila* embryos	Roth
FuGENE®HD Transfection Reagent	transfection	Promega
Glycine	blotting buffer	Merck
Isopropyl-β-D-thiogalactopyranosid (IPTG)	protein purification	Roth
Kanamycin	selection of *E.coli*	Roth
Lactate	Hoyer´s medium	Fluca
Leupeptin	protease inhibition	Roth
Lysozyme	protein purification	Biomol
Mercaptoethanol, 2-	protein npurification	Merck
Methanol LC/MS ultra	*Drosophila* embryo staining	Roth
Methylene blue	methylen blue solution	Sigma-Aldrich
Mowiol 4-88	immunohistology	Merck
N,N,N',N'-tetramethylethylenediamine (TEMED)	SDS-PAGE	Roth
n-Heptane	immunohistology	Roth
Oil 10 S VOLTALEF(R)	injection for germline transformation	VWR
Penicillin-Streptomycin	cell culture	Sigma-Aldrich

Pepstatin A	protease inhibition	Roth
Phosphatase inhibitor cocktail	phosphatase inhibition	Sigma-Aldrich
Phyenylmethylsulfonylfluoride(PMSF)	protease inhibition	Roth
p-Nitrobenzyl mesylate (PNBM)	kinase assay	Abcam
Protein G Plus Agarose	immunoprecipitation	Santa Cruz
Protino Glutathione Agarose 4B	protein purification	Macherey-Nagel
RNAse A	buffer P1/S1	Roth
Schneider´s *Drosophila* medium	cell culture	PAN Biotech
Sodium dodecyl sulfate (SDS) ultrapure	SDS-PAGE	Diagonal/AppliChem
Strep-Tactin-Sepharose 90% Suspension	immunoprecipitation	IBA GmbH
Tris Base	buffering	Sigma-Aldrich
Triton™ X-100	protein purification	Serva
Tween® 20	immunohistology	Roth

4.1.2 Solutions and buffer

Solutions and buffer were prepared with sterile H_2O and, if necessary, subsequently autoclaved.

Table 3 Solutions and buffer

solution/buffer	Composition	
APS	438 mM	APS
Blocking buffer	12,5 ml	TBS (20x)

	2,5 ml	10% Tween
	2,5 g	BSA
	7,5 g	Skim milk powder
	ad 250 ml	H_2O
Blotting buffer	6,17 M	Methanol
	399 mM	Glycine
	49,44 mM	Tris base
Buffer P1/S1	50 mM	Tris-HCl
	10 mM	EDTA
	100 µg/ml	RNase A
Buffer P2/S2	20 mM	NaOH
	3,5 mM	SDS
Buffer P3/S3	3 M	Potassium acetate
Coomassie Brilliant Blue (CBB) solution	15,61 M	Methanol
	46 mM	concentrated Coomassie Brilliant Blue
	1,67 M	Acetic acid
Embryoglue	50 cm	adhesive tape
	14 ml	n-heptane
Fixation solution	59,95 mM	Formaldehyde
	440 ml	PBS
	4,99 M	Heptane
GST elution buffer	30mM	reduced Glutathione
	50 mM	Tris-HCl pH 7.5
	150 mM	NaCl
Injection buffer (10x)	5mM	KCl
	0.1 mM	sodium phosphate, pH 6.8
Kinase buffer	50 mM	TRIS pH 7.5
	10 mM	$MgCl_2$
	1 mM	DTT
LEW washing buffer (300 mM)	300 mM	NaCl
		in PBS
LEW washing buffer (2 M)	2 M	NaCl

		in PBS
Loading dye (6x)	3 ml	30% Glycerol
	35 mg	Bromphenol blue
	10 ml	H_2O
Lysis buffer	1370 µg/ml	Pepstatin A
	10 µg/ml	Aprotinin
	40 µg/ml	PMSF
	10 µg/ml	Leupeptin
	5 ml	TNT buffer
Methylen blue solution	1 pinch	Methylen blue powder
		in TAE (0,1x)
Mowiol solution	0,4 g/ml	Mowiol
	1 g/ml	Glycerol
	2%	Tris-HCl (0,2M)
NB fixing solution	4% (v/v)	formaldehyde (37%)
	0.1 M	PIPES (1 M, pH6,9)
	0.3% (v/v)	Triton X-100 (10%)
	20mM	EGTA (0.1 M, pH8.0)
	1mM	$MgSO_4$ (1M)
	ad 10 ml	H_2O
PBS (10x) pH 7.4	1,37 mM	NaCl
	27 mM	KCl
	0,1 M	Na_2HPO_4
	20 mM	KH_2HPO_4
PBT	0,1 %	Tween 20 in PBS
SDS loading dye (2x)	6,4 ml	10% SDS
	1600 µl	Glycerol
	1 ml	Tris (1M)
	1600 µl	Bromphenol blue
	ad 16 ml	H_2O
SDS running buffer	0,96 M	Glycin
	125 mM	Tris
	3,46 mM	SDS

Stripping buffer	12,5 M	Methanol
	2,28 M	Acetic acid
T4 ligase buffer	400 mM	Tris-HCl
	100 mM	$MgCl_2$
	100 mM	DTT
	5 mM	ATP
TAE (1x)	20 mM	Tris
	1 mM	EDTA
	40 mM	AcOH
TBS (20x)	2,74 M	NaCl
	53,66 mM	KCl
	0,5 M	Tris-HCl
TBST	50 ml	TBS (20x)
	10 ml	10% Tween
	ad 1 l	H_2O
TNT buffer	150 mM	NaCl
	50 mM	Tris
	8 mM	Triton X-100
10 % Tween 20	41 mM	Tween 20
Washing buffer	300 mM	NaCl in PBS

4.1.3 Media and agarose plates

For cultivation of *E.coli* strains selective culture medium (LB_0 medium) or agar plates (LB_0 agar plates) with a dilution of the required antibiotic stock concentration were used under sterile conditions. For ampicillin a final concentration of 100 µg/ml was necessary whereas for kanamycin 50 µg/ml and for chloramphenicol 30 µg/ml were used. Agarose plates as well as all of the following media were stored at 4°C and preheated before using.

Table 4 Media and agarose plates

medium/agarose plate	composition	
Apple juice agar plates	1980 ml	H_2O
	60 g	Agar
	1020 ml	Apple juice
	51 g	Sugar
	10%	Nipagin
Freezing medium	45%	Conditioned medium
	45%	FBS
	10%	DMSO
Hoyer´s medium (ready to use)	50ml	H_2O
	30g	Gummi arabicum
	200g	Chloralhydrat
	16 ml	Glycerine
	1:1	Lactate
LB_0 medium	1%	Tryptone
	0,5%	Yeast extract
	1%	NaCl
	ad	H_2O
LB_0 agar plates	10%	Tryptone
	5%	Yeast extract
	5%	NaCl
	15%	Agar
	ad	H_2O
Schneider´s *Drosophila* medium		L-Glutamin
(ready to use)	0,40 g/l	$NaHCO_3$
	10%	FBS
	1%	Penicillin-Streptomycin
YTA medium	16%	Tryptone
	10%	Yeast extract
	5%	NaCl
	ad	H_2O

4.1.4 Oligonucleotides

The Oligonucleotides were designed with DNADynamo (BlueTractorSoftware, UK) and subsequently sent to Metabion international AG (Planegg/Steinkirchen, Germany), Microsynth AG (Balgach, Switzerland) or Sigma-Aldrich Chemie GmbH (Munich, Germany) for synthesizing. The freeze-dried oligonucleotides were resolved in autoclaved, de-ionized H_2O to a final concentration of 50 pmol/µl. After that, a 10 pM solution was prepared for further use and stored at - 20°C.

Following oligonucleotides listed in table 5 were used to achieve a specific mutation of the destined gene of interest.

Table 5 Oligonucleotides for mutagenesis

name	**sequence 5´- 3´**
Baz A522T-F	GGCATGCCAGCGGGAGCAACTGTAAGGA…GTC
Baz A638S-F	CTGGGTGTCTCTGTGAAGGGAAAGACGT…CTG
Baz A700S-F	CTGCTGAGCGTGAATGGAGTATCGCTGC…CAA
Baz A712T-F	AATGCCGAGGCCATGGAGACACTACGTC…ATG
Baz A741S-F	AAGATCTTGCGATCAGCGTCTTCCAGTG…CTG
Baz S574A-F	ATTCCGGTACAAAAATCCGCTAGCGCAC…CTG
Baz S638A-F	CTGGGTGTCGCTGTGAAGGGAAAGACGTGTTCGAAT
Baz S638D-F	AAGGCCGGACTGGGTGTCGACGTGAAGGGAAAGACG
Baz S700A-F	CTGCTGAGTGTGAATGGAGTAGCGCTGCGTGGG
Baz S700D-F	CTGAGCGTGAATGGAGTAGATCTGCGTGGGCAAAAC
Baz T522A-F	ATGCCAGCGGGAGCAGCTGTAAGGATTGTGGTC
Baz T522D-F	GCTGGAGCAGATGTAAGGATTGTGGTCTCCCGCCAG
Baz T712A-F	GCCGAGGCCATGGAGGCACTACGTCGGGCAATG
Baz T712D-F	AATGCCGAGGCAATGGAGGATCTACGTCGGGCA
BazS741A-F	AAGATCTTGCGATCAGCCGCTTCCAGTGACATTCTG
BazS741D-F	AAGATCTTGCGATCAGCCGATTCCAGTGACATTCTG
PAR-3 ΔaPKC-B	GTTGATCCAGTTCTTGCTGGAGGTGGAGATTTCGTTAA AACACGA
PAR-3 ΔPDZ2-3	AAAAAAATAGGCAAGAGGGGAGGTGGACAGCTTATT

	GTTGCAAGG
PAR-3 A453T-F	AGTACGACTGTAAGCAGTGGTTATAACACCAAAAAAATA
PAR-3 A534T-F	AGCACCAAGATGGAAGGTACCGTGAGCCTACTAGTCTTT
PAR-3 A604S-F	TCAGGATCTGCAGGCCTTGGTGTCTCTGTCAAAGGTAAC
PAR-3 A661T-F	AACCAAGATGCCATGGAGACCCTAAGAAGGTCTATG
PAR-3 S533A-F	GAAGTTGTTTCGCTCTTAAGAGCCACCAAGATGGAAGGA
PAR-3 S604A-F	TCTGCAGGACTTGGTGTCGCTGTCAAAGGTAACCGG
PAR-3 S667A-F	CTAAGAAGGTCTATGGCCACTGAAGGCAATAAACGA
PAR-3 S685A-F	ATTGTTGCGAGGAGAATAGCCAAGTGCAATGAGCTG
PAR-3 T453A-F	GTAAGCAGCGGTTATAACGCCAAAAAAATAGGCAAG
PAR-3 T468A-F	CAGCTTAAGAAAGGTGCAGAAGGCCTGGGATTCAGC
PAR-3 T468A-F2	ATCCAGCTTAAAAAAGGTGCAGAAGGTT…TTC
PAR-3 T476/481A-F	GGATTCAGCATCGCTTCTAGATGTAGCAATAGGTGGC
PAR-3 T534A-F	TCGCTGTTGAGAAGCGCCAAGATGGAAGGTACCGTGAGC
PAR-3 T661A-F	AACCAAGATGCCATGGAGGCCCTAAGAAGGTCTATG

Following oligonucleotides listed in table 6 were used for cloning and sequenzing of destined DNA constructs.

Table 6 Oligonucleotides for cloning and sequenzing

name	**sequence 5´- 3´**
Baz PDZ2-F	CACCATGGCCAATACCCGTAAACTGGG
Baz1108-NotI-R	GATAAAGCGGCCGCCTACAACGCCTGATGACCA
Baz948-NotI-F	GATAAAGCGGCCGCTTTCCAGCAACTTT…CAC
BazPDZ1-3pEntry-F	CACCATGGATGGTGAAATGCTGCTGATC
BazPDZ1pEntry-R	TCATCTCAACTCTGAGCTCTCCAA
BazPDZ1pGexNotI-F	AAAGCGGCCGCTTATGGATGGTGAAATGCTGCTG

	ATC
BazPDZ1pGexNotI-R	GATAAAGCGGCCGCTCATCTCAACTCTG…CAA
BazPDZ2pEntry-F	CACCATGGCCAATACCCGTAAACTGGG
BazPDZ2pEntry-R	TCACTCCTGCTGGCGGGA
BazPDZ2pGexNotI-R	AAAGCGGCCGCTTACTCCTGCTGGCGG
BazPDZ2pGexT436A-F	AAAGTCGACTAGCCAATGCCCGTAAACTGG
BazPDZ2pGexT436NotI-F	AAAGCGGCCGCTTGCCAATACCCGTAAACTGG
BazPDZ3pEntry-R	TCACGATCGCAAGATCTTGCGG
BazPDZ3pGexNotI-F	AAAGCGGCCGCATGAAGCATGACGGTGACTTG
BazPDZ3pGexNotI-R	AAAGCGGCCGCTCAGTCCAGAATGTCACTGGAA
BazPDZ3-R	GTGACTGTTACTGTGGTCCAG
GFP-Seq-F	CACATGGTCCTGCTGGAG
GFP-Seq-R	GTTTACGTCGCCGTCC
GST-Seq-F	TGCGTTCCCAAAATTAGTTTG
GST-Seq-R	GACGGGCTTGTCTGCTCCCG
M13-F	CGTTGTAAAACGACGGCCAG
M13-R	CAGGAAACAGCTATGAC
PAR-3-PDZ1-3 NotI R	AAAGCGGCCGCTCATCCAGGGGGGCTCCC
PAR-3-PDZ1-3 NotI R	AAAGCGGCCGCTCATCCAGGGGGGCTCCC
PAR-3-PDZ2 NotI F	AAAGCGGCCGCTTGGTTATAACACCAAAAAAAT
PAR-3-PDZ2 NotI F	AAAGCGGCCGCTTGGTTATAACACCAAAAAAAT
PAR-3-PDZ2 T453 NotI F	AAAGCGGCCGCTTGGCAAGAGGCTTAATATCCA
PAR-3-PDZ2 T453 NotI F	AAAGCGGCCGCTTGGCAAGAGGCTTAATATCCA
UASp-attB-seq-F	GCGTTAGGTCCTGTTCATTG

4.1.5 Plasmids

Plasmids were obtained from GE Healthcare Life Sciences (Chalfont St Giles, UK), Thermo Scientific (Waltham, Massachusetts, USA), Murphy lab (Baltimore, USA) and New England Biolabs (Frankfurt am Main, Germany).

Table 7 Plasmids

plasmid	description	source
pENTR™	Gateway cloning	lifetechnologies™
pGEX6P1	Gateway cloning	Amersham
pPGW	expression vector for *Drosophila* cells, UASp promoter, N-terminal GFP tag, ampicilin resistance	Murphy lab
USGW	UGW with OneStrep-Tag fused to the N-terminus of GFP	modified from DGRC
PWMattB	Gateway cloning	modified from DGRC
UGWattB	Gateway cloning	modified from DGRC

4.1.6 Commercial kits

The commercial kits shown in table 8 were used according to manufacturer´s instructions.

Table 8 Commercial kits

kit	application	company
BM Chemiluminescence Western Blotting Substrate	western blotting	Roche
In situ Cell Death Detection Kit, TMR red	TUNEL-assay for apoptosis detection	Roche
LR Clonase II Enzyme Mix	clonase reaction	lifetechnologies™

Nucleo Bond® PC 100	midi-preparation	Magery-Nagel
Nucleo Bond® PC 20	midi-preparation	Magery-Nagel
Nucleo Spin®Gel and PCR Clean-Up	PCR purification	Magery-Nagel
pEntr/D-Topo Cloning Kit	Gateway Cloning	lifetechnologies™
WesternBright ECL HPR Substrate	western blotting	Advansta

4.1.7 Antibodies

The primary antibodies used for western blotting (WB) and immunofluorescence (IF) are shown in table 9 and the corresponding secondary antibodies are listed in table 10.

Table 9 Primary antibodies

target	species	dilution for IF	dilution for WB	product/clone number	company/source
Actin	Mouse		1:1000	sc-47778	Santa Cruz
aPKC (PKCζ)	Rabbit	1:500	1:500	sc-216	Santa Cruz
Baz N-term	Rabbit	1:2000	1:2000		Wodarz et al., 1999
Baz PDZ1-3	Guinea pig	1:400	1:400		Shahab et al., 2015
Baz pS151	Rabbit		1:100		Krahn et al., 2009
Crb	Mouse	1:10		Cq4	DSHB, Tepass et al., 1990)
DE-Cadherin	Rat	1:20		DCAD2	DSHB, Oda et al., 1994
Dlg	Mouse	1:50		4F3	DSHB, Parnas et al., 2001
GFP	Chicken	1:1000	1:1000	GFP-1020	Aves Lab

GFP	Mouse		1:500	11814460001	Roche
GFP	Mouse	1:500	1:500	sc-9996	Santa Cruz
GFP	Mouse	1:500		A11120	Molecular Probes
Mir	Rat	1:1000			homemade
PAR-3	Rabbit		1:500	07-330	Millipore
PAR-6	Rat	1:500			homemade
PAR-6	Guinea pig	1:500			Kim et al., 2009
PAR-6	Rabbit	1:500			homemade
Sdt	Mouse	1:10			Bulgakova et al., 2010
SXL	Mouse	1:20		M114	DSHB, Bopp et al., 1991
α-tubulin	Mouse		1:1000	12G10	DSHB

Table 10 Secondary antibodies

antibody	**dilution**	**product number**	**company/origin**
Alexa Fluor 488- anti Guinea Pig	1:400	A-11073	Life Technologies
Alexa Fluor 488- anti Rat	1:400	A-11006	Life Technologies
Alexa Fluor 488- anti Rabbit	1:400	A-11034	Life Technologies
Alexa Fluor 488- anti Mouse	1:400	A-11001	Life Technologies
Alexa Fluor 488- anti Chicken	1:400	A-11039	Life Technologies
Alexa Fluor 568-anti Guinea Pig	1:400	A-11075	Life Technologies
Alexa Fluor 568-anti Rat	1:400	A-11077	Life Technologies
Alexa Fluor 568-anti Chicken	1:400	A-11041	Life Technologies
Alexa Fluor 647-anti Guinea Pig	1:400	A-21450	Life Technologies
Alexa Fluor 647-anti Rat	1:400	A-21247	Life Technologies
Alexa Fluor 647-anti Rabbit	1:400	A-21244	Life Technologies

Alexa Fluor 647-anti Mouse	1:400	A-21235	Life Technologies
Alexa Fluor 647-anti Chicken	1:400	A-21449	Life Technologies
HRP-anti Guinea Pig	1:10000	5220-0366	Medac Diagnostics
HRP-anti Rat	1:10000	5220-0284	Medac Diagnostics
HRP-anti Rabbit	1:10000	VWRKDPV R55HRP	Medac Diagnostics
HRP-anti Mouse	1:10000	VWRKDPV M55HRP	Medac Diagnostics
HRP-anti Chicken	1:10000	5220-0373	Medac Diagnostics

4.1.8 Enzymes

The restriction enzymes are shown in table 11. In table 12 all specific enzymes like polymerases or kinases are listed.

Table 11 Restriction enzymes

enzyme	interface	buffer	company
BamHI	G↓GATCC	BamHI buffer	Fermentas/Thermo Scientific
BglI	GCCNNNN↓NGGC	orange	Fermentas/Thermo Scientific
BglII	A↓GATCT	orange	Fermentas/Thermo Scientific
Bpu1102I(BlpI)	GC↓TNAGC	yellow	Fermentas/Thermo Scientific
BseRI	GAGGAG$(N)_{10}$↓	CutSmart® Buffer	New England BioLabs
Bsp119I(BstBI)	TT↓CGAA	yellow	Fermentas/Thermo Scientific
$Bts^{\alpha}I$	GCAGTGNN↓	CutSmart® Buffer	New England BioLabs
DpnI	Gm6A↓TC	yellow	Fermentas/Thermo Scientific

Eco130I(StyI)	C↓CWWGG	orange	Fermentas/Thermo Scientific
Eco147I(StuI)	AGG↓CCT	blue	Fermentas/Thermo Scientific
Eco321(EcoRV)	GAT↓ATC	red	Fermentas/Thermo Scientific
EcoRI	G↓AATTC	EcoRI buffer	Fermentas/Thermo Scientific
HindIII	A↓AGCTT	red	Fermentas/Thermo Scientific
KpnI	GGATC↓C	NEBuffer 1.1	New England BioLabs
MlsI	TGG↓CCA	red	Fermentas/Thermo Scientific
NotI	GC↓GGCCGC	orange	Fermentas/Thermo Scientific
PstI	CTGCA↓G	orange	Fermentas/Thermo Scientific
PsyI(Tth111I)	GACN↓NNGTC	blue	Fermentas/Thermo Scientific
PvuII	CAG↓CTG	green	Fermentas/Thermo Scientific
SacII	CCGC↓GG	blue	Fermentas/Thermo Scientific
SpeI	A↓CTAGT	yellow	Fermentas/Thermo Scientific
XhoI	C↓TCGAG	red	Fermentas/Thermo Scientific

Table 12 Specific enzymes

enzyme	**company**
ACCUZYME™ DNA Polymerase	Bioline
cAMP-dependent Protein Kinase (PKA), catalytic subunit	New England BioLabs

FastAP Thermosensitive Alkanine Phosphatase	Thermo Scientific
GST-PKCζ	Sigma-Aldrich
T4 DNA Ligase	Fermentas/Thermo Scientific
Taq Polymerase	homemade

4.1.9 Marker

Markers were used for quantification analysis in agarosegel electrophoresis as well as SDS-PAGE.

Table 13 Marker

Marker	**Company**
Blue Prestained Protein Standard Broad Range (11-190 kD)	New England Biolabs
GeneRuler^{TM} 1 kb DNA Ladder	Thermo Scientific
PageRuler^{TM} Prestained Protein Ladder	Thermo Scientific

4.1.10 Fly lines

Fly lines were bought from different sources listed in table 14 or generated using the PhiC31-Integrase system (*Ubi::GFP-Baz* variants, *UASp::aPKC^{CAAX}*, *UASp::Crb*, *UASp::Sdt-myc*; attP25C=attP40, attP86F=ZH-86Fb and attP65B=VK00033) (Chapter 4.2.4.2). Germ line clones were generated according to the dominant female sterile technique (Chou et al., 1993) (Chapter 4.2.4.3). For generating embryos which express GFP-Baz variants with maternally and zygotically mutant *baz$^{815-8}$* background, virgins of *baz$^{815-8}$* FRT19A / FRT19A, hs::Flp, OvoD1; Ubi::GFP-Baz-variants rescue crosses were mated with hemizygous mutant males expressing Baz_{wt} or Baz_{5xA} (*baz$^{815-8}$*/Y; Ubi::GFP-$Baz_{wt/5xA}$) or wild type males expressing Baz_{7xA}.

Table 14 Fly lines

fly line	description	chromosome	source
apkc^{k06403}FRT42B	*apkc* null allele	2	Wodarz et al., 2000
baz$^{815-8}$ FRT19A	*baz* null allele	1	Krahn et al., 2010b; McKim et al., 1996
sdt^{K85}	Stop codon in *Sdt L27N*	1	Berger et al., 2007
dag::GAL4	ubiquitous expression in daughterless gene pattern, GAL4 driver line	3	Bloomington stock collection
hs::Flp, OvoD1	germ line clonal analysis	1	Bloomington stock collection
mat67::GAL4	ubiquitous maternally expression, GAL4 driver line	3	Bloomington stock collection
par-6 $^{\Delta 226}$ FRT19A	*par-6* null allele	1	Krahn lab stock collection
UAS::PAR-1-shRNA	expression of dsRNA for RNAi of par-1 under the control of UAS	3	TRiP GL00253 and TRiP HMS00405

4.1.11 Cell lines

S2R *Drosophila* Schneider Cells were cultivated at 25°C.

Table 15 Cell lines

cell line	description	source
S2R *Drosophila* Schneider cells	late embryonic stage	DGRC

4.1.12 Bacterial strains

Bacterial strains were cultivated on agar plates at 37°C and selected via specific resistances.

Table 16 Bacterial strains

bacterial strain	genotype	application	source
DH5α	*φ80dlacZΔM15, Δ(lacZYAargF)U169, deoR, recA1, endA1,hsdR17(rK-,mK+), phoA, supE44, λ-, thi-1, gyrA96, relA1*	amplification of plasmid DNA	Invitrogen
BL21 Star™(DE3)	F– *omp*T *hsd*SB(rB–, mB–) *gal dcm rne*131	expression of recombinant protein	invitrogen

4.1.13 Disposables

All used disposables listed in table 17 were disposed according to their usage via autoclaving or waste separation.

Table 17 Disposables

disposables	manufacturer
96 Biosphere® Filter Tips, 0.1 – 10 µl	Sarstedt
96 Biosphere® Filter Tips, 2 – 20 µl	Sarstedt
Autoclave tape, 50 m	Brand
Cell Scraper 25 cm	Sarstedt
centrifuge tube, 15 ml	Sarstedt
centrifuge tube, 50 ml	Sarstedt
Cuvettes, 10 x 4 x 45 mm	Sarstedt
Delicate Task Wipes – White	Kimberly-Clark
Folded Filters (Qual.), Ø 240 mm	Sartorius stedim
Micro tube, 1.5 ml	Sarstedt

Microscope Cover Glasses, 24 x 50 mm	Marienfeld
Microscope Cover Glasses, Ø 22 mm	Thermo Scientific
Microscope Slides, 25 x 75 x 1.0 mm	Thermo Scientific
Multiply® -Pro cup, 0.2 ml	Sarstedt
Nitril Extra-Sensitiv 24 cm	NitriSense
Parafilm "M"	Bemis
Pipette tip, 1000 µl	Sarstedt
Pipette tip, 20 µl	Sarstedt
Pipette tip, 200 µl	Sarstedt
SafeSeal micro tube, 2 ml	Sarstedt
Serological pipette, 10 ml	Sarstedt
Serological pipette, 2 ml	Sarstedt
Serological pipette, 5 ml	Sarstedt
Super RX Fujifilm	Fujifilm
TC-Dish 150, Standard	Sarstedt
TC-Flask T25, Stand., Vent. Cap	Sarstedt
TC-Flask T75, Stand., Vent. Cap	Sarstedt
TC-Plate 12 Well, Standard, F	Sarstedt
TC-Plate 24 Well, Standard, F	Sarstedt
TC-Plate 6 Well, Standard, F	Sarstedt
Transfer pipette, 3.5 ml	Sarstedt
Transfermembran, vliesvestärkte NC	Hartenstein
WHATMAN Paper 460 x 570	VWR

4.1.14 Devices

Table 18 Devices

device	application	company
5050 ELV	autoclave	Tuttnauer
AxioCam MRc camera	transmitted light microscopy	Zeiss
Axiovert 200	microscope	Zeiss

BL 1500 S	chemical balance	Sartorius
Bunsenbrenner LABOGAZ 470	flame treatment	Roth
Centrifuge 5810R	centrifuge	Eppendorf
ChemiDoc™ MP	transilluminator	Biorad
CT 15 RE	table centrifuge	Hitachi
Duomex 1030	platform shaker	Heidolph
Eco-Mini System E	SDS-PAGE	Analytik Jena
Evolution™ 201/220 UV-Vis-Spektrophotometer	spectrophotometer	Thermo Scientific
Femtotips® II microinjection capillary	Injection for germline transformation	Eppendorf
Fusion FX7	western blot developing	Peqlab
Heraeus T 6200	drying chamber	Thermo Scientific
Heraeus UT 6120	drying chamber	Thermo Scientific
Light table	Agarose gel analysis	Danubia
LSM 710 Meta confocal microscope	confocal microscopy	Zeiss
Mastercycler nexus gradient	thermocycler	Eppendorf
Micromanipulator InjectMan NI2	Injection for germline transformation	Eppendorf
Nanodrop1000	spectrometer (AG Meister)	Thermo Scientific
Nanodrop2000	spectrometer	Thermo Scientific
Pellet Mixers and Cordless Motor	homogenizing *Drosophila* embryos	VWR
Pipetboy	electric pipetting aid	Integra
Pipettes	pipetting	Eppendorf
Rotiphorese® PROclamp MINI Tank-Blotting-System	Western Blot	Roth
Rotiphorese® Unit PROclamp MINI complete set	SDS-PAGE	Roth
Sonopuls HD 2070/2200	protein purification	Bandelin

Stereo zoom microscop	binocular	Motic
Thermomixer comfort	heating block	Eppendorf
Unitron	incubator shaker	Infors HT
UV slider	transilluminator	Intas
Vortex Genie 2	vortex mixer	Intas

4.1.15 Data bases and software

Data bases and software used as a support for this work are shown in table 19.

Table 19 Data bases and software

data bases/software	**application**
Adobe Photoshop	image editing program
DNA Dynamo	sequence analysis
Flybase	database for *Drosophila* genetics
GIMP	image editing program
IMAGEJ	image editing program
NCBI	databases for biomedical and genomic information
ZEN 2010 Software	microscope software

4.2 Methods

4.2.1 Molecular biology methods

4.2.1.1 Polymerase chain reaction (PCR)

The polymerase chain reaction (PCR) (Mullis et al., 1986) was used to amplify specific DNA fragments *in vitro*. The PCR method contains a series of many cycles where the double stranded DNA first becomes denaturated at 95°C. Afterwards two oligonucleotides can anneal to the previously originated single stranded DNA at 55 - 65°C. This procedure is called annealing step. In the following step, called elongation, a DNA polymerase together with a mix of the four dNTPs elongates the annealed oligonucleotides at the 3´ end until two double stranded DNA fragments are formed again. The duration of this elongation step depends on the length of the amplified fragment. Through repetition of these steps for 30 - 40 cycles the target DNA fragment can be produced in high amounts. Additionally the PCR method enables mutations or deletions of target gene fragments and also allows the gene of interest to become marked with an epitope like GFP. Furthermore the newly formed DNA fragments can also be controlled via PCR.

Standard PCR reactions were performed with 20 - 100 ng/µl of plasmid DNA together with 200 nM of forward and reverse primer in 25 µl or 50 µl total reaction volume according to the required amount of PCR product. Furthermore 250 µM of each dNTP together with 0.02 µl polymerase per µl of total volume in the corresponding reaction buffer were added. For most applications the homemade Taq polymerase was used whereas for site-directed mutagenesis the bought ACCUZYME^{TM} DNA Polymerase from Bioline was applied. Table 20 showes the standard thermocycler PCR program for the used “Master Cycler Nexus Gradient” from Eppendorf.

Table 20 Standard thermocycler PCR program

thermocycler program			
5 min	95°C	initial denaturation	
30 s	95°C	denaturation	x 30 cycles
30 s	55-65°C	annealing, according to primer pair	
1 – 2 min/kb	72°C	elongation, according to construct length	
15 min	72°C	final elongation	
∞	10°C	storage	

Afterwards the PCR products were purified from agarose gels using the "Nucleo Spin® Gel and PCR CleanUp" kit from Macherey-Nagel according to manufacturer's instructions and eluted in 26 µl distilled water.

4.2.1.1.1 Mutagenesis PCR

The site-directed mutagenesis was used to perform point mutations, replace amino acids and delete or insert single or multiple adjacent amino acids. For adding point mutations in ORFs cloned into pENTR or pGEX6P1 vectors, special oligonucleotides were designed, which contained the desired mutation and an additional silent mutation to identify the mutated vector via an extra restriction site. Mutagenesis PCR reactions were performed using 300 ng template DNA together with 125 ng of the designed primer. Furthermore 125 µM of each dNTP together with 0.02 µl ACCUZYME^{TM} DNA Polymerase per µl of total volume in the corresponding reaction buffer with 1 µl DMSO were added. Table 21 showes the mutagenesis thermocycler PCR program for the used "Master Cycler Nexus Gradient" from Eppendorf.

Table 21 Mutagenesis thermocycler PCR program

thermocycler program			
5 min	95°C	initial denaturation	
20 s	95°C	denaturation	x 25 cycles
1 min	55°C	annealing	
2 min/kb +2min safety	72°C	elongation	
40 min	72°C	final elongation	
∞	12°C	storage	

After performing the PCR the initial template DNA was removed via digesting 14 µl of the PCR product with 1.5 µl DpnI for at least 6 hours at 37°C. Afterwards the mixture was transformed into DH5α cells as described in 4.2.1.5.

4.2.1.2 Agarose gel electrophoresis

The agarose gel electrophoresis was used to analyze DNA fragments resulting from enzymatic digestion or PCR product purification according to their length from other fragments in an electric field (140 V for 20 - 30 minutes). The assembly of the agarose gels varied according to the expected size of the DNA or PCR samples, which were mixed with the respective amount of 6x loading dye solution. Usually 1 % (or 2 % for small fragments) agarose gels containing 0.5 µg/ml ethidium bromide in TAE buffer were prepared. For purification of PCR products the agarose gels were prepared without ethidiumbromide and stained after running in a methylene blue solution. To evaluate the correct size of the samples, 10 µl of GeneRuler 1 kb DNA Ladder from Thermo Scientific were applicated in parallel. To analyze and document the samples after running the agarose gel was transferred to an UV transilluminator from Intras or ChemiDoc™ MP from Biorad or a light table from Danubia for cutting out bands from a methylene blue stained gel.

4.2.1.3 Molecular cloning

The process of molecular cloning consists of a set of experimental methods that are applied to assemble recombinant DNA fragments. First of all the DNA fragment has to be mutated and/or amplified via PCR (4.2.1.1) and subsequently purified. Afterwards the destination vector and the PCR product were digested with the corresponding restriction enzymes, prior to ligation. In order to cleave 1 µg of the required vector DNA in the cloning process, 2 µl enzyme were added together with 4 µl corresponding buffer and incubated overnight at 37°C. Afterwards the cutted

vector DNA was purified by methylene-blue stained agarose gel. In case the vector was cutted with only one enzyme a dephosphorylation step had to be done in order to prevent religation. Therefore 1 µl of FastAP Thermosensitive Alkanine Phosphatase from Thermo Scientific were added to 26 µl of purifed vector DNA in the corresponding buffer and incubated at least 30 minutes at 37°C. Afterwards, the Fast AP was inactivated by incubating the mix at 75°C for 20 minutes.

In the last step of the cloning process the prepared insert and vector has to be ligated using the T4 ligase. For this purpose, three ligations, two ligations with different concentrations of the components to achieve good conditions for different constructs and one control ligation without insert to check if the vector is already religated again were prepared according to the setup protocol in table 22. The ligation setups were incubated overnight at room temperature and then transformed into DH5α cells as described in 4.2.1.5.

Table 22 Setup for ligation

	control	**ligation 1:1**	**ligation 1:4**
H_2O	17.3 µL	16.8 µL	15.3 µL
T4 ligase buffer	2 µL	2 µL	2 µL
Vector	0.5 µL	0.5 µL	0.5 µL
Insert	-	0.5 µL	2 µL
T4 ligase	0.2 µL	0.2 µL	0.2 µL

4.2.1.4 Subcloning via Entry/GatewayTM technology

The *Drosophila* Gateway™ technology has been developed to clone genes of interest into diverse destination vectors for usage in *Drosophila* cell culture or flies without time consuming and labor intensive procedures like in classical molecular cloning processes. To use this technology first of all the gene of interest has to be cloned into the pENTR™ vector. Via the LR recombination reaction the requested ORF, flanked by *attL1* and *attL2* recombination sites, is transferred into any of the destination vectors of the *Drosophila* Gateway™ Vector Collection (Murphy Lab), which are flanked by *attR1* and *attR2* recombination sites. This is catalyzed by the λ integrase

(Gateway® LR Clonase™), which recombines the *attL1* and *attL2* flanked ORF with the *attR1* and *attR2* flanked destination vector. Hereby the ORF is exchanged by the *ccdB* gene of the destination vector. Because of the differences between the recombination sites of the ENTRY clone and the destination vector, this process is direction-specific and the desired destination vector with the gene of interest is selectable via ampicillin resistance and a lack of toxicity of the *ccdB* gene product for standard laboratory strains of *E. coli* (Figure 6). For the recombination reaction, 50 - 100 ng of the pENTR™ clone, 150 ng of the destination vector and 0.4 µl of the Gateway® LR Clonase™ were mixed and incubated for approximately 2 hours at 25°C. Afterwards the mix was transformed into DH5α cells (4.2.1.5). After growing of the transformed *E. coli* clones the success of the recombination reaction was analyzed via Mini preparation (4.2.1.6.1) and analytical digest with appropriate restriction enzymes according to manufacturer's instructions (Thermo Scientific).

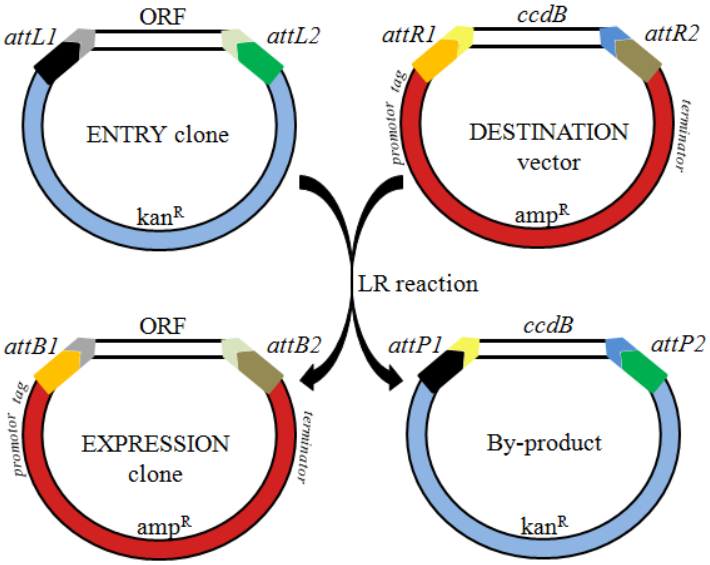

Figure 6 The Gateway™ LR in vitro recombination reaction

The recombination cassette, consisting of the ORF, flanked with the *attL1* and *attL2* recombination site of the ENTRY clone, is recognized by the λ integrase, which can recombine it with the *attR1* and *attR2* recombination site of the destination vector. This reaction creates the expression clone and a by-product, carrying the toxic *ccdB* gene (adapted from: https://emb.carnegiescience.edu/drosophila-gateway-vector-collection).

4.2.1.5 Transformation of chemical competent *E. coli* cells

Chemical competent *E.coli* strains, listed in table 16, were transformed with plasmid DNA in order to amplify the amount of DNA (with DH5α cells) or to express recombinant protein (with BL21 Star™ (DE3) cells). First of all 100 µl *E.coli* cell solution was thawed on ice, subsequently mixed with 100 - 1000 ng (3000 - 5000 ng for BL21 Star™ (DE3) cells) of plasmid DNA and incubated for 30 - 45 minutes on ice. Afterwards a heat-shock at 42°C for 1 minute was performed and immediately cooled on ice for 5 minutes. Thereon 200 µl LB medium were added to the sample and incubated shaking for one hour at 37°C. Finally the transformed cells were plated on prewarmed, antibiotic-selective LB agar plates under sterile conditions and incubated overnight at 37°C. Afterwards the grown colonies were picked and analyzed by Mini preparation (4.2.1.6.1).

4.2.1.6 Isolation of plasmid DNA via alkaline lysis

4.2.1.6.1 Mini Preparation

For the isolation and analysis of plasmid DNA from genetically modified *E.coli* transformants single colonies were inoculated in 2 ml LB medium and incubated for at least 6 hours or overnight at 37°C. Afterwards 1.5 µl of the cell suspension was pelleted by centrifugation for 1 minute at 6000 rpm. After discarding the supernatant the pellet was resuspended in 100 µl of buffer P1 which includes 100 µg/ml of RNase A. Thereafter 200 µl of buffer P2 were added and mixed very well, succeeded by 150 µl buffer P3 and inversion for 3 - 4 times. The samples were centrifuged for 6 minutes at 14000 rpm and 4°C. Subsequently the supernatant was transferred into new Eppendorf tubes, filled with 900 µl pure ethanol, mixed and centrifuged for 12 minutes at 15000 rpm in order to precipitate the DNA. The supernatant was discarded and the DNA pellet was washed with 1 ml of 70% ethanol by centrifuging for 5 minutes at 12000 rpm. Thereafter the supernatant was completely removed and

the pellet dried at 65°C in a drying cabinet for 12 minutes. Then the pellet was dissolved in 25 µl distilled H_2O. The dissolved DNA was tested via analytical digest with restriction enzymes according to manufacturer´s instructions (Thermo Fisher) and agarose gel electrophoresis (4.2.1.7).

4.2.1.6.2 Midi Preparation

To get larger amounts of clean plasmid DNA, successfully transformed *E.coli* colonies, analyzed by Mini preparation (4.2.1.6.1) and analytical digestion (4.2.1.7), were inoculated in 55 ml LB medium with according antibiotics. To purifiy the plasmid DNA a Midi preparation with the NucleoBond® PC 20 Kit from Macherey-Nagel was performed according to manufacturer´s instructions with the same principle as the Mini preparation (4.2.1.6.1), the alkaline lysis with SDS. For even larger amounts of plasmid DNA, the NucleoBond® PC 100 Kit from Macherey-Nagel was performed. For the standard NucleoBond® PC 20 Kit protocol 50 ml of the overnight grown cell suspension was centrifuged at 5000 rpm for 5 minutes, the pellet was then resuspended in 3 ml buffer S1 (provided with the kit or homemade), 3 ml lysis buffer S2 were added, mixed and incubated for 3 minutes at room temperature. Afterwards 3 ml of neutralization buffer S3 were added, inverted for several times and centrifuged for 8 minutes at 10000 rpm at 4°C. In the meantime the columns (provided with the kit) were prepared by adding 1 ml of N2 equilibration buffer. The supernatant of the prepared Midi preparation was filtered and loaded on the column. Afterwards the column was washed twice with the N3 wash buffer (provided with the kit). Subsequently the DNA could be eluted with 1 ml N5 elution buffer (provided with the kit), mixed with 0.75 ml isopropanol by inverting several times and centrifuged for 30 minutes at 15000 rpm at 4°C. The DNA pellet was washed with 70% ethanol followed by a centrifugation step for 5 minutes at 15000 rpm at 4°C. The supernatant was discarded and the pellet was fully dried at 65°C in a drying cabinet. Thereafter the pellet was dissolved in sterile distilled water, the concentration was measured at the NanoDrop1000/2000 from Thermo Scientific and adjusted to 1 µg/µl. For sequencing 1.2 µg plasmid DNA together with 30 pmol of sequencing primer were filled up to 15 µl with distilled water and sent to Seqlab/Microsynth (Göttingen, Germany).

4.2.1.7 Analysis of plasmid DNA via analytical digestion

To control and identify successfully transformed *E.coli* colonies after Mini preparation (4.2.1.6.1) the analytical digestion was performed. For this restriction enzymes from Fermentas/Thermo Scientific were used corresponding to manifacturer´s instructions. The restriction enzymes were chosen according to their ability to cut the plasmid DNA in specific pattern, which made it possible to distinguish between the correct plasmid DNA of interest and wrong constructs. The theoretically construction of the analytical digestion was achieved by the software DNADynamo.

4.2.2 Biochemical methods

4.2.2.1 Protein extraction from *Drosophila* embryos

To extract proteins from *Drosophila* embryos in order to perform an analysis of the containing proteins or their interactions in a co-immunoprecipitation, embryo lysates had to be made. First the chorion of the respective embryos was removed by incubation for 4 - 5 minutes in 5% sodium hypochloride. The embryos were washed and collected in 1.5 ml Eppendorf tubes as described in 4.2.5.1. Afterwards 100 - 300 µl of lysis buffer according to the amount of collected embryos were added in order to homogenize the embryos with a pellet mixer and cordless motor from VWR. The lysis buffer consists of TNT buffer with a final concentration of 10µg/ml of aprotinin and leupeptin, 40 µg/ml of PMSF and 1370 µg/ml of pepstatin A and additionally of 19.62 mg/ml of chantharidine and/or 1:100 dilution of phosphatase inhibitor cocktail from Sigma Aldrich if the phosphorylation status of the protein of interest had to be retained. Afterwards the homogenate was shaken on ice for 20 minutes and subsequently centrifuged for 10 minutes at 15000 rpm at 4°C. The supernatant was

transferred into a new Eppendorf tube and the protein concentration of the lysate was measured as described in 4.2.2.3.

4.2.2.2 Protein extraction from *Drosophila* Schneider cells

Similar to the extraction of proteins from *Drosophila* embryos described in 4.2.2.1 also proteins derived from transfected *Drosophila* S2R cells were analyzed in terms of their interactions in a co-immunoprecipitation. Therefore transfected S2R cells (4.2.3.1) were scraped from their cell culture flask or plate with a cell scaper, homogenized with a 5 ml glas pipette, transferred into a 15 ml centrifuge tube and centrifuged for 5 minutes at 12000 rpm at room temperature. The supernatant was discarded very precisely with a yellow tip to avoid residues of cell culture medium. After that the pellet was resuspended with a yellow tip in 400 µl of lysis buffer, containing TNT buffer with a final concentration of 10µg/ml of aprotinin and leupeptin, 40 µg/ml of PMSF and 1370 µg/ml of pepstatin A and additionally of 19.62 mg/ml of chantharidine and/or 1:100 dilution of phosphatase inhibitor cocktail from Sigma Aldrich if the phosphorylation status of the protein of interest had to be retained. Afterwards the homogenate was shaken on ice for 15 minutes, centrifuged for 10 minutes at 15000 rpm at 4°C and the supernatant transferred into a new Eppendorf tube. The protein concentration of the lysate was measured as described in 4.2.2.3.

4.2.2.3 Measurement of protein concentration

To estimate the total concentration of protein in a lysate (4.2.2.1 and 4.2.2.2) or eluate after protein purification (4.2.2.7) the Bradford method with the Roti-Quant reagent from Roth was used. Therefore Roti-Quant reagent was diluted 1:5 with distilled water. 1-10 µl of protein solution, depending on the expected concentration, were mixed with 1 ml of the diluted Roti-Quant reagent and transferred into a cuvette. The absorption was measured at 595 nm with the Evolution™ 201/220 UV-

Vis-Spektrophotometer from Thermo Scientific with an integration time of 2 seconds. For calibration a BSA standard curve was used.

4.2.2.4 Co-immunoprecipitation

To analyze protein-protein interactions, *Drosophila* embryo lysates as described in 4.2.2.1 or *Drosophila* S2R cell lysates as described in 4.2.2.2 were made first. A 10 µl aliquot for the input sample was taken from these lysates and boiled with 10 µl 2x SDS loading buffer for 5 minutes at 95°C. The remaining lysate was incubated for 1.5 hours with either 16 µl of blocked Strep-Tactin® Sepharose® beads or antibody tagged Protein G Plus Agarose beads. The used Strep-Tactin® Sepharose® beads were before blocked overnight at 4°C with 5% BSA in TNT buffer whereas the used Protein G Plus Agarose beads were incubated overnight at 4°C with 5% BSA in TNT buffer and the desired antibody in the corresponding dilution. Afterwards the samples were centrifuged for 2 minutes at 3500 rpm and washed twice with TNT buffer. The beads were centrifuged again, the supernatant removed, 16 µl of 2xSDS buffer added and boiled for 5 minutes. The analysis was achieved by SDS-PAGE (4.2.2.5).

4.2.2.5 SDS-PAGE

The denaturating discontinuous SDS polyacrylamid gel electrophoresis, short SDS-PAGE, is used to separate proteins according to their size in an electric field. The polyacrylamide gels, consisting of a stacking gel for concentration of the proteins before running on a starting point and a running gel for separation of the proteins according to their size, were made either with 7.5 % or 10 % running gel concentration. Table 23 shows the used composition of the gel.

Table 23 Polyacrylamid gel composition

component	stacking gel	running gel (7.5%)	running gel (10%)
Acrylamid	800 µl	5.2 ml	7 ml
1 M Tris-HCl	(pH 6.8) 600 µl	(pH 8.8) 8 ml	(pH 8.8) 7.9 ml
H_2O	3.6 ml	7.4 ml	5.6 ml
10% SDS	50 µl	200 µl	210 µl
10% APS	26 µl	106 µl	60 µl
TEMED	5 µl	10 µl	10 µl

The protein samples were boiled with 2x or 5x SDS loading buffer according to their concentration for 5 minutes at 95°C. After loading the prepared protein samples into the polyacrylamide gel pockets, 5 µl of the PageRuler™ Prestained Protein Ladder from Thermo Scientific or 10 µl of the Blue Prestained Protein Standard Broad Range (11-190 kD) from NEB were also loaded to compare the molecular weight size of the samples. During the first half of this work the Rotiphorese® Unit PROclamp MINI complete set from Roth was used whereas at a later time the Eco-Mini System E from Analytic Jena was bought. After running the SDS-PAGE the polyacrylamide gel was stained either with Coomassie Brilliant Blue (CBB) solution from Thermo Scientific according to manufacturer´s instructions to analyze the size and amount of protein in the sample or further used in western blot, described in 4.2.2.6, to detect protein interactions more precisely.

4.2.2.6 Western blot

To support the subsequent detection of the required proteins separated by SDS-PAGE (4.2.2.5), the polyacrylamide gel containing the separated proteins was applied to the western blotting chamber Rotiphorese® PROclamp MINI Tank-Blotting-System from Roth. For this a so called “blotting sandwich” according to manufacturer´s instructions with whatmanpaper and the nitrocellulose membrane, where the proteins should be blotted on, was prepared. The transfer of the proteins to the membrane lasted 75 minutes at 100 V at 4°C and was performed in blotting buffer. Afterwards the nitrocellulose membrane was incubated with blocking buffer for at least 30 minutes to prevent background signal. The blocked membrane could now be cutted to prevent wasting antibody for not used parts of the membrane and

subsequently incubated with primary antibody in blocking buffer diluted according to table 9. After an overnight incubation with the primary antibody the membrane was washed three times for 20 minutes with TBS-T buffer and incubated for 2 hours with the corresponding secondary antibody diluted in blocking buffer according to table 10. Afterwards the membrane was again washed three times for 20 minutes with TBS-T buffer before it was covered with BM Chemiluminescence Western Blotting Substrate from Roche or WesternBright ECL HPR Substrate from Advansta for 2 minutes according to manufacturer´s instructions. Subsequently the chemiluminescence analysis of the protein samples on the nitrocellulose membrane was performed in the Fusion FX7 Western Blot developer from Peqlab according to manufacturer´s instructions.

4.2.2.7 Protein purification

GST-tagged proteins were purified from bacterial cultures in order to analyze the required proteins later on in an *in vitro* kinase assay (4.2.2.8). For the expression of GST-tagged protein BL21 Star^{TM} (DE3) cells were first transformed with the desired plasmid DNA as described in 4.2.1.5.. A pre-culture from these successfully transfected BL21 Star^{TM} (DE3) cells in LB medium was inoculated overnight at 37°C and 200 - 250 rpm with the corresponding antibiotics. Afterwards 2 - 5 ml of the grown pre-culture were transferred to 100 - 150 ml of YTA medium and incubated at 37°C and 200 - 250 rpm until they reached mid-log phase at an OD_{600} of 0.6 - 0.7. To induce expression of the recombinant protein 0.5 mM Isopropyl-β-D-thiogalactopyranosid (IPTG), 3% KH_2PO_4 and 2% pure ethanol were added. Thereafter the culture was incubated overnight shaking at 18°C. After centrifuging the culture for 5 minutes at 5000 rpm the pellet was frozen for at least 30 minutes at -80°C. In the meantime a LEW lysis buffer was prepared containing LEW washing buffer (300 mM NaCl in PBS) with a final concentration of 10µg/ml of aprotinin and leupeptin, 40 µg/ml of PMSF and 1370 µg/ml of pepstatin A, 10 mM ß-mercaptoethanol and 1% triton X-100 to increase the permeability of the cell membrane as well as to keep the native conformation of the protein during the procedure. After resuspending the thawed pellet in 8 ml LEW lysis buffer the cell

suspension was shaken on ice for 30 minutes and afterwards sonicated for 3 cycles of 15 seconds + 30 seconds on ice with an amplitude of 98 %. In the next step lysozyme was added to a final concentration of 1 mg/ml, mixed and incubated for several minutes standing on ice. The sample was centrifuged for 15 minutes at 20000 rpm and 4°C. To select GST-tagged proteins from the suspension the supernatant was collected and incubated with 15 µl of Protino Glutathione Agarose 4B beads from Macherey-Nagel for 2 hours shaking at 4°C. After that the beads were washed once with LEW washing buffer (300 mM NaCl) with 1% triton X-100, once with LEW washing buffer with 2M NaCl and once with LEW washing buffer (300 mM NaCl) without additives. After the washing steps the beads were incubated with 150 µl GST elution buffer for 1 hour shaking at 4°C. Subsequently the protein concentration from the eluate was measured according to the Bradford method described in 4.2.2.3 and the eluted protein solution could be used for the *in vitro* kinase assay (4.2.2.8). The eluted proteins were analyzed for degradation on a Coomassie Brilliant Blue stained SDS-PAGE gel (4.2.2.5).

4.2.2.8 *In vitro* kinase assay

The kinase assay method allows analyzing kinase directed phosphorylation of target proteins *in vitro*. For this purpose 2 µg of purified protein as described in 4.2.2.7 were incubated with 100 ng of commercially bought kinase, for example GST-PKCζ from Sigma-Aldrich, together with a final concentration of 10µg/ml of aprotinin and leupeptin, 40 µg/ml of PMSF and 1370 µg/ml of pepstatin A, 19.62 mg/ml phosphatase inhibitor chantharidine and 100 µM ATP in kinase buffer (50mM TRIS pH 7.5, 10mM $MgCl_2$, 1mM DTT). Finally 0.3µCi[$_{\gamma\text{-}32}$ATP] were added in the radioactive lab, mixed and incubated for 1 hour at 30°C. Afterwards the kinase reaction was terminated by adding 2x SDS loading buffer and boiling for 5 minutes at 95°C. A SDS-PAGE as described in 4.2.2.5 was performed and the expected phosphorylation of the proteins was detected in the darkroom of the photo lab with Super RX Fujifilm films at different time points.

Another kinase assay variant performed with ATPγS was used in the last months of this work. For this purpose 0.5 µl of 100mM ATPγS instead of 0.3µCi[$_{\gamma\text{-}32}$ATP] were added to the mixture described above. The samples were incubated 1 hour at 25°C with mixing in between. Afterwards 1 µl PNBM was added, incubated at 22°C for 2 hours, boiled with 2x SDS loading buffer and a SDS-PAGE analysis with a following western blot was performed as described in 4.2.2.5 and 4.2.2.6. .

4.2.3 *Drosophila* cell culture

Drosophila S2R Schneider cells from the *Drosophila* Genomics Resource Center (DGRC) were cultivated in Schneider´s *Drosophila* medium from PAN biotech with 10 % FBS and 1% Penicillin-Streptomycin at 25°C. The S2R cells were passaged twice a week by firstly washing the semi-adherent cells with medium to get rid of old medium and particles. Subsequently the cells were scraped with a sterile cell scraper in 5 ml complete Schneider´s *Drosophila* medium and resuspended with a 5 ml serological pipette. This cell suspension was diluted 1:10 in fresh complete Schneider´s *Drosophila* medium in new T25 cell culture flasks and incubated at 25°C. For transfections T25 cell culture flasks with a dense layer of S2R cells were washed, the cells resuspended as described above and distributed in a 6 well plate (usually 0.6 – 2 x 10^6 cells in 2 ml). In case of immunostaining a sterile coverslip was placed in each well additionally.

4.2.3.1 Transfection with FuGene®HD Transfection Reagent

Transfection of *Drosophila* S2R cells was achieved with the FuGENE®HD Transfection Reagent from Promega according to manufacturer´s instructions. Therefore a transfection mix was prepared under sterile conditions mixing 95 µl prewarmed Schneider´s *Drosophila* medium without any additives with 2 µg of plasmid DNA (0.75 µg per construct if two constructs were used). After shortly

prewarming and mixing the FuGENE®HD Transfection Reagent, 2 µl of this reagent (1.5µl per construct if more than one construct was used) were added, immediately mixed for 5 seconds and incubated at room temperature for 15 minutes. Afterwards the transfection mix was distributed over the cells and incubated at 25°C for 2 - 5 days. In case of GFP-tagged recombinant proteins the transfection rate was screened by fluorescence microscopy.

4.2.4 Fly genetics

4.2.4.1 *Drosophila melanogaster* breeding conditions

Drosophila breeding flies were maintained in glas vials with sponge plug filled with standard food (0.8 % agar, 2.2 % sugar beet molasses, 8.0 % malt extract, 1.8 % brewer´s yeast, 1.0 % soy flour, 8.0 % maize meal, 0.3 % nipagin) with sprinkles of dry yeast on top at 18°C, 21°C, 25°C or 29°C depending on the experimental setup. These glas vials, already filled with standard food, were received from the Department of Developmental Biology at the University of Regensburg. The fly stock vials were exchanged in intervals of 3 to 5 weeks at 18°C. An artificial lighting was used to achieve a 12 hour day/night rhythm.

For the collection of *Drosophila* embryos in order to perform immunostainings or get embryonic lysates, flies were kept in special cages of two different sizes where the bottom consisted of an apple juice agar plate with yeast paste made from baker´s yeast and water. The flies laid their eggs on these plates, which were exchanged after special time points in order to get different embryonic stages.

4.2.4.2 The PhiC31 integrase system

Transgenic fly lines were generated using the PhiC31 integrase system. The PhiC31 integrase, a recombinase isolated from the bacteriophage PhiC31, mediates the site-specific integration of a transgene between two specific 34 bp attachment sites, called *attB* in the donor plasmid and *attP* in the target site, integrated into the genome of flies (Thorpe et al., 2000). This reaction is unidirectional, as the recombination event produces two different sites, the *attR* and the *attL* site, which cannot act as functional substrates for the PhiC31 integrase (Figure 7). For the generation of Ubi::GFP-Baz variants, UASp::aPKC^{CAAX}, UASp::Crb and UASp::Sdt-myc lines in this study the PhiC31-Integrase system was used.

Plasmid DNA from a Midi preparation (4.2.1.6.2), carrying the respective transgene, were introduced into the germline via microinjection into the pole cell region of preblastoderm embryos. For this purpose an injection mix was prepared, consisting of 200 ng plasmid DNA in 10x injection buffer (5 mM KCl, 0.1 mM sodium phosphate, pH 6.8) and sterile water to a final volume of 50 µl. This injection mix was centrifuged at least for 30 minutes at 15000 rpm and 16°C before usage. 30 minutes old *Drosophila* embryos of the fly line carrying the desired target site were dechorionised, arranged in a side directed row on a block of apple juice agar and transferred to a cover slip, which was coated with embryo glue. After a short drying step the embryos were covered with Oil 10 S VOLTALEF® and the injection mix was injected into the pole cell region of the embryos with an Femptotips®II microinjection capillary by a micromanipulator InjectMan NI2 from Eppendorf. After an incubation of the injected embryos at 18°C overnight and 21°C for 12 hours the hatched larvae were collected into *Drosophila* vials with mashed food. Developed adults were crossed to w-; Gla/CyO flies for the transgenic fly selection.

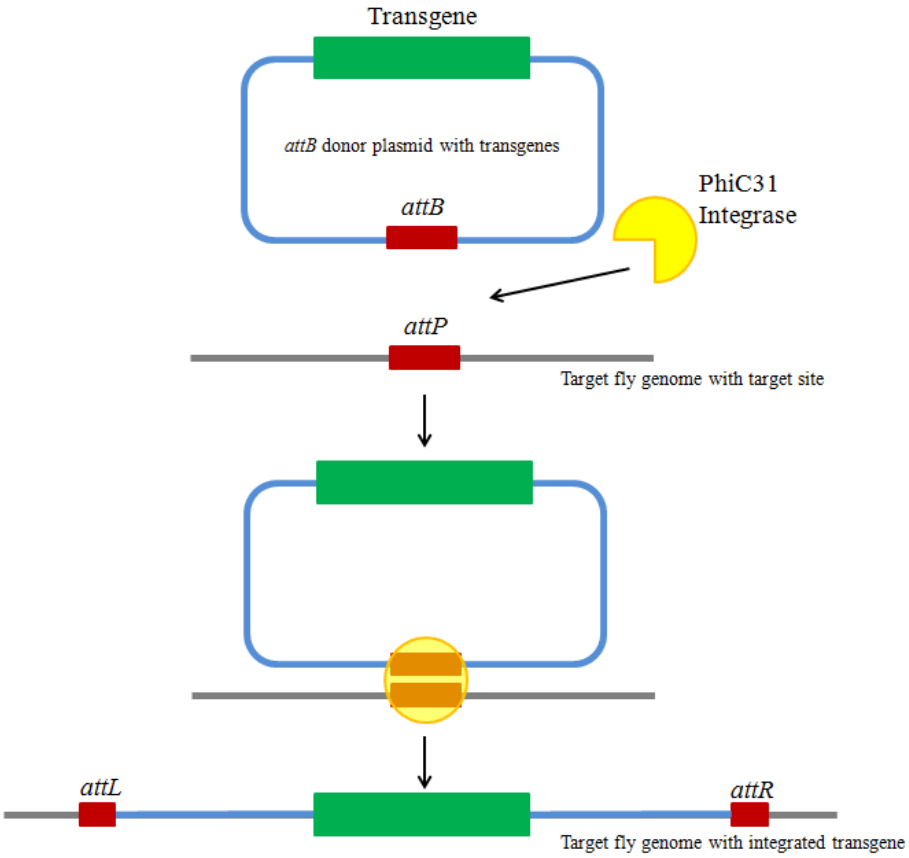

Figure 7 The PhiC31 integrase system

The PhiC31 Integrase system provides a method for unidirectional integration of transgenes into specific loci on the genome of flies between two attachment sites called *attB* in the donor plasmid and *attP* in the target site. The recombination results in an *attL* and an *attR* site, which cannot act as functional substrates for the PhiC31 integrase (adapted from: http://www.systembio.com/phic31).

4.2.4.3 The dominant female sterile technique

The dominant female sterile technique (Chou et al., 1993) was used to generate *Drosophila* germline clones. Germline dependent, dominant female sterile mutations in the *ovo* gene (ovo^D mutants) results in a blocked egg production because of the decay of female germ cells during early oogenesis. The ovo^D mutants can be applied to remove non recombinant cells in the FLP/FRT mediated recombination screens in order to get mutations that create phenotypes in germline clones, whereby FLP stands for flipase and FRT for FLP recombinase-target. Therefore these mutations have to be placed on the FRT selective chromosome arm. The FLP recombinase achieves recombination between the two FRT sites on homologous chromosomes.

The egg chambers, which lost the *ovo*^{D} are homozygous for the other FRT chromosome arm and will be viable, whereas the *ovo*^{D} transgene carrying germ cells, where no recombination occurred, will die (Figure 8). With this method genetic screens can be made for lethal mutation by creating maternal-effect phenotypes derived from homozygous mutant germline clones (St. Johnston, 2002).

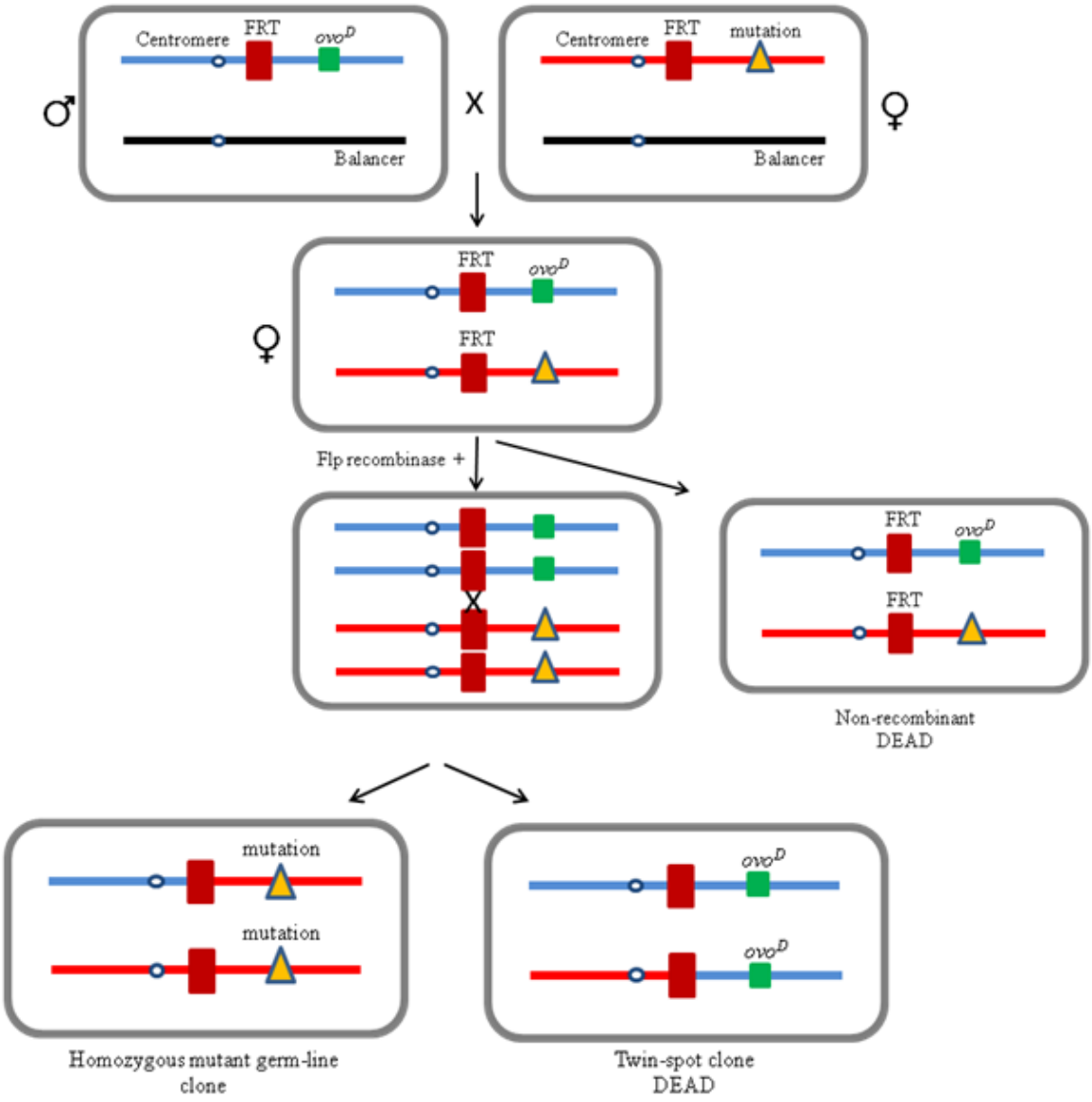

Figure 8 The dominant female sterile technique

The dominant female sterile *ovo*^{D} mutants show blocked egg production because of the decay of female germ cells during early oogenesis. The *ovo*^{D} mutants are used to remove non recombinant cells in the FLP/FRT mediated recombination screens thereby creating phenotypes in germline clones. Therefore these mutations have to be placed on the FRT chromosome arm against which a selection should be conducted. The FLP recombinase achieves recombination between the two FRT sites on homologous chromosomes. The egg chambers, which lost the *ovo*^{D} are homozygous for the other FRT

chromosome arm and will be viable, whereas the *ovo*^{D} transgene carrying germ cells, where no recombination occurred, will die (adapted from St. Johnston, 2002).

Moreover the the FLP/FRT mediated recombination is used in germline and somatic *Drosophila* cells to achieve mutant clones via mitotic recombination (Theodosiou and Xu, 1998). In this work the generation of embryos, which were maternally and zygotically mutant for *baz*$^{815\text{-}8}$ and expressed GFP-Baz variants, were achieved by crossing virgins of *baz*$^{815\text{-}8}$ FRT19A/FRT19A, hs::Flp, OvoD1; Ubi::GFP-Baz-variants with hemizygous mutant males expressing Baz_{wt} or Baz_{5xA} (*baz*$^{815\text{-}8}$/Y; Ubi::GFP-$Baz_{wt/5xA}$) or wild type males expressing Baz_{7xA}. In this connection the FLP recombinase was expressed under control of a heatshock promoter, which was induced by a heatshock of larvae at 37°C for 2 hours for two times with a gap of 24 hour in between.

4.2.4.4 The UAS-GAL4 system

The binary UAS-GAL4 system (Brand and Perrimon, 1993) was used for overexpression analysis in *Drosophila* embryos. GAL4 is a transcription factor derived from yeast, which is expressed in *Drosophila* under control of a tissue specific promoter that binds to UAS, an upstream activating sequence. Binding of GAL4 to UAS results in the expression of a target gene downstream of UAS. The activation of the UAS/GAL4 system is achieved by crossing transgenic GAL4 fly strains (diver lines) with a transgenic UAS fly strain (responder line). The offspring will show an expression of the gene of interest downstream of UAS in all cells, where GAL4 is expressed.

4.2.4.5 Lethality test

To analyze the lethality of a respective *Drosophila* fly line a lethality test was made at 25°C by firstly collecting 300 embryos of the same age and arrange them in rows on apple juice agar plates in a cage with yeast paste between the rows. Every day the embryos were analyzed in respect of their developmental stage, if they had died or if possible survivors have hatched to adults. The plates were watered every day to avoid drying out of the plates. All died stages and also all adult fly survivors were counted and analyzed.

4.2.5 Histology

4.2.5.1 Fixation and immunostaining of *Drosophila* embryos

The *Drosophila* flies were kept in special cages where the bottom consisted of an apple juice agar plate with yeast paste made from baker´s yeast and water. The flies layed their eggs on these plates, which were exchanged after special time points, for example after 3 hours to get very early embryonic stages or overnight to get very old embryonic stages. The embryos were first released from the plate carefully with water and a brush. Afterwards the plates were covered with 5 % sodium hypochloride for 4 - 5 minutes until the chorion of the embryos was dissolved. The embryos in the suspension were filtered through a mesh with a vacuum pump and washed thoroughly with water to clean and collect the embryos. Thereafter the dechorionized embryos were fixed in a scintillation tube with 2 ml of 4 % formaldehyde in PBS and 3 ml n-heptane for 20 minutes on a shaker. The lower phase was removed and 3 ml methanol LC/MS ultra from Roth were added. The suspension was mixed in order to dissolve the vitteline membrane and the embryos were washed three times with methanol LC/MS ultra, transferred into a 1.5 ml Eppendorf tube and stored at - 20°C for at least one hour.

Fixed embryos had to be washed first three times with PBT (0.1% Tween 20 in PBS) at room temperature on a shaker. Thereafter a blocking step was performed using 5 % BSA in PBT for at least 30 minutes at room temperature on the shaker. The embryos were then incubated overnight at 4°C with the first antibody diluted in PBT with 5 % BSA according to the desired dilution. After that the embryos were again washed three times with PBT for 20 minutes at room temperature on the shaker before getting incubated with the secondary antibody in PBT with 5 % BSA according to the desired dilution for 2 hours. The DAPI staining was performed with 1:1000 DAPI (5 µg/ml) in PBT for 20 minutes. After another two washing steps with PBT for 20 minutes at room temperature on the shaker the embryos were transferred on an object slide without liquid and embedded with 50 µl Mowiol and a cover slip.

4.2.5.2 Detection of apoptosis in *Drosophila* embryos

Apoptosis in *Drosophila* embryos was detected with the "In Situ Cell Death Detection Kit, TMR red" from Roche. The so called TUNEL (TdT-mediated dUTP-X nick end labelling) assay could be performed as apoptosis is indicated by DNA degradation, which creates single- and double- stranded DNA breaks, also called nicks. In the TUNEL assay both types of DNA breaks are recognized by labelling the free 3'-OH termini with modified nucleotides, the TMR-dUTP, in an enzymatic reaction. The terminal deoxynucleotidyl transferase (TdT) catalyzes the polymerization of the modified nucleotides to the 3'-end of single-and double-stranded DNA.

The TUNEL assay for apoptosis detection in *Drosophila* embryos was made at the end of the embryo immunostaining as described in 4.2.5.1. Directly after the staining with secondary antibody, liquid was removed and the embryos were incubated with a mix of 45 µl of Label Solution and 5 µl of Enzyme Solution (provided in the "In Situ Cell Death Detection Kit, TMR red" from Roche) for 1 hour at 37°C in the dark. Afterwards the embryos were washed three times with PBT for 20 minutes at room temperature on the shaker and stained with DAPI according to the protocol described in 4.2.5.1. The apoptotic cells of the embryos were detected by the incorporated red

fluorescent TMR-dUTP into the damaged DNA strands under the fluorescence microscope.

4.2.5.3 Confocal microscopy

Images were taken on the laser scanning confocal microscope Zeiss LSM 710 Meta confocal microscope with the 25xNA 0.8 or 63x NA 1.2 water objectives and ZEN 2010 software from ZEISS. For processing images afterwards Adobe Photoshop and IMAGE J (version1.43m, NIH, USA) were used.

4.2.5.4 Cuticle preparation of *Drosophila* embryos

To analyze the cuticle, relevant *Drosophila* embryos were firstly collected from apple juice agar plates by dechorionizing as described in 4.2.5.1. Afterwards the embryos were transferred on an objective slide with a tip and covered with approximately 50 µl of Hoyer´s medium with lactate and a cover slip. The samples ware incubated overnight at 65°C and analyzed under a transmitted light microscope with a EC Plan-Neofluor 2.5x/0.075 Pol M27 objective and an AxioCam MRc camera from Zeiss.

5 Results

5.1 Localization of aPKC is shifted in early development of *Drosophila* embryonic epithelia

The correct positioning of components of the PAR complex to the apical membrane is a prerequisite for the proper polarization of epithelial cells, thus several important and in part redundant mechanisms are involved. Accordingly, the positioning and stabilization of Baz at the apical junctions during late cellularization until early gastrulation requires the kinase aPKC, which is in turn recruited to the cell junctions by Baz at the same time (Wodarz et al., 2000; Rolls et al., 2003). However, it is still not completely understood, how aPKC acts in positioning Baz to the apical junctions.

Therefore, an analysis of wild type *Drosophila* embryonic epithelium, which was fixed and stained according to 4.2.5.1, showed, that in embryonic stage 6, which corresponds to the timeframe between late cellularization and early gastrulation, endogenous Baz and aPKC colocalize at the apical junctions of *Drosophila* embryonic epithelial cells (Figure 9a), whereas Crb is not expressed at this developmental stage. As the formation of the AJ is not completed, Baz and aPKC accumulate at the broad apico-lateral cell-cell contacts.

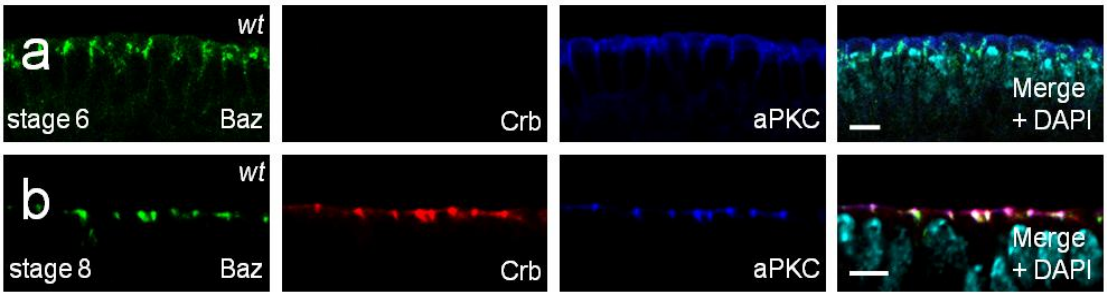

Figure 9 Localization of Baz and aPKC in early Drosophila embryonic development

Drosophila wildtype embryos stained with antibodies against Baz, Crb and aPKC. (a) stage 6 embryo displays a colocalization of Baz and aPKC, whereas Crb is not expressed yet. (b) stage 8 embryo shows Crb expression and its colocalization with aPKC at a more apical position than Baz staining. Device: Zeiss LSM 710 Meta confocal microscope; Scale bar = 5 µm.

In contrast, with the beginning of Crb expression during embryonic stage 8, when germ band elongation proceeds, a substantial portion of aPKC segregates from Baz and colocalizes with Crb (Harris and Peifer, 2005; Krahn et al., 2010a; Morais-de-Sá et al., 2010). The localization of the associated Baz and aPKC is restricted to the apical cell-cell junctions, whereas the Crb and aPKC staining showed a more apical localization than the Baz staining (Figure 9b). This observation showed that before the onset of Crb expression during epithelial development, recruitment of aPKC to the apical junctions seems to be dependent on Baz.

5.2 Baz PDZ domains and aPKC-binding region are involved in aPKC binding

Baz can interact with aPKC via two described regions, a fragment comprising the second to third PDZ domain and the conserved aPKC-binding motif, also known as conserved region 3 (CR3) (Figure 4) (Izumi et al., 1998; Lin et al., 2000; Wodarz et al., 2000; Nagai-Tamai et al., 2002; Rolls et al., 2003; Horikoshi et al., 2009; Morais-de-Sá et al., 2010).

To examine which of these two regions of Baz is crucial for aPKC-binding, a co-immunoprecipitation of endogenous aPKC with transfected One-Strep-GFP-Baz variants, which were detected by GFP, in *Drosophila* S2R cells was performed (Figure 10). The *Drosophila* S2R cells were transfected using the FuGENE®HD Transfection Reagent according to the protocol described in 4.2.3.1. The protein extraction from S2R cells as well as the co-immunoprecipitation was performed according to the protocols described in 4.2.2.2 and 4.2.2.4, respectively.

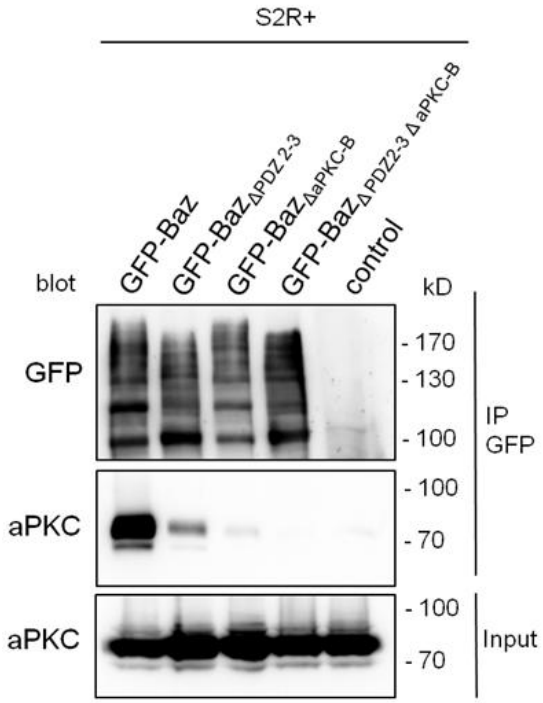

Figure 10 Co-Immunoprecipitation of endogenous aPKC with transfected Baz variants in S2R cells

Western blot detection identified bound proteins of the immunoprecipitation of transfected OneStrep-GFP-Baz variants, which were detected by the GFP-tag and co-immunoprecipitated endogenous aPKC (ca. 70kD). Transfection was performed with the FuGENE®HD Transfection Reagent according to 4.2.3.1. As a control untransfected S2R cell lysates were used.

The analysis of the resulting western blot showed that indeed, both regions are involved in binding of aPKC. In detail, deletion of the PDZ domain two to three of the GFP-tagged Baz, named as GFP-Baz$_{\Delta PDZ2-3}$ in figure 10, strongly reduced the amount of co-immunoprecipitated aPKC in contrast to wild-type Baz. Moreover a deletion of the aPKC-binding motif, annotated as GFP-Baz$_{\Delta aPKC-B}$, almost abolished aPKC binding as seen in a very slight aPKC band detected in the western blot in figure 10. Finally, a deletion of both regions in Baz showed a completely inhibition of a detectable interaction with aPKC, meaning that GFP-Baz $_{\Delta PDZ2-3,\Delta aPKC-B}$ is not anymore able to bind endogenous aPKC.

A remarkable finding in the western blot analysis showed, that in the positive control, the GFP-tagged wild type Baz exhibited a much more intensely binding of aPKC than the accumulated binding of the deletion constructs. This may indicate that both interaction domains function synergistically in binding to aPKC.

5.3 Baz/PAR-3_{PDZ2-3} domain is phosphorylated by aPKC at multiple residues

The correct stabilization of Baz/PAR-3 at the apical cell-cell contacts is accomplished by an activation of Baz/PAR-3 via the kinase aPKC. More in detail, aPKC is able to phosphorylate Baz at certain residues corresponding to the conserved aPKC consensus phosphorylation site motif (Chapter 3.5) within the two described binding regions of aPKC discussed above (Chapter 5.2) (Izumi et al., 1998; Lin et al., 2000; Wodarz et al., 2000; Nagai-Tamai et al., 2002; Rolls et al., 2003; Horikoshi et al., 2009; Morais-de-Sá et al., 2010). For the mammalian homologue PAR-3, an interaction with aPKC has been described within the conserved aPKC-binding motif at the serine at position 827 (Izumi et al., 1998; Lin et al., 2000; Nagai-Tamai et al., 2002; Horikoshi et al., 2009; Morais-de-Sá et al., 2010).

To analyze these specific residues of Baz/PAR-3 for phosphorylation of aPKC, a general screen of possible phosphorylation sites according to the aPKC phosphorylation site motif (Chapter 3.5) was performed. Before the start of this work, Sabrina Wohlhaupter started with the screen of aPKC phosphorylation sites for the *Drosophila* Baz, which led finally to an identification of five serines/threonines as targets of aPKC kinase activity: the threonine at position 522 (T522), the serine 638 (S638) and 700 (S700), the threonine 712 (T712) and the serine 741 (S741). Sophia Weiß performed during her Bachelorthesis in the time of this work the corresponding screen for PAR-3 and identified nine possible phosphorylation sites of aPKC in the PAR-3_{PDZ2-3} region: T453, T468, T476, T481, S533, S604, T661, S667 and S685. The alignment in figure 11 between Baz and PAR-3 shows the phosphorylation sites within the PDZ domains of both proteins as well as the homologue regions. It was achieved using the Needleman-Wunsch algorithm, which creates an optimal end-to-end alignment including gaps between the two protein sequences (Chakraborty and Bandyopadhyay, 2013).

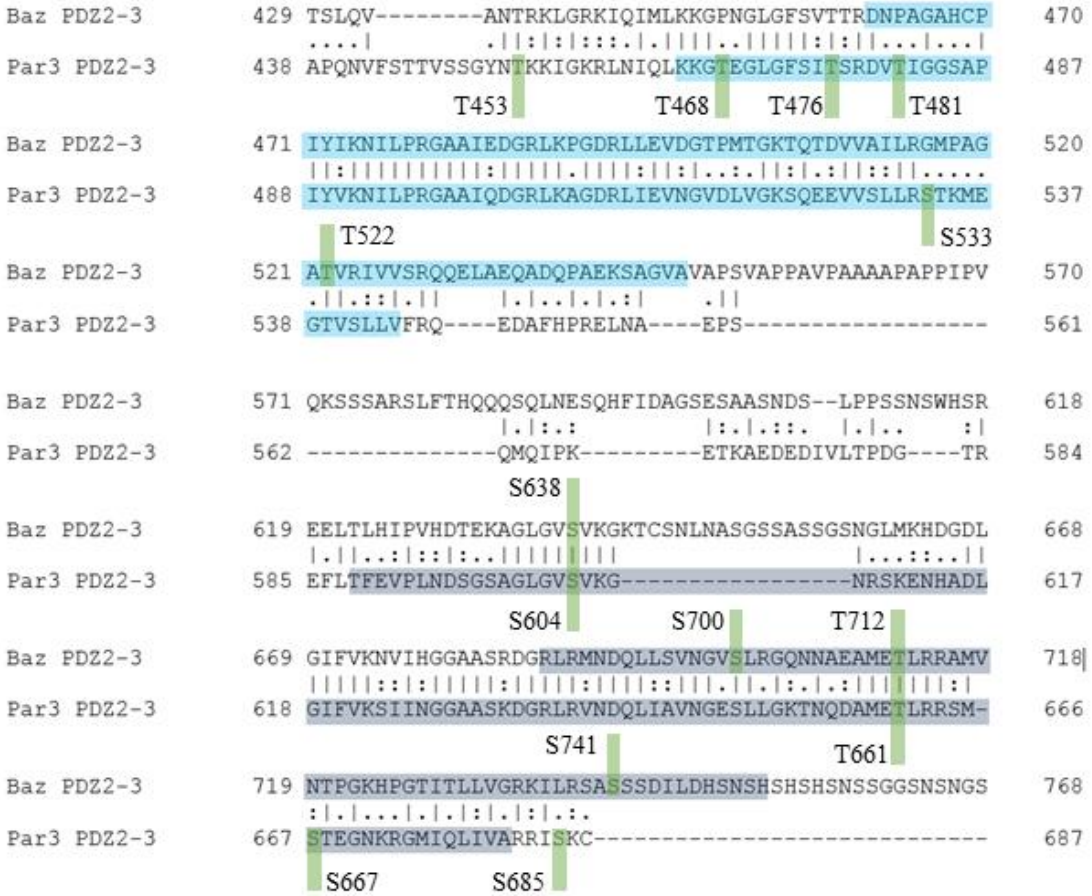

Figure 11 Alignment between Baz and PAR-3 PDZ 2-3 domains

Alignment between Baz (upper line) and PAR-3 (lower line) PDZ2-3 domains and the identified phosphorylation targets of aPKC (green) for both proteins. The PDZ 2 domain is shown in blue, the PDZ 3 domain is shown in grey. (Figure from Bachelorthesis Sophia Weiß)

To identify these serines/threonines as functional targets of aPKC kinase activity, all residues were replaced by an alanine in a GST-fused Baz/PAR-3 protein. The exchange of the serine/threonine by an alanine was achieved using mutagenesis PCR as described in 4.2.1.1.1, transformation into BL21 Star^{TM} (DE3) cells, according to 4.2.1.5, and protein purification performed as described in 4.2.2.7. Afterwards the possible phosphorylatable residues of the received GST-tagged Baz/PAR-3 variants were analyzed in a kinase assay with aPKC (4.2.2.8).

Initially, the replacement of all five residues by alanine in GST-Baz$_{PDZ1-3}$, annotated as GST-Baz$_{PDZ1-3,\ T522A,\ S628A,\ S700A,\ T712A,\ S741A}$ = Baz $_{PDZ1-3\ 5xA}$, showed no

phosphorylation of the recombinant protein by aPKC anymore, meaning that these five serines/threonines are the phosphorylation targets of aPKC in the three PDZ domains of Bazooka (Figure 12a). In contrast, the positive control GST-Baz_{PDZ1-3} with all five residues according to wild type situation exhibited a clear phosphorylation of aPKC (Figure 12a).

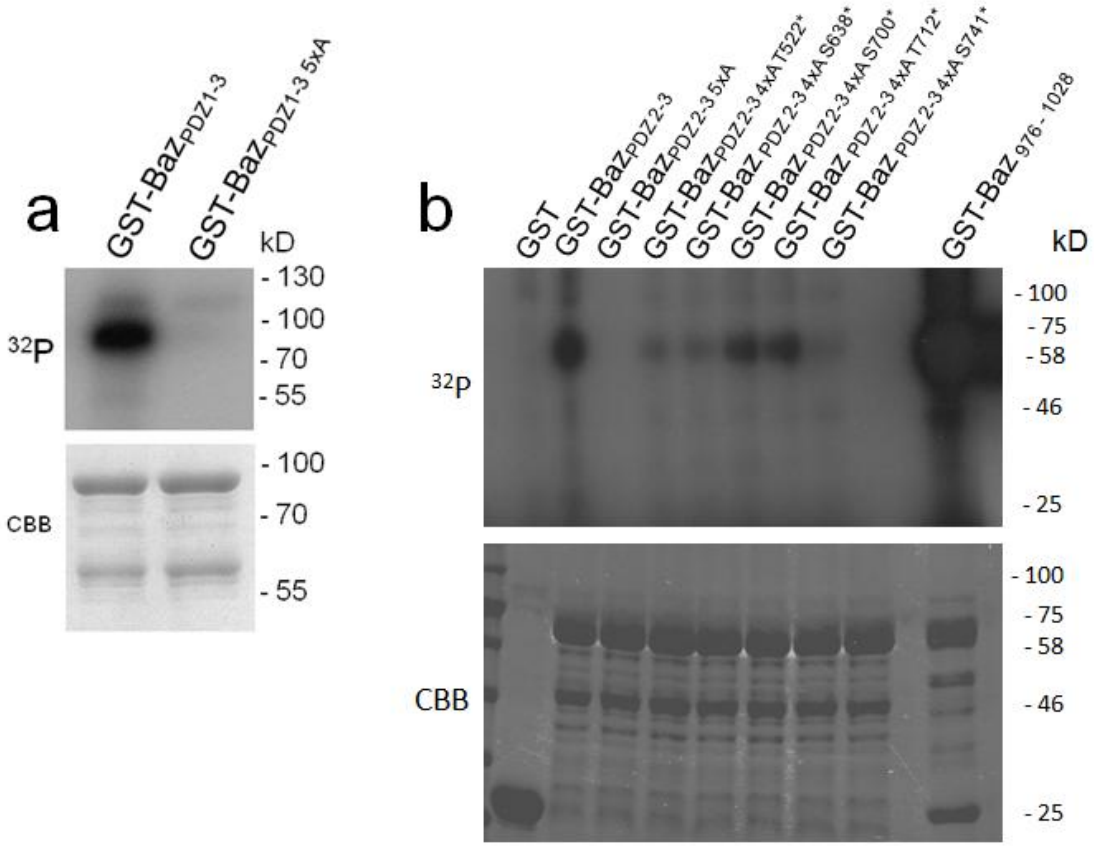

Figure 12 Phosphorylation targets of aPKC in $Baz_{PDZ\ 2-3}$

Kinase Assay of (a) GST-tagged Baz_{PDZ1-3} (ca. 75kD) and (b) GST-tagged Baz_{PDZ2-3} (ca. 60kD) variants to analyze aPKC kinase directed phosphorylation *in vitro*, according to 4.2.2.8 (GST = ca. 25 kD; aPKC autophosphorylation = ca. 130 kD). GST-PKCζ from Sigma-Aldrich was used together with radioactive labeled $_{\gamma\text{-}32}$ATP. CBB indicates coomassie brilliant blue staining for the inputs.

To get a closer look we next performed a phosphorylation analysis using GST-Baz_{PDZ2-3}, as the five residues are only in the region between Baz PDZ domain two and three. Replacing all five serines/threonines by an alanine, shown in figure 12b as $Baz_{PDZ\ 2-3,\ T522A,\ S628A,\ S700A,\ T712A,\ S741A}$ = $Baz_{\ PDZ2-3\ 5xA,}$ confirmed the abolished phosphorylation of aPKC as already seen in the initial experiment of figure 12a.

Furthermore, by replacing just four serines/threonines by an alanine and thereby leaving one residue intact, we were able to verify these findings, as in these recombinant proteins the residue marked with an asterix was able to be phosphorylated by aPKC and showed in the kinase assay a corresponding phosphorylation band, although weaker detectable than Baz_{PDZ2-3} (Figure 12b). The GST-Baz_{PDZ2-3} variants were here annotated as GST-$Baz_{PDZ\ 2-3\ 4xA\ T522*}$, GST-$Baz_{PDZ2-3\ 4xA\ S628*}$, GST-$Baz_{PDZ2-3\ 4xA\ S700*}$, GST-$Baz_{PDZ2-3\ 4xA\ T712*}$ and GST-$Baz_{PDZ2-3\ 4xA\ S741}$*, respectively (Figure 12b). Moreover a C-terminal control fragment on Baz, GST-$Baz_{916-1028}$, which includes the aPKC-binding region with the serine 980, showed a very strong phosphorylation in comparison to non mutated GST-Baz_{PDZ2-3} as well as the variants with one serine/threonine left. To the end of this work massspectrometry analysis were performed in order to identify the phosphorylation sites of Baz_{PDZ2-3} precisely, but were still under progress.

For the mammalian homologue PAR-3, corresponding experiments were performed to clearly identify all targets for aPKC phosphorylation in the PDZ domain region of this protein. In the initial experiment, all nine possible phosphorylation residues for aPKC were replaced by an alanine, resulting in a GST-tagged PAR-$3_{PDZ2-3,\ T453A,\ T468A,\ T476A,\ T481A,\ S533A,\ S604A,\ T661A,\ S667A,\ S685A}$ = GST-PAR-$3_{PDZ2-3\ 9xA}$, whereby more precisely the included threonine 453 is positioned directly before the start of the PDZ2 domain. In a kinase assay experiment with ATPγS and GST-PKCζ from Sigma-Aldrich according to 4.2.2.8, the GST-PAR-$3_{PDZ2-3\ 9xA}$ variant, where all phosphorylation targets of aPKC were mutated, showed no phosphorylation signal anymore in comparison to the wild type GST-PAR-3_{PDZ2-3}, meaning that aPKC was not able to phosphorylate this mutated protein anymore (Figure 13).

According to the experiments done with *Drosophila* Baz, we also had a particularized look on each single phosphorylation residue of PAR-3 for aPKC. However, the GST-tagged PAR-3_{PDZ2-3} constructs, where eight residues were replaced by an alanine and consequently one serine or threonine was left intact, showed, that the last two serines, the serine at position 667 and 685, were not phosphorylated by GST-aPKCζ in GST-PAR-$3_{PDZ2-3\ 8xA\ S667*}$ and GST-PAR-$3_{PDZ2-3\ 8xA\ S685*}$, respectively (Figure 13). As a consequence, the serine at position 667 and 685, which were initially identified according to the aPKC phosphorylation site motif, are no targets for aPKC phosphorylation of PAR-3. Summarizing the results

of this kinase assay led to the finding that PAR-3_{PDZ2-3} exhibits seven aPKC phosphorylation sites: T453, T468, T476, T481, S533, S604 and T661.

As the threonine at position 476 and the threonine at position 481 are only separated by five amino acids, we could only design one oligonucleotide for the mutagenesis PCR that replaces both threonines by an alanine. Consequently a final result, which would show the possible phosphorylation of these single threonines, is missing.

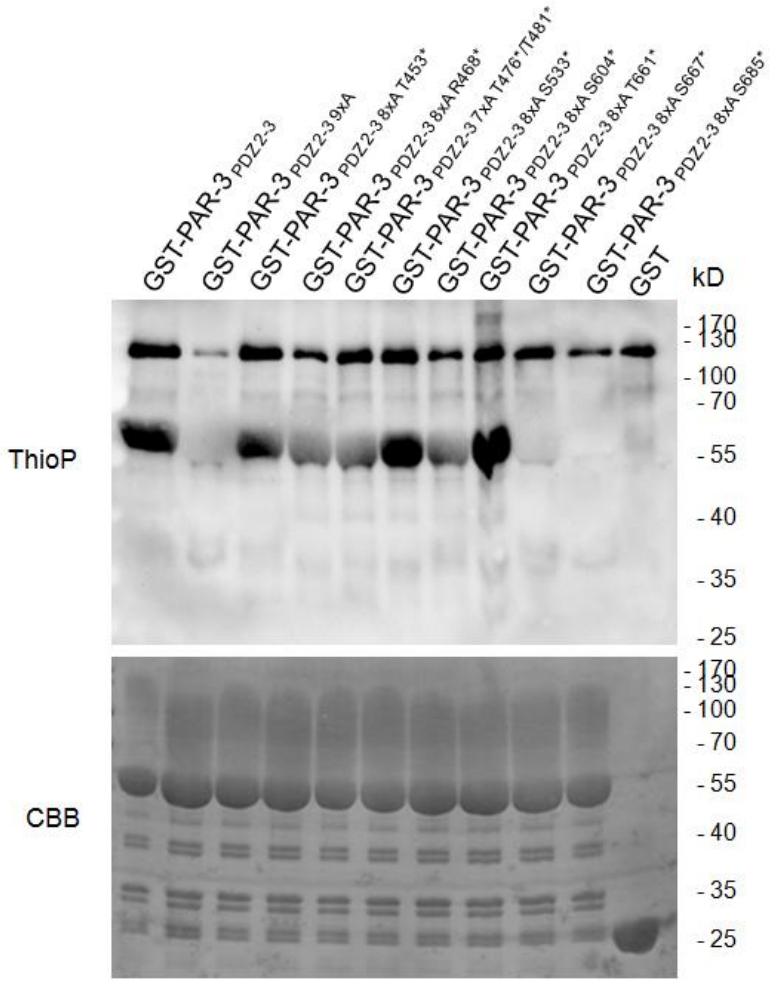

Figure 13 Phosphorylation targets of aPKC in PAR-3_{PDZ2-3}

Kinase assay of GST-tagged PAR-3_{PDZ2-3} variants (ca. 55kD) to analyze aPKC kinase directed phosphorylation *in vitro*, according to 4.2.2.8 (GST = ca. 25 kD; aPKC autophosphorylation = ca. 130 kD). GST-PKCζ from Sigma-Aldrich was used together with ATPγS. CBB indicates coomassie brilliant blue staining for the inputs.

5.4 The impact of aPKC-mediated phosphorylation of Baz_{PDZ2-3} *in vivo*

After the successfully identification of the aPKC-mediated phosphorylation sites in Baz_{PDZ2-3} it was of special interest to have a detailed look on the impact of these phosphorylations *in vivo*. For this purpose *Drosophila* embryonic epithelial cells were focused, which derived from transgenic fly lines created with the PhiC31-Integrase system (4.2.4.2), with GFP-tagged Baz variants expressed under an ubiquitous promoter (*Ubi::GFP-Baz*). Through these settings overexpression artifacts could be prevented and protein levels comparable to endogenous Baz could be achieved. As proof a western blot analysis was made to compare Baz in embryonic lysates from embryos mutant for baz^{815-8} (*baz* null allele), which express *Ubi::GFP-Baz* with endogenous Baz in lysates of w^{1118} flies. Indeed, both samples showed comparable protein levels of Baz (Figure 14). As the Baz of the baz^{815-8}; GFP-Baz flies is fused to a 27kD large GFP-tag, the GFP-Baz band migrated slower in the western blot analysis compared to endogenous Baz in lysates of w^{1118} flies.

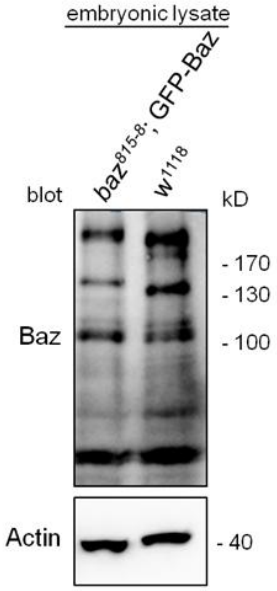

Figure 14 Comparison of Baz protein level in Drosophila embryonic lysates of baz^{815-8}; Ubi::GFP-Baz and w^{1118} flies

Western blot detection identified comparable Baz protein levels in lysates from embryos mutant for baz^{815-8}; *Ubi::GFP-Baz* and w^{1118} embryos. As a loading control the actin level of both samples was analyzed.

For the analysis of the impact of aPKC-mediated phosphorylation at Baz_{PDZ2-3} domain in *Drosophila* embryonic epithelium, embryos of the different wild type fly lines, possessing either GFP-tagged wild type Baz_{wt}, GFP-tagged Baz_{5xA} ($Baz_{T522A, S628A, S700A, T712A, S741A}$ = Baz_{5xA}), where all five phosphorylation targets of aPKC are replaced by an alanine or GFP-tagged Baz_{5xD} ($Baz_{T522D, S628D, S700D, T712D, S741D}$ = Baz_{5xD}), where the five phosphorylation targets are exchanged by an aspartatic acid to mimic phosphorylation, were collected, fixed and immunostained according to the protocol described in 4.2.5.1.

The confocal laser scanning microscopy of the samples revealed, that the transgenic GFP-Baz_{wt} as well as GFP-Baz_{5xA} and GFP-Baz_{5xD} displayed a correct localization at the apical junctions in polarized epithelial cells in the stage 12 of wild type embryos (Figure 15). This finding confirmed previous studies, which showed that the three PDZ domains are dispensable for Baz localization on a wild type background (Krahn et al., 2010b; McKinley et al., 2012).

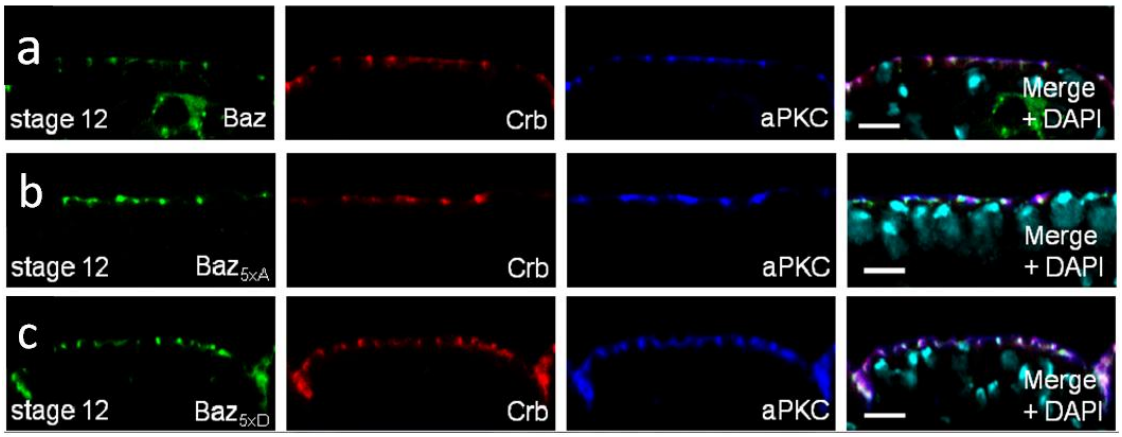

Figure 15 Expression of GFP-tagged Baz variants in fully polarized Drosophila wild type embryonic epithelia (stage 12)

Drosophila wildtype embryos expressing (a) GFP-Baz, (b) GFP-Baz_{5xA} and (c) GFP-Baz_{5xD}, stained with antibodies against Baz, Crb and aPKC in embryonic stage 12 showed correct localization at the apical junctions. Device: Zeiss LSM 710 Meta confocal microscope; Scale bar = 5 µm.

Since the PAR complex is crucial for early development in *Drosophila* embryonic epithelia (Lin et al., 2000; Chen and Zhang, 2013), we had a closer look on embryonic stage 6, the transition from late cellularization to early gastrulation when

Crb is not yet expressed (Figure 16). In this experimental approach wild type GFP-tagged Baz as well as GFP-Baz_{5xD} localized correctly to the forming apical junctions comparable to endogenous Baz (Figure 9). However GFP-Baz_{5xA} exhibited an almost complete cytosolic localization in embryonic stage 6 epithelial cells, meaning that the five phosphorylation sites of aPKC in the Baz_{PDZ2-3} domains show an influence on early embryonic epithelial development in *Drosophila in vivo.*

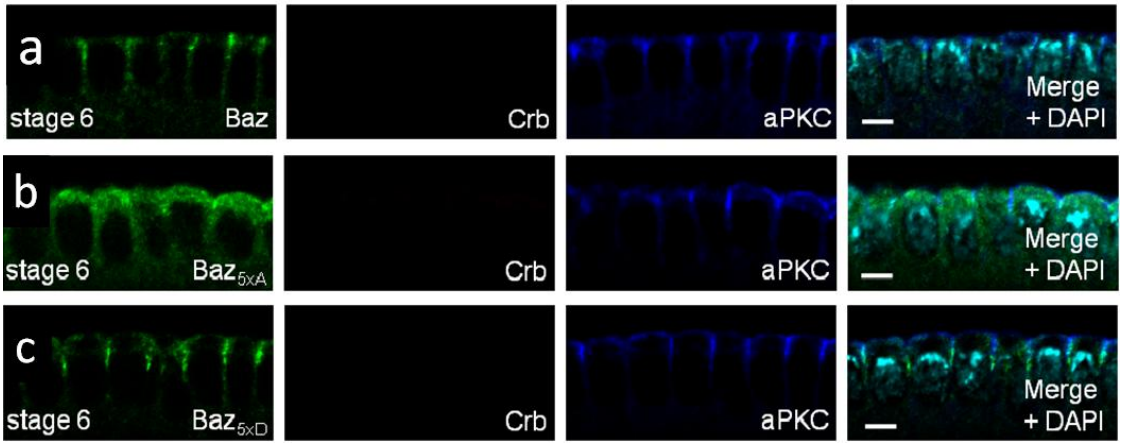

Figure 16 Expression of GFP Baz variants in Drosophila wild type embryonic epithelia during late cellularization/early gastrulation (stage 6)

Drosophila wildtype embryos expressing (a) GFP-Baz, (b) GFP-Baz_{5xA} and (c) GFP-Baz_{5xD}, stained with antibodies against Baz, Crb and aPKC in embryonic stage 6 showed correct localization of GFP-Baz (a) and GFP-Baz_{5xD} (c) at the apical junctions, whereas GFP-Baz_{5xA} (b) showed an almost complete cytosolic localization. Device: Zeiss LSM 710 Meta confocal microscope; Scale bar = 5 µm.

5.5 Phosphorylation of Baz_{PDZ2-3} is important for aPKC binding and protein stability

With the findings, that beside the aPKC-binding region in the CR3 also the PDZ2-3 domains of *Drosophila* Bazooka contributes to aPKC binding (Chapter 5.2) and the identification of the five phosphorylation sites within the Baz_{PDZ2-3} domain (Chapter 5.3), the question arose, if these phosphorylations also have an influence on the binding between Baz and aPKC.

To investigate this issue, a co-immunoprecipitation of endogenous aPKC was performed using transfected GFP-tagged Baz variants in *Drosophila* S2R cells according to the protocol described in 4.2.3.1. The protein extraction from S2R cells as well as the co-immunoprecipitation was conducted according to the protocols described in 4.2.2.2 and 4.2.2.4, respectively (Figure 17a).

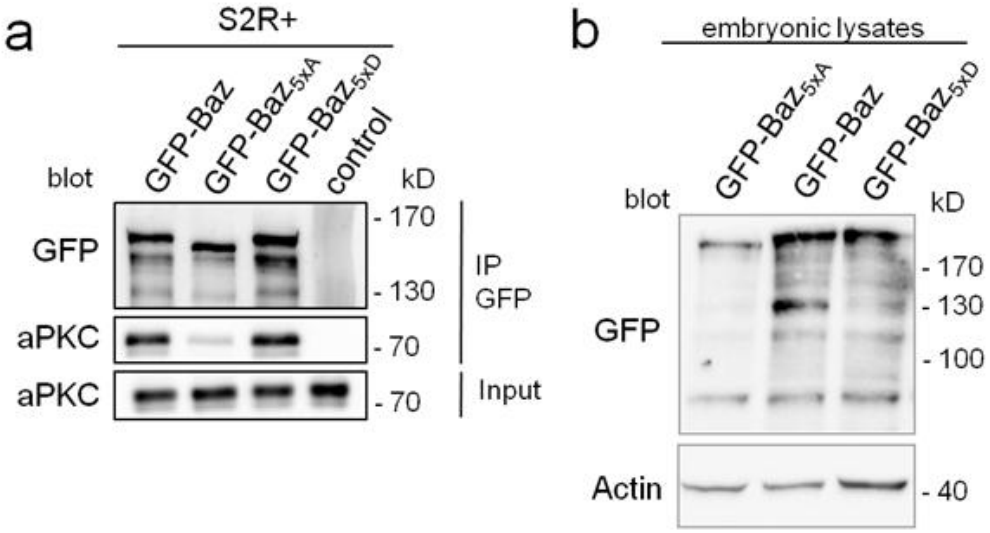

Figure 17 Co-Immunoprecipitation of endogenous aPKC with GFP-tagged Baz variants in transfected S2R cells

Western blot detection identified (a) bound proteins of the immunoprecipitation of transfected GFP-Baz/ GFP-Baz_{5xA}/ GFP-Baz_{5xD}, which were detected by the GFP-tag and co-immunoprecipitated endogenous aPKC (ca. 70kD). Transfection was performed with the FuGENE®HD Transfection Reagent according to 4.2.3.1. As a control untransfected S2R cell lysates were used. In (b) protein level of GFP-Baz variants were compared, which showed a reduced protein level of GFP-Baz_{5xA}. As a loading control the actin level (ca. 42 kD) of the samples was analyzed.

The western blot analysis showed that GFP-Baz as well as the phosphomimetic version GFP-Baz_{5xD} were able to provide robust binding of endogenous aPKC whereas the GFP-Baz_{5xA} variant revealed a decreased association with endogenous aPKC in lysates of transfected S2R cells, indicated by the detection of co-immunoprecipitated aPKC in figure 17a. Moreover the GFP-Baz_{5xA} variant exhibited a faster migration in SDS-PAGE compared to wild type Baz or the phosphomimetic version GFP-Baz_{5xD}, which led to the suggestion that these residues are important for aPKC-binding and moreover also phosphorylated *in vivo*, too.

A comparison of GFP-Baz, GFP-Baz_{5xA} and GFP-Baz_{5xD} *Drosophila* embryonic lysates emphasized that GFP-Baz $_{5xA}$ exhibited a reduced protein level compared to wild type Baz or the phosphomimetic GFP-Baz_{5xD} variant as GFP-Baz_{5xA} protein was much weaker detectable in western blot analysis shown in figure 17b. Out of these results the conclusion was made that it seems that the phosphorylation of Baz_{PDZ2-3} by aPKC stabilizes Baz itself.

5.6 Phosphorylation of Baz_{PDZ2-3} by aPKC is important for early *Drosophila* embryonic development

In order to get closer insights into the *in vivo* mechanisms resulting from the phosphorylation of Baz_{PDZ2-3} by aPKC, *baz*-deficient flies with ubiquitously expressed Baz rescue constructs were analyzed in detail.

First of all zygotically mutant baz^{815-8} (*baz* null allele) flies are not able to survive until adulthood and die already until the end of embryogenesis. This phenotype could be fully rescued by Baz_{wt} as well as by the phosphomimetic Baz_{5xD} variant. Contrary to expectation Baz_{5xA} was able to rescue the zygotically mutant baz^{815-8} flies similar to Baz_{wt} as well as Baz_{5xD} and beyond the rescued flies did not possess any obvious defects. As in these zygotically mutant baz^{815-8} flies a certain amount of maternally provided Baz stays until around embryonic stage 11, it seems that Baz_{5xA} as well as Baz_{5xD} mutations are dispensable for late embryonic development, larval stages, pupal development and adult flies, at the time when no maternally endogenous Baz is working anymore.

To verify this hypothesis *baz* germ line clones, which do not possess a maternal and zygotic contribution of endogenous wild type Baz, were used in order to enable and analyze an impact of the Baz_{5xA} as well as Baz_{5xD} mutations in early *Drosophila* embryonic development *in vivo*. Therefore the corresponding embryos were collected, fixed and immunostained according to the protocol described in 4.2.5.1. and analyzed using the confocal laser scanning microscopy.

The embryos of *baz* germ line clones displayed a complete embryonic lethality and could be fully rescued by GFP-Baz_{wt} (Figure 18). Wild type GFP-tagged Baz

localized correctly to the apical junctions during late cellularization/early gastrulation (stage 6) (Figure 18a, d), when Crb is not expressed and furthermore during proceeding embryonic development after Crb expression (stage 8/9) in these embryos (Figure 18b, c). Accordingly a z-stack projection through the epithelial cells x-y-axis of GFP-Baz_{wt} embryos, maternally and zygotically mutant for baz^{815-8}, confirmed the observations that GFP-Baz_{wt} is able to rescue the *baz* germ line clone phenotype (Figure 18d). In the square of each staining made with the ZEN Blue software a projection through completely 8 µm of epithelial cells was made using single slices with a thickness of 0.76 µm of a stage 6 embryo. It illustrated a clear cortical localization of Baz and aPKC. At top and on the side of the square in figure 18d the side view is shown, which revealed the colocalization of Baz and aPKC to the apical junctions (Figure 18d). Furthermore another staining using Baz, PAR-6 and the lateral marker Dlg confirmed the correct localization of the PAR complex component PAR-6 during early embryonic development in stage 6 (Figure 18e) until later developmental stages (stage 9, Figure 18f). Also the lateral marker Dlg possessed a normal localization along the later plasma membrane.

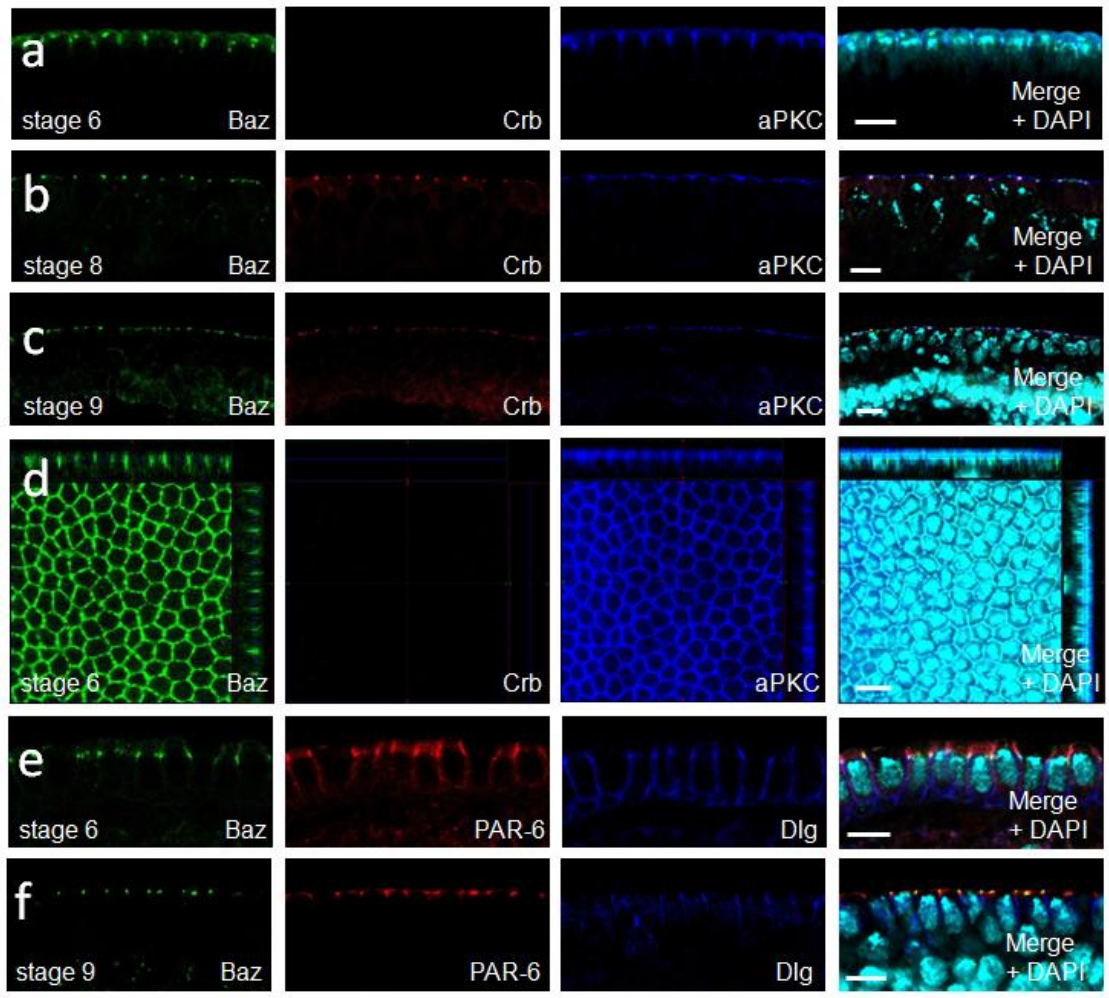

Figure 18 Expression of GFP-Baz$_{wt}$ in baz$^{815-8}$ mutant background

Expression of GFP-Baz$_{wt}$ in embryos which are maternally and zygotically mutant for *baz*$^{815-8}$ shows correct localization of (a, d) Baz and aPKC in embryonic stage 6 to the apical junctions as well as (b, c) Baz, Crb and aPKC in stage 8 and 9 after Crb expression and (e, f) Baz, PAR-6 at the apical junctions and Dlg lateral localization in stage 6 and 9, respectively. (d) shows a z-stack projection in embryonic stage 6 using a 8 µm frame according to the epithelial cell size with single slice thickness of 0.76 µm. The square of each channel shows an x-y axis projection with the respective side views. Device: Zeiss LSM 710 Meta confocal microscope; Scale bar (a, d) = 5 µm (b, c, e, f) = 10 µm.

By way of comparison GFP-Baz$_{5xA}$ in maternally and zygotically *baz*$^{815-8}$ - mutant background was analyzed with the same experimental settings as made for the wild type Baz rescue described above. The expression of GFP-Baz$_{5xA}$ in these embryos revealed a cytoplasmic mislocalization of GFP-Baz$_{5xA}$ and aPKC during late cellularization/early gastrulation (stage 6) (Figure 19a, d), before the onset of Crb expression. Thereby a considerable amount of aPKC was observed at the free apical membrane, which is contradictory to the aPKC localization in control epithelia.

Accordingly to the Baz wild type rescue experiments in *baz*$^{815-8}$ - mutant rescue, also for the Baz_{5xA} rescue a z-stack projection analysis through the epithelial cells x-y axis of embryonic stage 6 was performed (Figure 19d). Exactly like for the Baz_{wt} rescued *baz*$^{815-8}$- mutant embryos a square of each immunostaining made with the ZEN Blue software indicates a projection through completely 8 µm of epithelial cells using single slices with a thickness of 0.76 µm of a stage 6 embryo. The z-stack projection confirmed the mislocalization of GFP-Baz_{5xA} and aPKC to the cytoplasm. Moreover the side view panels clearly showed the cytoplasmic accumulation of GFP-Baz_{5xA} and aPKC (Figure 19d).

Another very important finding was, that Crb, which becomes expressed from late gastrulation onwards, showed an initial cytoplasmic mislocalization in embryonic stage 8 similar to Baz_{5xA} and aPKC in GFP-Baz_{5xA} rescued embryos, maternally and zygotically mutant for *baz*$^{815-8}$ (Figure 19b). However, with the transition to stage 9, initially cytoplasmic mislocalized Crb as well as aPKC were rescued to the cortex, although at aberrant positions (Figure 19c).

Moreover an immunostaining of the GFP- Baz_{5xA} rescued *baz*$^{815-8}$ embryos with PAR-6 and Dlg revealed a loss of PAR-6 from the apical cell-cell contacts in embryonic stage 6, whereas the staining of the lateral marker Discs large (Dlg) exhibited normal localization (Figure 19e). However, the corresponding immunostaining of embryonic stage 9 revealed that also PAR-6 localization similar to Crb and aPKC localization seems to be rescued to some degree to the cortex (Figure 19f).

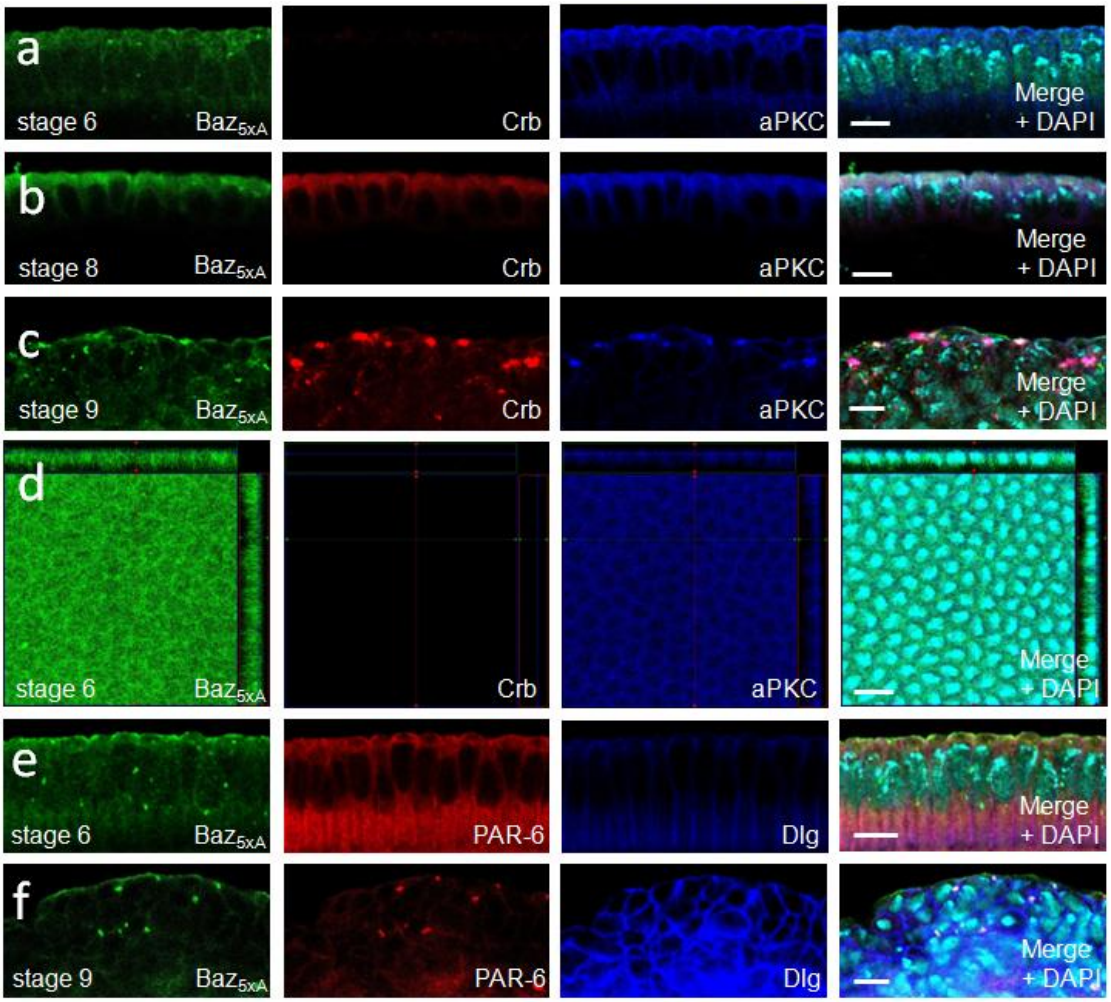

Figure 19 Expression of GFP-Baz$_{5xA}$ in baz$^{815-8}$ mutant background

Expression of GFP-Baz$_{5xA}$ in embryos which are maternally and zygotically mutant for *baz*$^{815-8}$ shows mislocalization of (a, d) Baz and aPKC in embryonic stage 6, (b, c) Baz, Crb and aPKC in stage 8 and 9 after Crb expression, (e, f) Baz, PAR-6 mislocalization and Dlg lateral localization in embryonic stage 6 and 9. (d) shows a z-stack projection in embryonic stage 6 using an 8 µm frame according to the epithelial cell size with single slice thickness of 0.76 µm. The image of each channel shows an x-y axis projection with the respective side views. Device: Zeiss LSM 710 Meta confocal microscope; Scale bar (a, d) = 5 µm (b, c, e, f) = 10 µm.

In an additional experiment the formation of AJ during epithelial development in the Baz$_{5xA}$ mutant embryos with *baz*$^{815-8}$ background were analyzed in order to get a closer insight into the cellular morphology in regard to the Baz$_{PDZ2-3}$ phosphorylation. In this context GFP-Baz$_{5xA}$ rescued embryos, maternally and zygotically mutant for *baz*$^{815-8}$, were immunostained with DE-Cadherin and analyzed with the confocal laser scanning microscopy. The Baz$_{5xA}$ mutant epithelial cells showed a diffuse cytoplasmic DE-Cadherin staining in comparison to wild type

control (Figure 20a, c), which demonstrated that these mutant epithelia failed to establish regular apical AJ in early embryonic epithelial development (stage 6). Furthermore in later stages, the epithelia of the Baz_{5xA} mutant embryos in the *baz*$^{815-8}$ background showed a severely disturbed epithelial morphology in comparison to the GFP-Baz_{wt} rescued epithelia of the *baz*$^{815-8}$ mutant embryos, which is illustrated in an onview image of the epithelia of GFP-Baz_{wt} and GFP-Baz_{5xA} rescued embryos in figure 20b and d, respectively. Moreover the top view images shown in figure 20b and d revealed an impaired AJ assembly at cell-cell contacts of certain groups of cells in the GFP-Baz_{5xA} rescued embryonic epithelia instead of the AJ assembly in the GFP-Baz_{wt} rescued embryos at the apical circumference of each cell.

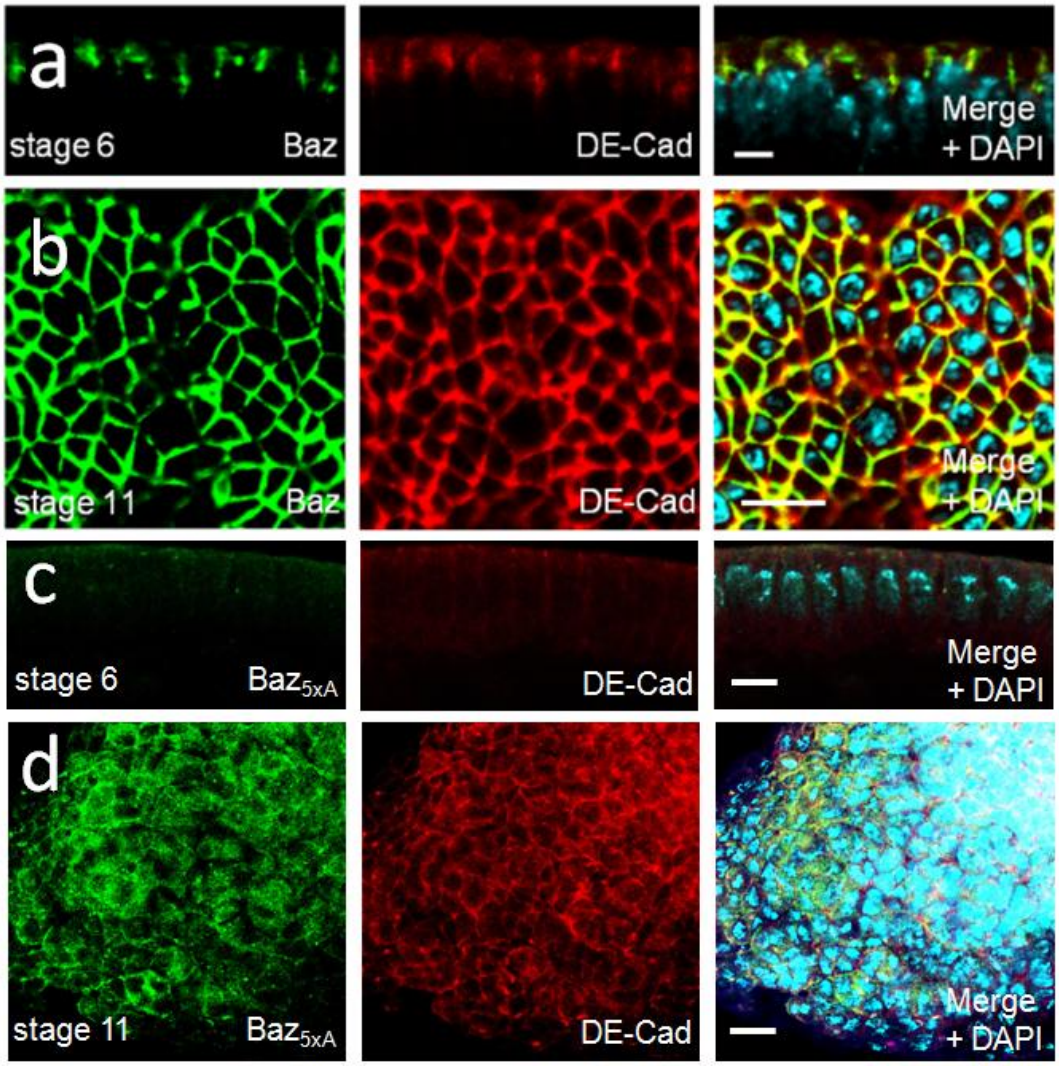

Figure 20 AJ assembly of GFP-Baz$_{5xA}$ embryos in baz$^{815-8}$ mutant background

Expression of GFP-Baz_{5xA} in embryos which are maternally and zygotically mutant for *baz*$^{815-8}$ shows (c) impaired AJ assembly in early embryonic stage 6 in comparison to (a) wild type Baz rescued *baz*$^{815-8}$ mutant embryos. (d) Onview of stage 11 Baz_{5xA} mutant embryonic epithelia in the *baz*$^{815-8}$ background shows severely disturbed epithelial morphology in comparison to (b) the GFP-Baz_{wt}

rescued epithelia, and (d) irregular AJ formation at certain groups of cells instead of (b) the apical circumference of each cell. Device: Zeiss LSM 710 Meta confocal microscope; Scale bar (a, c) = 5 µm (b, d) = 10 µm.

The severe cellular defects of the Baz_{5xA} mutant embryos in the *baz*$^{815\text{-}8}$ background have to be related to embryonic lethality, which was confirmed by a TUNEL assay to detect apoptotic cells in *Drosophila* embryos with the "In Situ Cell Death Detection Kit, TMR red" from Roche according to the protocol described in 4.2.5.2. In this approach the Baz_{5xA} mutant embryos displayed an increased apoptosis in the epidermis indicated by an increase of TUNEL-stained apoptotic cells illustrated in figure 21b in comparison to the Baz_{wt} rescued embryos in the *baz*$^{815\text{-}8}$ background (Figure 21a), which possessed almost no TUNEL-stained, apoptotic cells.

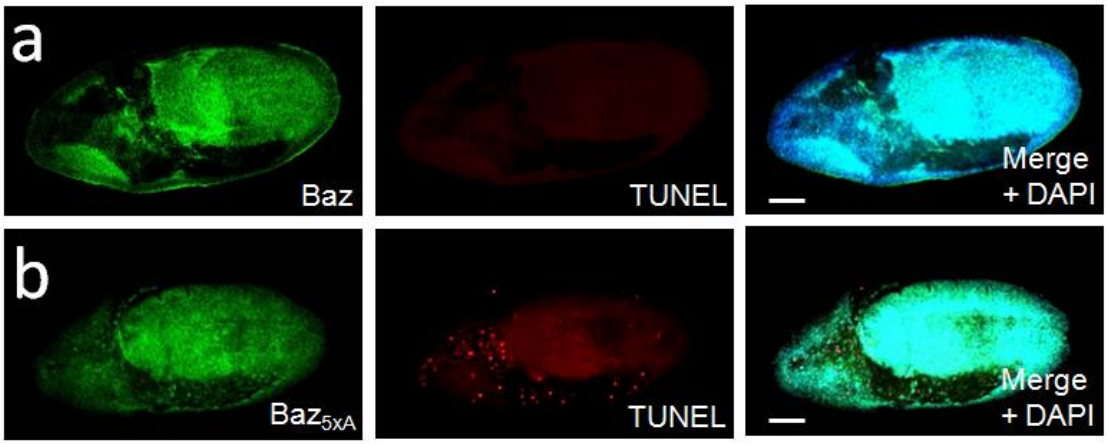

Figure 21 Apoptosis detection in GFP-Baz$_{wt}$ and GFP-Baz$_{5xA}$ rescued baz$^{815\text{-}8}$ mutant embryos

Apoptosis detection in *Drosophila* embryos expressing (a) GFP-Baz_{wt} and (b) GFP-Baz_{5xA} in embryos which are maternally and zygotically mutant for *baz*$^{815\text{-}8}$. For the TUNEL staining the "In Situ Cell Death Detection Kit, TMR red" from Roche was used as described in 4.2.5.2 and according to manufacturer´s instructions. (b) GFP-Baz_{5xA} rescued embryos exhibited increased apoptosis in the epithelial tissue compared to (a) wild type Baz rescued embryonic epidermis. Device: Zeiss LSM 710 Meta confocal microscope; Scale bar = 50 µm.

Taken together the findings described in this chapter indicate that the phosphorylation of $Baz_{PDZ2\text{-}3}$ by aPKC is fundamentally important for the early polarization of *Drosophila* epithelia as well as for the AJ formation of epithelial cells and are to a certain degree rescued by the ectopic expression of Crb from embryonic stage 9 onwards (Figure 19).

5.7 aPKC mediated phosphorylation of Baz_{PDZ2-3} is crucial for early *Drosophila* embryonic development due to a lack of Crb expression

The findings above (Chapter 5.6) indicated that the phosphorylation of Baz_{PDZ2-3} by aPKC is highly important in early embryonic epithelial development, from late cellularization until early gastrulation (stages 5-7) before the onset of Crb expression (stage 8). Moreover it is reported, that Baz and Crb compete for binding of aPKC in maturing epithelia and in the follicular epithelium (Harris and Peifer, 2005; Morais-de-Sá et al., 2010). As a consequence, establishment of early embryonic epithelial polarization seems to be highly dependent on the Baz mediated recruitment of aPKC via phosphorylation of Baz_{PDZ2-3} by aPKC in the absence of Crb.

To analyze this hypothesis in detail a maternally expression of the Crb complex components Sdt and Crb in Baz_{5xA}-mutant embryos, using the UASp/GAL4 system and the maternal driver line *mat67::GAL4*, was performed (Figure 22a). The z-stack projection analysis of these mutant embryos revealed that the cytoplasmic mislocalization of aPKC and GFP-tagged $Baz_{5xA,}$ observed in the Baz_{5xA} rescued embryos, maternally and zygotically mutant for baz^{815-8} (Figure 19a, d), could be partly rescued to the apical junctions by the earlier maternal expression of Sdt and Crb. However the embryos still exhibited a disturbed epithelial morphology (Figure 22a).

From the other point of view another experimental setup was achieved using Baz_{5xA} expressing embryos mutant for both *baz* and *sdt* (baz^{815-8}, sdt^{K85};Baz_{5xA}) (Figure 22b, c). The configuration of these mutants resulted in a destablilization of Crb due to the loss of its adapter protein Sdt. The baz^{815-8}, sdt^{K85}; GFP-Baz_{5xA} mutant embryos displayed strong polarity defects with severely disrupted epithelial morphology, illustrated in the onview image in figure 22c, and cytoplasmic mislocalized aPKC in later embryonic stages (stage 9) (Figure 22b, c). Moreover GFP-Baz_{5xA} and aPKC did not accumulate in aggregates in these baz^{815-8}, sdt^{K85}; Baz_{5xA} mutant embryos as observed during stage 9 in the Baz_{5xA} mutant embryos (Figure 19c). As a control to that single *sdt* mutants were immunostained and analyzed. The loss of Sdt did not

lead to an effect on the localization of Baz and aPKC, which were similar to wild type situation located at the apical junctions in embryonic stage 9 (Figure 22d).

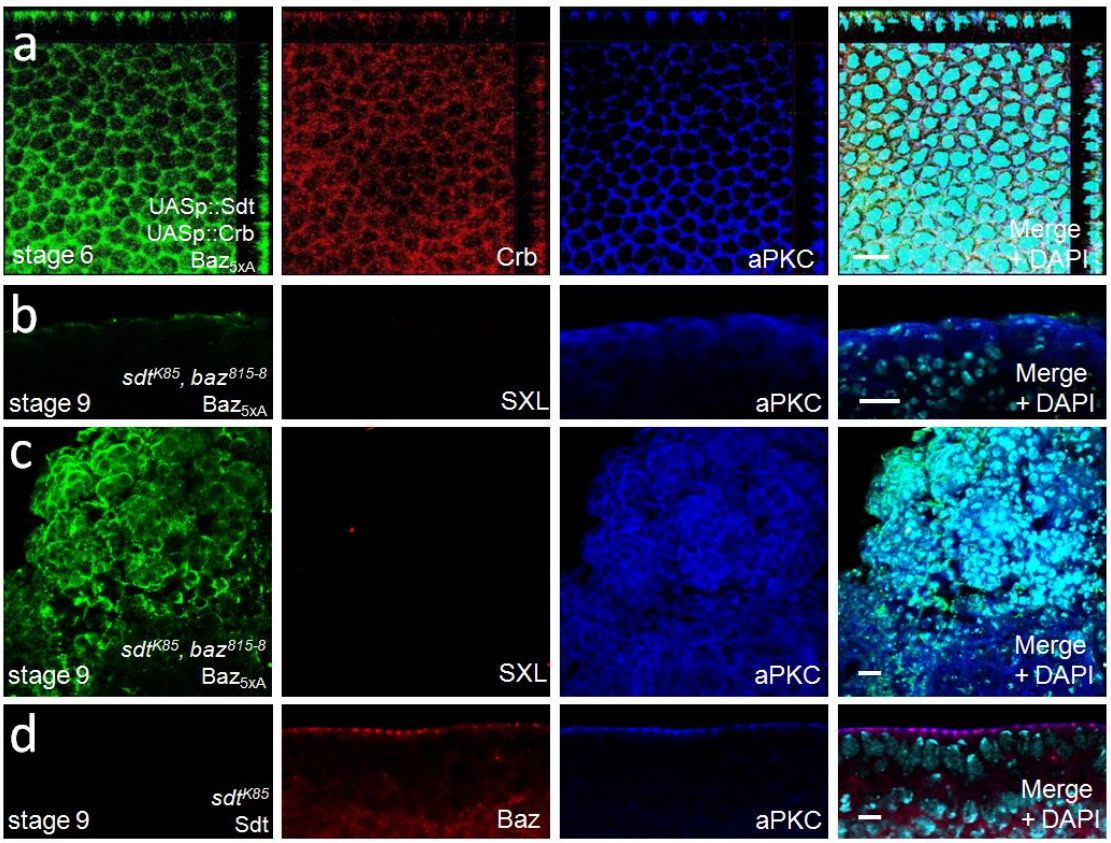

Figure 22 Baz_{PDZ2-3} phosphorylation functions in redundancy with Crb

(a) stage 6 GFP-Baz_{5xA} embryos which are maternally expressing Crb and Sdt show partly rescue; Z-stack projection using an 8 µm frame according to the epithelial cell size with single slice thickness of 0.76 µm; the image of each channel shows an x-y axis projection with the respective side views. (b, c) GFP-Baz_{5xA} embryos which are double mutant for baz^{815-8} and sdt^{K85} show severely disrupted epithelial morphology (c, onview) with weak membrane association of Baz_{5xA} and cytoplasmic accumulation of aPKC; hemizygous mutant embryos were identified by the missing sexlethal (SXL) expression. (d) *sdt* mutant embryos in stage 9 show normal localization of Baz and aPKC to the apical junctions. Device: Zeiss LSM 710 Meta confocal microscope; Scale bar = 10 µm.

As a conclusion the data observed in the rescue experiment of Baz_{5xA}-mutant embryos with maternally expression of Sdt and Crb as well as in the baz^{815-8}, sdt^{K85}; GFP-Baz_{5xA} mutants, which showed a destabilisation of Crb, indicated that Crb is able to act redundantly with Baz_{PDZ2-3} phosphorylation in order to recruit aPKC to the cortex and thereby establish apical-basal polarity in the embryonic epidermis.

5.8 Phosphorylation of Baz_{PDZ2-3} by aPKC is important to restrict basolateral PAR-1 activity

The activity of the PAR complex is counterbalanced by basolateral polarity proteins in order to achieve and maintain distinct cortical domains. Thereby aPKC controls the localization of the basolateral kinase PAR-1 (Benton and St. Johnston, 2003a). Vice versa PAR-1 is able to phosphorylate Baz at two conserved serines at position 151 and 1085 in *Drosophila* in order to exclude Baz from the basolateral domain (Benton and St. Johnston, 2003a; Hurd et al., 2003; Krahn et al., 2009; McKinley and Harris, 2012).

As PAR-1 is influencing the components of the PAR complex via phsophorylation of Baz and on the other way is phosphorylated by aPKC itself the assumption came up whether the cytoplasmic accumulation of aPKC and GFP-Baz_{5xA} observed in Baz_{5xA} mutant embryos is due to an aberrant PAR-1 activity. In a comparison of embryonic lysates derived from baz^{815-8} mutant embryos with Baz_{5xA} or wild type Baz rescue, the PAR-1 mediated phosphorylation at serine 151 (pS151) of Baz during cellularization/early gastrulation was analyzed (Figure 23). Through quantification of the intensity of the bands corresponding to full length Baz (marked with an asterix in Figure 23), the western blot analysis revealed that Baz_{5xA} in *baz*-mutant embryos in comparison to wild type Baz in *baz*-mutant embryos showed a decreased total Baz protein level of Baz_{5xA} but a more than twofold increase in phosphorylation at S151 in Baz_{5xA}.

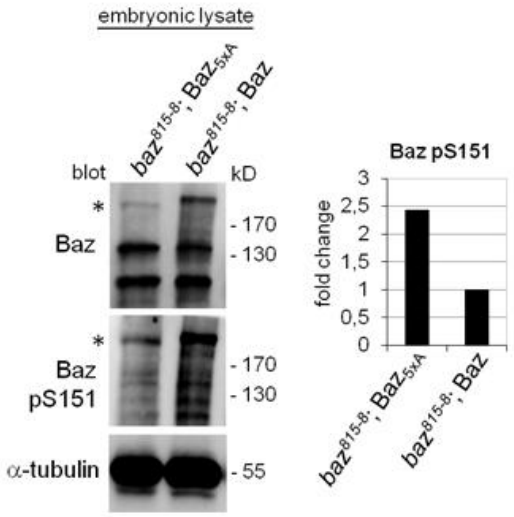

Figure 23 Comparison of embryonic lysates derived from baz$^{815-8}$ mutant embryos with Baz$_{5xA}$ or wild type Baz rescue

The intensity of bands corresponding to full length Baz (asterisk, ca. 190 kD) was quantified. The phosphorylation of serine 151 was normalized against the total Baz level and the phosphorylation of wild type Baz was set as 1. As a loading control the α-tubulin level of the samples was analyzed.

To analyze the influence of the PAR-1 phosphorylation in consideration of the Baz$_{PDZ2-3}$ phosphorylation by aPKC *in vivo*, an experimental setup was established with Baz$_{5xA}$ mutant embryos that maternally express a small hairpin RNA against PAR-1 mRNA (McKinley and Harris, 2012). Thereby a knock down of PAR-1 in Baz$_{5xA}$ mutant embryos was achieved (Figure 24a). The results out of this experiment showed, that the maternal expression of PAR-1 shRNA, thereby downregulating PAR-1 activity in Baz$_{5xA}$ mutant embryos, rescued aPKC and PAR-6 and to a certain degree also Baz$_{5xA}$ cortical localization during late cellularization/early gastrulation (embryonic stage 6). As the basolateral exclusion of aPKC is lost because of the reduced PAR-1 activity, aPKC staining displayed a more lateral membrane accumulation compared to wild type situation (Figure 24a).

To get a closer insight into the phosphorylation of Baz by PAR-1, another experimental approach was provided, using mutations of the two PAR-1 phosphorylation sites of Baz, the serine at position 151 and 1085, respectively, to an alanine in Baz$_{5xA}$ embryos maternally and zygotically mutant for *baz*$^{815-8}$, annotated as Baz$_{7xA}$ mutant embryos (Figure 24b). The immunostained Baz$_{7xA}$ mutant embryos showed a clear membrane targeting of the GFP-tagged Baz$_{7xA}$, which extended over

the entire lateral plasma membrane (Figure 24b). Moreover the aPKC staining revealed a cytoplasmic accumulation (Figure 24b) similar to the staining in Baz_{5xA} mutant embryos (Figure 19a, d).

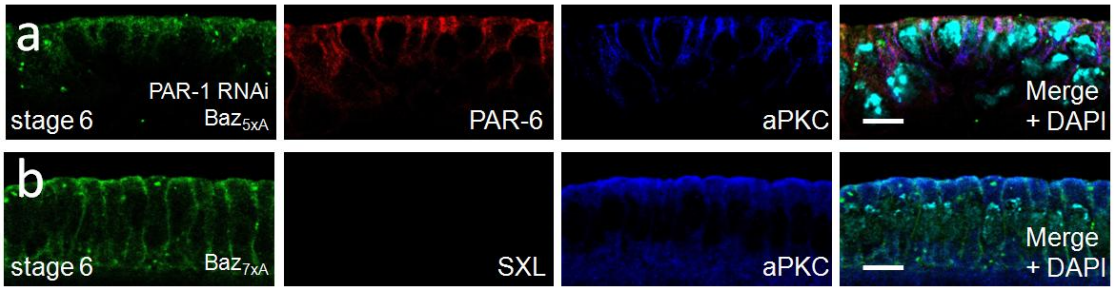

Figure 24 Baz_{PDZ2-3} phosphorylation by aPKC is important to control PAR-1 activity

(a) GFP-Baz_{5xA} embryos which are maternally expressing PAR-1 shRNA show partly rescue of aPKC and PAR-6 localization to the cortex and weak rescue of Baz_{5xA} during embryonic stage 6. (b) GFP-Baz_{7xA} in embryos which are maternally and zygotically mutant for baz^{815-8} show rescue to the membrane, whereas aPKC is mislocalized to the cytoplasm. Hemizygous mutant embryos were identified by the missing sexlethal (SXL) expression. Device: Zeiss LSM 710 Meta confocal microscope; Scale bar = 10 µm.

Taken together the data in this chapter suggest, that impaired Baz_{PDZ2-3} phosphorylation leads to an aberrant PAR-1 activity, indicated in the increased phosphorylation level at the serine 151 of the Baz_{5xA} mutants, which can be rescued by downregulation of PAR-1 (Figure 24a) or mutation of the PAR-1 phosphorylation sites of Baz (Figure 24b).

5.9 The impact of kinase activities on the phosphorylation of Baz_{PDZ2-3}

The kinase activity of aPKC plays an essential role in the right positionining and function of polarity components in epithelial cells, consequently an analysis of the influence of the aPKC activity in connection with the findings in the Baz_{5xA} mutant embryos (Figure 19) was made.

Therefore an experimental setup was provided using Baz_{5xA} mutant embryos in the *baz*$^{815-8}$ background, which exhibited a maternal expression of aPKC^{CAAX}, a constitutive active variant of the kinase due to an additional farnesylation motif (Sotillos et al., 2004). The z-stack projection analysis of the immunostaining of these mutant embryos revealed a rescued localization of aPKC and PAR-6 and to a certain degree of Baz_{5xA}, although the cell morphology and the cell size were severely disturbed in these embryos (Figure 25a).

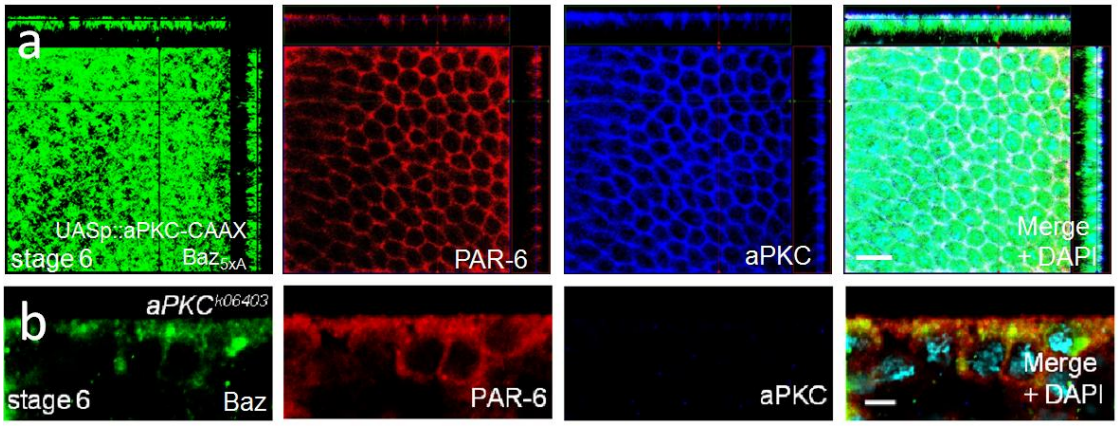

Figure 25 Impact of aPKC activity in early epithelial development

(a) stage 6 GFP-Baz_{5xA} embryos which are maternally expressing aPKC^{CAAX} show partly rescue of PAR-6 and aPKC and a weak rescue of GFP-Baz_{5xA} localization; z-stack projection using an 8 µm frame according to the epithelial cell size with single slice thickness of 0.76 µm; the image of each channel shows an x-y axis projection with the respective side views. (b) embryos maternally and zygotically mutant for *aPKC*^{k06403} show Baz cortical, but aberrant localization and PAR-6 cytoplasmic accumulation in embryonic stage 6. Device: Zeiss LSM 710 Meta confocal microscope; Scale bar = 10 µm.

In another experimental setup an immunostaining of the core components of the PAR complex, Baz, PAR-6 and aPKC in embryos which were maternally and zygotically mutant for *apkc* (*aPKC*^{k06403}) was conducted. Contrary to expectations, the analysis of these mutant embryos showed a relatively cortical localization of endogenous Baz and a cytoplasmic PAR-6 accumulation during embryonic stage 6 (Figure 25b).

This seems to be contradictory to the findings of the localization of Baz_{5xA} (Figure 19), which is entirely cytoplasmic during early gastrulation of Baz_{5xA} mutant embryos. In order to explain this fact, the hypothesis was made, wether some of the serines/threonines of Baz_{PDZ2-3} which are phosphorylated by aPKC can be

phosphorylated by another kinase, too. By searching for possible candidates a kinase assay was made which revealed that Baz_{PDZ1-3} can be phosphorylated by the protein kinase A (PKA). Moreover the kinase assay experiment also revealed, that the phosphorylation of Baz by PKA is decreased but still detectable in $Baz_{PDZ1-3\ 5xA}$ (Figure 26a). These findings indicated that some serines or threonines in the Baz_{PDZ1-3} region are phosphorylated by both kinases, aPKC and PKA.

To gain a detailed consideration of all phosphorylation targets another kinase assay analysis was made, using the same GST- tagged Baz_{PDZ2-3} variants as for the previous kinase assay with aPKC (Figure 12b), where just four serines/threonines were replaced by an alanine thereby leaving one residue intact. This experiment revealed, that one phosphorylation residue, the threonine on position 741 of Baz can be also phosphorylated by PKA (Figure 26b). Moreover also the Baz 976-1028 fragment including the aPKC-binding motif is also phosphorylated by PKA.

These data indicate that the relatively cortical localization of endogenous Baz observed in *apkc* mutant embryos (Figure 25b) is due to a rescuing activity of the kinase PKA by Baz_{PDZ2-3} phosphorylation at the serine at position 741.

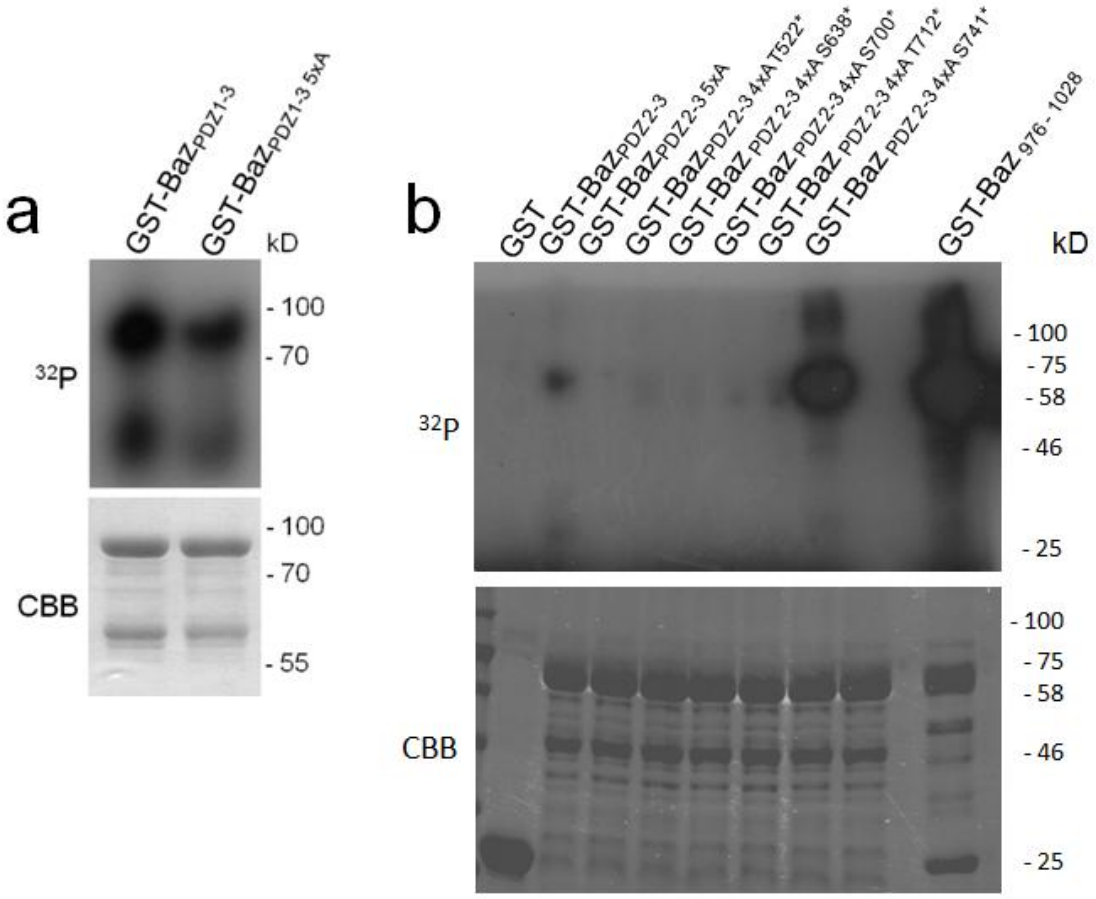

Figure 26 Phosphorylation targets of PKA in Baz$_{PDZ2-3}$

Kinase assay of (a) GST-tagged Baz$_{PDZ1-3}$ (ca. 75kD) and (b) GST-tagged Baz$_{PDZ2-3}$ (ca. 60kD) variants to analyze PKA kinase directed phosphorylation *in vitro*, according to 4.2.2.8. cAMP-dependent PKA,catalytic subunit from New England Biolabs was used together with radioactive labeled $_{\gamma\text{-}32}$ATP (GST = ca. 25 kD). CBB indicates coomassie brilliant blue staining for the inputs.

5.10 The impact of PAR-6 on the kinase activity of aPKC

PAR-6, the third core component of the PAR complex beside aPKC and Baz/PAR-3, is known to associate with aPKC and Baz/PAR-3 via the formation of a PAR-6/aPKC heterodimer. Thereby its PDZ domain can bind to Baz/PAR-3, whereas its PB1 binding domain can interact with aPKC. Moreover PAR-6 can interact through its semi CRIB *Drosophila* motif with the small GTPase Cdc42 (Lin et al., 2000; Joberty et al., 2000; Suzuki et al., 2001; Suzuki et al., 2003; Garrard et al., 2003; Peterson et al., 2004) (Figure 4; Chapter 3.6).

During this work, Silke Wiesner from the Max-Planck Institute for Developmental Biology in Tübingen, Germany, detected another domain of PAR-6, namely a C-terminal PDZ-binding motif (PBM). C-terminal PBMs are classified into three general specificity classes: type I PBM (-X-S/T-X-Φ $_{COOH}$), type II PBM (-X- Φ -X-Φ $_{COOH}$), and type III PBM (-X-D/E-X-Φ $_{COOH}$), whereby X stands for any residue and Φ for a hydrophobic residue (Javier and Rice, 2011; Nourry et al., 2003). In the carboxy terminal end of *Drosophila* as well as human PAR-6 a type II PBM (-X- Φ -X- Φ $_{COOH}$) can be found, whereby for the human PAR-6 the C-terminal protein sequence "GFSL" shows the two needed hydrophobic amino acids phenylalanine ("F") and leucine ("L") and the *Drosophila* PAR-6 possesses two hydrophobic leucines in the C-terminal peptide sequence "VLHL", respectively (Figure 27, grey shades).

PAR-6 [Homo sapiens]

```
  1 MARPQRTPAR SPDSIVEVKS KFDAEFRRFA LPRASVSGFQ EFSRLLRAVH QIPGLDVLLG
 61 YTDAHGDLLP LTNDDSLHRA LASGPPPLRL LVQKREADSS GLAFASNSLQ RRKKGLLLRP
121 VAPLRTRPPL LISLPQDFRQ VSSVIDVDLL PETHRRVRLH KHGSDRPLGF YIRDGMSVRV
181 APQGLERVPG IFISRLVRGG LAESTGLLAV SDEILEVNGI EVAGKTLDQV TDMMVANSHN
241 LIVTVKPANQ RNNVVRGASG RLTGPPSAGP GPAEPDSDDD SSDLVIENRQ PPSSNGLSQG
301 PPCWDLHPGC RHPGTRSSLP SLDDQEQASS GWGSRIRGDG SGFSL
```

PAR-6 [Drosophila melanogaster]

```
  1 MSKNKINTTS ATAASDTNLI EVKSKFDAEF RRWSFKRNEA EQSFDKFASL IEQLHKLTNI
 61 QFLILYIDPR DNDLLPINND DNFGRALKTA RPLLRVIVQR KDDLNEYSGF GTMKPRNLIG
121 SILMGHTPVK TKAPSISIPH DFRQVSAIID VDIVPETHRR VRLLKHGSDK PLGFYIRDGT
181 SVRVTASGLE KQPGIFISRL VPGGLAESTG LLAVNDEVIE VNGIEVAGKT LDQVTDMMVA
241 NSSNLIITVK PANQRTLTST HRGSFSRNSQ LSSGSHHTNN TNTSDEIEHD DQDDIVDLTG
301 VTLDESPTST SAGNHNHQPP LSSSPSSHHQ QAASNASTIM ASDVKDGVLH L
```

Figure 27 Protein sequences of human and fly PAR-6

Protein sequence data from NCBI Databases for *Homo sapiens* (GenBank: BAB16105.1) and *Drosophila melanogaster* (GenBank: AAD15927.1) show both a possible type II PBM at the last four aminos acids, shadowed in grey (from: https://www.ncbi.nlm.nih.gov/pubmed/).

With this finding the question arose, if the alleged PBM of PAR-6 is functional and important for the establishment of *Drosophila* embryonal epithelial polarity.

To identify the influence of the supposed PBM module of PAR-6 *in vivo*, flies lacking this PBM peptide sequence, were analyzed using different approaches.

Firstly the lethality of fly strains possessing a *par-6* mutant (*par-6*^{V226} null allele) background, which were rescued either with wild type PAR-6 or with PAR-6 lacking the supposed PBM sequence were analyzed (*par-6; PAR-6* and *par-6; PAR-6ΔPBM* in figure 28). The lethality test was provided as described in 4.2.4.5. This experiment showed that the embryonic lethality was considerably increased in PAR-6ΔPBM rescued flies up to 44 % +/- 1 % in comparison to the wild type PAR-6 rescued flies which showed an embryonic lethality of 15 % +/- 3 %. Consequently only 33% +/- 2 % of the PAR-6ΔPBM rescued flies survived until adulthood, wereas the wild type PAR-6 rescued flies showed a survival rate of 63 % +/- 5 %. Dag::GAL4 embryos were used as a control which showed a wild type embryonic lethality of 4 % +/- 1 % and a survíval rate of 75 % +/- 4 %. These findings concluded that the found PBM sequence of PAR-6 seems to have an *in vivo* impact on the *Drosophila* embryonic development. Notably, the larval and pupal lethality was without remarkable findings.

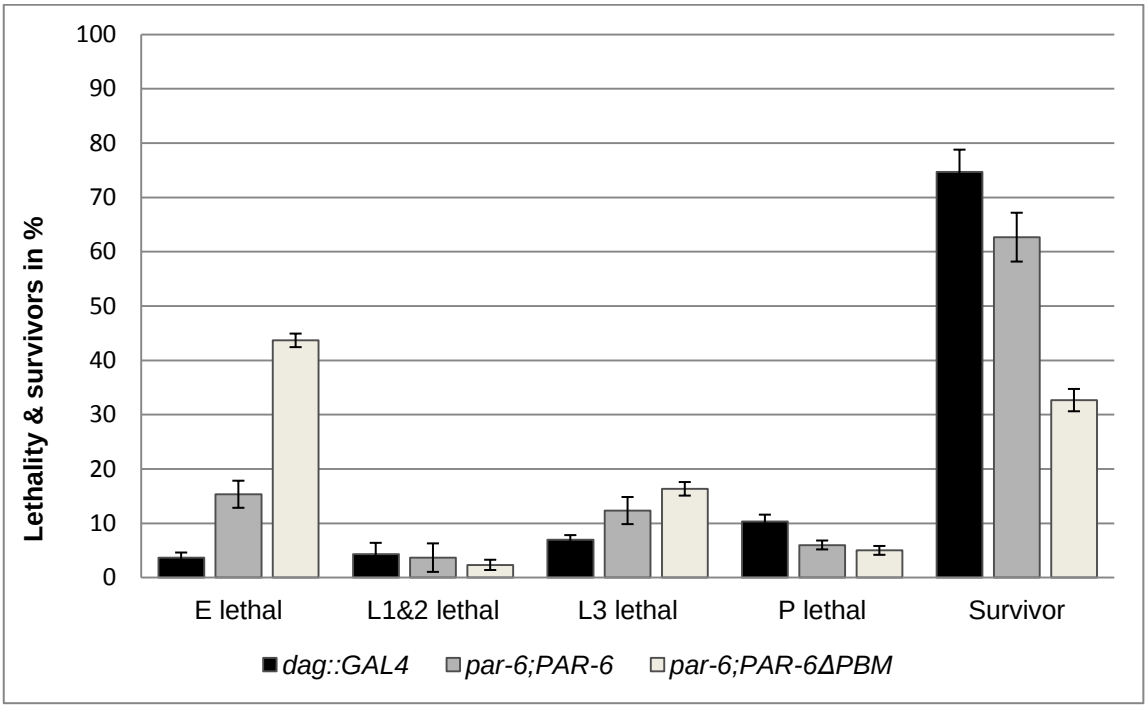

Figure 28 Lethality test of PAR-6 delta PBM flies

Lethality test was performed according to 4.2.4.5 at 25°C using 300 embryos of the same stage for each genotype. As control wild type Dag::GAL4 embryos (black) were used which showed a normal embryonic lethality of 4 % +/- 1 % and a survíval rate of 75 % +/- 4 %. The *par-6* mutant background could be rescued by wild type PAR-6 (grey) to 63 % +/- 5 % survivors whereas the PAR-6ΔPBM (beige) rescued flies showed only a survival rate of 33 % +/- 2 %. E = embryonic; L1&L2 = larval stages 1 & 2; P = pupal. Error bars indicate standard deviations.

However these findings could not be verified in an analysis of cuticles of these embryos (4.2.5.4). Both fly strains, *par-6; PAR-6* and *par-6; PAR-6ΔPBM*, showed similar cuticle phenotypes, therefore no notable difference could be detected. Most of the analyzed embryos displayed a shortening of the cuticle and head defects with impaired segmentation (Figure 29).

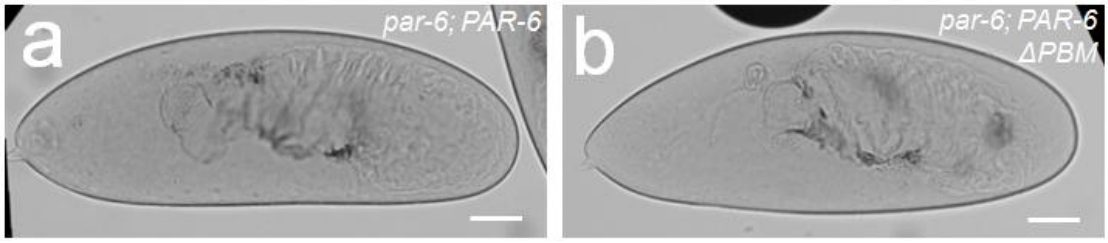

Figure 29 Curicle preparation of PAR-6 and PAR-6ΔPBM rescued par6^{V226}flies

The analysis of cuticle preparations of *Drosophila* embryos derived from *par-6; PAR-6* and *par-6; PAR-6ΔPBM* fly strains showed no significantly difference between the phenotypes. Embryos were dechorionized, embedded with Hoyer´s medium with lactate and incubated at 65°C overnight. Device: EC Plan-Neofluar 2.5x/0.075 Pol M27 objective and an AxioCam MRc camera from Zeiss.

To get a closer look into the impact of the the supposed PBM module of PAR-6 *in vivo*, immunostaining analysis were made with embryos derived from *par-6* mutant background rescued with either wild type PAR-6 or PAR-6 lacking the PBM or the PDZ domain or both, respectively. In a first approach the early epithelial development was scanned in PAR-6ΔPBM and PAR-6ΔPDZ embryos with *par-6* mutant background (Figure 30a, b). The analysis of embryonic stage 6 of both fly strains showed, that aPKC is still able to locate at the forming apical junction although its adaptor protein PAR-6 is lacking the PBM module (Figure 30a) or the PDZ domain (Figure 30b), respectively. Nevertheless, in PAR-6ΔPDZ embryos with *par-6* mutant background Baz displayed a cytosolic accumulation whereas in PAR-6ΔPBM embryos with *par-6* mutant background Baz was still able to locate at the apical junctions together with aPKC (Figure 30a, b). Notably, the GFP-tagged PAR-6ΔPBM showed still a small amount of located protein to the apical junctions compared to the almost completely cytosolic GFP-PAR-6ΔPDZ, although GFP-PAR-6ΔPBM also displayed cytosolic mislocalization.

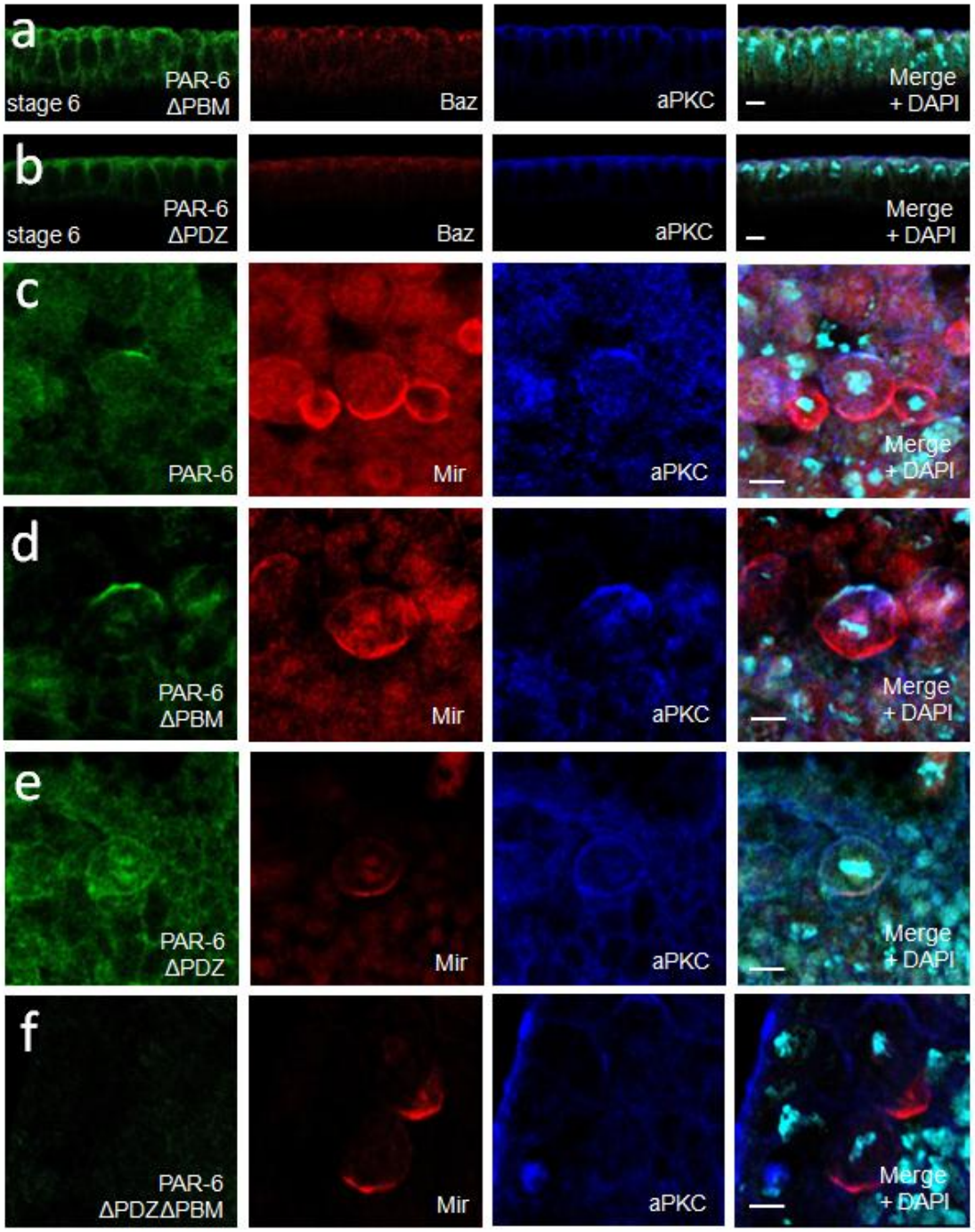

Figure 30 Immunostainings of epithelia and neuroblasts of PAR-6 mutants

(a, b) immunostaining of GFP-PAR-6ΔPBM (a) and GFP-PAR-6ΔPDZ (b) rescued embryonic epithelial cells with *par-6* mutant background shows mislocalization of Baz in GFP-PAR-6ΔPDZ rescued embryos. (c-f) embryonic neuroblast staining of GFP-PAR-6 (c), GFP-PAR-6ΔPBM (d), GFP-PAR-6ΔPDZ (e) and GFP-PAR-6ΔPDZΔPBM rescued embryos with *par-6* mutant background shows mislocalization of GFP and aPKC staining in PAR-6ΔPDZ and PAR-6ΔPDZΔPBM rescued embryos. Device: Zeiss LSM 710 Meta confocal microscope; Scale bar (a, b) = 5 µm (c-f) = 10 µm.

Furthermore the polarity of embryonic neuroblasts at early stages of neurogenesis (embryonic stage 9-11) in embryos lacking the PBM or the PDZ domain or both

domains of PAR-6 was investigated using immunostainings with the cell fate determinant Miranda (Mir), which usually locates opposite (basal) to the PAR complex components (apical) in metaphase neuroblasts. In this analysis, wild type control GFP-PAR-6 in *par-6* mutant embryos showed in metaphase neuroblasts a clear apical localization together with aPKC on the opposite side of the Mir staining, as illustrated in figure 30c. Nevertheless for GFP-PAR-6ΔPBM only very slight abnormalities could be observed, whereby GFP-PAR-6ΔPBM still displayed a cortical localization in neuroblasts together with aPKC, although in this embryos GFP-PAR-6ΔPBM and aPKC showed a more non-homogenous distribution compared to the wild type GFP-PAR-6 neuroblasts (Figure 30d). In contrast, GFP-PAR-6ΔPDZ was not anymore able to locate correctly at the opposite side of Mir but rather showed a slightly localization around the whole cortex and in the cytoplasm together with the aPKC staining (Figure 30e). In a double mutant embryo for PAR-6ΔPBM and PAR-6ΔPDZ no detectable localization of the GFP-PAR-6 ΔPDZΔPBM as well as aPKC could be found in metaphase neuroblasts (Figure 30f).

Taken together the results of the immunostainings of epithelial cells and neuroblasts indicate, that the PAR-6 PDZ domain plays an important role in the correct location of Baz and aPKC and that the suggested PAR-6 PBM domains seems to have a supporting function in the establishment of epithelial and neuroblast polarity.

6 Discussion

Polarity is a fundamental mechanism to establish and maintain function of epithelial cells. Epithelia are characterized by apical-basal polarity. This apical-basal polarization and the formation of cell-cell junctions are important key steps in the development of epithelia to provide barrier formation, directed transport and mechanical integrity of the tissue.

The PAR complex, consisting of the core components Bazooka/PAR-3, PAR-6 and aPKC, plays an important role in the establishment of the apical-basal polarity in epithelial cells and is the first to become unequally localized, thereby controlling the localization of additional complexes functioning further downstream in the regulation of cell polarity.

Within this study, the interaction between Baz and the kinase aPKC as well as the positioning and function of phosphorylation events of Baz by aPKC were analyzed in detail. The analysis in this study showed that substantially aPKC-binding is accomplished by both aPKC-binding domains of Baz (PDZ2-3 and CR3). Additionally phosphorylation sites of Baz and the human PAR-3 by aPKC were identified and analyzed *in vivo* in the fly. Thereby, detailed considerations of the chronology of the *Drosophila* embryonic epithelial development showed that in the early epithelial development, Baz phosphorylation by aPKC at the PDZ domains two to three is fundamentally important for the recruitment of aPKC. Furthermore after Crb expression from embryonic stage 8 onwards Baz and Crb function to some extent redundantly to determine the apical domain of epithelial cells and both further direct the formation of apical junctions by recruiting aPKC. On the other hand, establishment of correct apical to basal polarity also depends on the interaction between Baz and the basolateral kinase PAR-1. Impaired Baz PDZ-phosphorylation by aPKC results in a destabilization of Baz and disturbed apical targeting of aPKC with a simultaneous excessive activity of PAR-1. Consequently, aPKC fails to regulate AJ assembly, leading to massive defects in epithelial polarity. However, the data in this study show that another kinase, PKA, is able to phosphorylate Baz within the PDZ2-3 domain, thereby also providing a recruitment of Baz to the apical

junctions. Moreover, the first observations indicate a C-terminally located PDZ binding motif of PAR-6, which seems to support the establishment of epithelial and neuroblast polarity.

6.1 Structural and functional analysis of the Baz_{PDZ2-3} phosphorylation by aPKC

In the first part of this work, the interaction between Baz/PAR-3 and aPKC was analyzed in detail. First of all it was shown that aPKC initially co-localizes together with Baz to the apical junctions. However upon the onset of Crb expression during *Drosophila* embryonic stage 8 a substantial portion of aPKC is shifted towards Crb (Chapter 5.1; Figure 9). This led to the conclusion that before the onset of Crb expression during epithelial development, recruitment of aPKC to the apical junctions depends on Baz. This theory is supported by the finding that embryos, which are maternally and zygotically mutant for *baz* show a cytoplasmatic mislocalization of aPKC (Wodarz et al., 2000). Moreover the positioning and stabilization of Baz at the apical junctions during embryonic stage 6 has been shown to require aPKC, which is in turn simultaneously recruited to the cell junctions by Baz (Wodarz et al., 2000). Additionally a couple of reports showed that during embryonic stage 8 a substantial portion of aPKC segregates from Baz and colocalizes with Crb (Harris and Peifer, 2005; Krahn et al., 2010a; Morais-de-Sá et al., 2010). However to clarify this issue, quantification analysis would help to messure the precise ratio of co-localizing proteins.

An investigation of the binding affinity of the two described interaction regions of Baz with aPKC, the Baz_{PDZ2-3} domain and the conserved Baz-aPKC-binding motif (CR3), was conducted (Chapter 5.2) (Izumi et al., 1998; Lin et al., 2000; Wodarz et al., 2000; Nagai-Tamai et al., 2002; Rolls et al., 2003; Horikoshi et al., 2009; Morais-de-Sá et al., 2010). The co-immunoprecipitation of endogenous aPKC with transfected GFP-Baz variants in *Drosophila* S2R cells revealed that both regions are involved in binding to aPKC and that the PDZ2-3 domain and the aPKC-binding motif of Baz may function synergistically in binding aPKC, which was shown by the

observation, that the wild type Baz control exhibited a much more intensely binding of aPKC than the accumulated binding of the deletion constructs (Figure 10).

In further experiments in this work it could be shown, that the Baz_{PDZ2-3} phosphorylation influences the binding of Baz to aPKC, as Baz_{5xA} binds much less aPKC compared to Baz_{wt} or the phosphomimetic version Baz_{5xD} in cell lysates derived from transfected *Drosophila* S2R cells (Chapter 5.5, Figure 17a). Usually a kinase and a substrate shortly associate in order to achieve phosphorylation of the substrate and thereafter disconnect again, which is also known as the "kiss-and-run" principle. Thereafter the phosphomimetic version Baz_{5xD} should bind less than wild type and the phosphodeficient version Baz_{5xA} should bind stronger. Nevertheless the co-immunoprecipitation revealed a strong affinity of Baz and aPKC, therefore beside the substrate function of Baz it could also serve as a scaffold for aPKC recruitment and stabilization at the apical cell-cell contacts. Corresponding to that, in neuroblasts it was found that the cell fate determinant Numb requires binding by Baz before being phosphorylated by aPKC, which gives a hint to the scaffolding function of Baz (Wirtz-Peitz et al., 2008). Baz may act thereby as a co-factor for aPKC kinase activity and substrate specificity (Wirtz-Peitz et al., 2008). Another indication for the hypothesis, that Baz functions as a co-factor for regulating aPKC was found during dorsal closure of *Drosophila* embryos, where Baz seems to inhibit aPKC to provide re-arrangement of Actin-Myosin filaments (David et al., 2013). Moreover it is reported that in the mammalian system the PAR-3 aPKC-binding region competes with the pseudosubstrate domain of aPKC for binding of the substrate pocket, which could lead to an unfolding of the autoinhibited kinase and thereby activation of aPKC (Wang et al., 2012).

A comparison of GFP-Baz, GFP-Baz_{5xA} and GFP-Baz_{5xD} *Drosophila* embryonic lysates emphasized that GFP-Baz_{5xA} exhibited a reduced protein level compared to wild type Baz or the phosphomimetic GFP-Baz_{5xD} variant (Figure 17b). This result further suggests that the phosphorylation of Baz_{PDZ2-3} by aPKC stabilizes Baz itself.

However, the reduced protein level observed for the GFP-Baz_{5xA} embryonic lysates (Figure 17b) as well as the reduced binding affinity of $Baz_{PDZ2-3\ 5xA}$ to aPKC (Figure 10 and 17a) could also be observed due to a structural misfolding of the mutated protein, thereby leading to wrong interpretations of the data. This would mean that the faster migration of GFP-Baz_{5xA} observed in SDS-PAGE (Figure 17a) and the

reduced stability of GFP-Baz_{5xA} (Figure 17b) is due to a disrupted protein structure because of mutation events rather than a loss of phosphorylation. Nevertheless crystallisation studies of $Baz_{PDZ2\text{-}3\ 5xA}$ would help to gain a more detailed knowledge about the molecular structure of the protein.

Using the aPKC phosphorylation site motif (Chapter 3.5) and a corresponding kinase assay analysis, phosphorylation residues in the PDZ two to three region of *Drosophila* Baz and mammalian PAR-3 were identified. The *in vitro* kinase assay with GST-tagged Baz variants (Chapter 5.3, Figure 12) clearly showed that replacing the predicted five phosphorylation targets of $Baz_{PDZ2\text{-}3}$ by alanines, thereby disturbing the ability of aPKC to phosphorylate these positions, led to a loss of phosphorylation by aPKC for $Baz_{PDZ2\text{-}3\ 5xA}$, demonstrating that the five serines/threonines at the positions 522, 638, 700, 712 and 741 of $Baz_{PDZ2\text{-}3}$ are phosphorylation targets of aPKC.

As the used kinase in this experiment was a bought GST-tagged human PKCζ from Sigma Aldrich at high concentrations, one concern could be that the experiment was interspecies and thereby not reliable. aPKC is a highly conserved protein from fly to man and moreover the positive control of the phosphorylation of the CR3 of Baz within a fragment encompassing position 976-1028 (Figure 12b), revealed a strong phosphorylation ability of the human aPKC on the known phosphorylation site for aPKC at *Drosophila* Baz serine 980 (Izumi et al., 1998; Lin et al., 2000; Nagai-Tamai et al., 2002; Horikoshi et al., 2009; Morais-de-Sá et al., 2010). Furthermore, this experiment showed, that the phoshorylation of the reported serine 980 in comparison to the PDZ2-3 domain phosphorylation of Baz by aPKC is much more intensely, meaning that the aPKC-binding motif is highly important for Baz phosphorylation by aPKC, whereas the $Baz_{PDZ2\text{-}3}$ fragment showed a minor phosphorylation by aPKC. In this context, the kinase assay in figure 12b additionally revealed, that not all found target sites of aPKC in $Baz_{PDZ2\text{-}3}$ are equally phosphorylated but rather showed different degrees of detectable phosphorylation. Thereby the serine at position 700 and the threonine at position 712 of Baz possessed the highest levels of phosphorylation. This means that these two phosphorylation targets of aPKC might be most relevant for the $Baz_{PDZ2\text{-}3}$ phosphorylation and are maybe supported by the phosphorylation of the three other found phosphorylation sites. Therefore it seems, that the phosphorylation of $Baz_{PDZ2\text{-}3}$ plays a different role

than the phosphorylation at Baz-CR3, whereby the *in vivo* studies presented in this work may give a first hint to a temporally importance in the development of polarity, to be exact in the very early embryonic stages. However, to clarify this issue precisely, confirmations are needed to show that these predicted residues are also phosphorylated *in vivo*. One evidence for this could be, that the full length Baz in which all five phosphorylation targets of aPKC in Baz_{PDZ2-3} were replaced by alanine migrates slightly faster in SDS-PAGES compared to wild-type Baz or the phosphomimetic version Baz_{5xD} (Figure 17a), which leads to the suggestion that these residues are phosphorylated *in vivo*, too. On the other hand, the faster migration in SDS-PAGE as well as the reduced stability of Baz_{5xA} could be also due to a disrupted structure of the protein rather than a loss of phosphorylation *in vivo*. To the end of this work massspectrometry analysis were performed in order to identify the supposed phosphorylation sites of Baz_{PDZ2-3} precisely, but were still under progress, therefore no convincing evidences are received so far. Consequently a final evidence which demonstrates, that Baz_{PDZ2-3} is phosphorylated *in vivo* is still missing.

For the mammalian homologue PAR-3 corresponding experiments using ATPγS and GST-tagged PAR-3_{PDZ2-3} constructs were performed to clearly identify all targets for aPKC phosphorylation in the PDZ domain region of this protein (Chapter 5.3, Figure 13). Within this experiment it was found that PAR-3_{PDZ2-3} exhibits seven aPKC phosphorylation sites: T453, T468, T476, T481, S533, S604 and T661. However the threonine 476 and 481 are only separated by five amino acids, therefore these residues were not separately analyzed and a final result, which would show the possible phosphorylation of these single threonines, is missing here. Moreover, the autophosphorylation band of aPKC at around 130 kD seems to be weakened in the GST-PAR-$3_{PDZ2-3\ 9xA}$ sample, which could lead to the supposition, that here the activity of aPKC was impaired compared to the other samples. However, also for the mammalian PAR-3 equally to *Drosophila* Baz *in vivo* experiments have to be done to verify these first results.

6.2 The relevance of Baz_{PDZ2-3} phosphorylation in early epithelial development

In the second part of this work, the impact of aPKC-mediated Baz_{PDZ2-3} phosphorylation *in vivo* was examined. In previous studies it has been revealed that the PDZ domains of Baz are dispensable for proper localization of Baz to the apical junctions on a *Drosophila* wild type background (Krahn et al., 2010b; McKinley et al., 2012), which could be confirmed in this study (Chapter 5.4, Figure 15). Nevertheless in this work it was shown that in early embryonic epithelial cells at the transition from late cellularization to early gastrulation (embryonic stage 6) the GFP-tagged phosphodeficient variant Baz_{5xA} exhibited an almost complete cytosolic localization, wereas the wild type GFP-Baz as well as the phosphomimetic GFP-Baz_{5xD} indicated a normal localization to the forming apical junctions (Figure 16). This gives an important hint that the PDZ phosphorylation of Baz by aPKC plays an important role in early epithelial development at a timepoint, when other apical polarity proteins like Crb are not expressed yet and moreover, that the Baz PDZ phosphorylation becomes dispensable in later embryonic development.

To gain a better understanding about the role of Baz PDZ phosphorylation by aPKC *in vivo*, further analysis using *baz*-deficient flies with ubiquitously expressed rescue constructs were conducted. Zygotically mutant baz^{815-8} (*baz* null allele) flies die until the end of embryogenesis and can be fully rescued by Baz_{wt} as well as Baz_{5xA} and Baz_{5xD}. This observation was another evidence to elucidate the *in vivo* function of the Baz PDZ phosphorylation as these fly strains still possessed maternally enogenous Baz until around embryonic stage 11, which was able to rescue early epithelial development. Again this observation showed that the PDZ phosphorylation is dispensable in late tissue development at the time when no maternally provided Baz might rescue anymore.

Corresponding to that, the analysis in this work using *baz* germ line clones which do not possess a maternal or zygotic contribution of endogenous Baz clearly verified the impact of Baz PDZ phosphorylation in early *Drosophila* epithelial development *in vivo*. The expression of GFP-Baz_{5xA} in maternally and zygotically baz^{815-8} - mutant background embryos revealed a cytoplasmic mislocalization of GFP-$Baz_{5xA,}$ aPKC

and PAR-6 during late cellularization/early gastrulation (embryonic stage 6) (Chapter 5.6, Figure 19), before the onset of Crb expression. Interestingly, Crb showed an initial cytoplasmic mislocalization in embryonic stage 8 similar to Baz_{5xA} and aPKC in GFP-Baz_{5xA} rescued embryos, maternally and zygotically mutant for *baz*$^{815-8}$ (Figure 19b). However, with the transition to stage 9, initially cytoplasmic mislocalized Crb as well as aPKC and PAR-6 were rescued to the cortex, although at aberrant positions (Figure 19c, e) because of the already disturbed epithelial architecture. These findings further confirmed the early contribution of Baz PDZ phosphorylation to epithelial development and moreover, that with the beginning of Crb expression, the PAR-proteins aPKC and PAR-6 and to some extent also the mutated Baz are rescued to the cortex.

Furthermore also the analysis of the establishment of the AJ (Figure 20) and the cell morphology reinforced the importance of Baz_{PDZ2-3} phosphorylation for AJ formation of epithelial cells. The GFP-Baz_{5xA} embryos in maternal and zygotic *baz*$^{815-8}$ - mutant background possessed severe morphology aberrations with AJ only formed at the apical circumference of certain groups of cells (Figure 20d). As these severe cellular defects of the Baz_{5xA} mutant embryos in the *baz*$^{815-8}$ background should have an influence on embryonic lethality, the provided TUNEL assay confirmed the increase of apoptotic cells in *Drosophila* Baz_{5xA} mutant embryos (Figure 21b).

Taken together the findings in this work clearly point to the fact that the phosphorylation of Baz_{PDZ2-3} by aPKC is fundamentally important for the early polarization of *Drosophila* epithelia as well as for the AJ formation of epithelial cells, which are to a certain degree rescued after the ectopic expression of Crb from embryonic stage 9 onwards. Accordingly Baz PDZ phosphorylation seems to work redundantly together with Crb or another at the moment unknown protein after stage 9 onwards. This hypothesis is further strengthened by the fact that Baz and Crb compete for binding of aPKC in maturing epithelia and in the follicular epithelium (Harris and Peifer, 2005; Morais-de-Sá et al., 2010).

Nevertheless as it was shown that GFP-Baz_{5xA} embryos exhibited a lower protein level compared to GFP-Baz_{wt} and GFP-Baz_{5xD} (Figure 17b), the observed mislocalization of GFP-Baz_{5xA} could also derive from insufficient protein levels rather than a deficiency of Baz PDZ phosphorylation.

In this context the experiments in this study clearly showed that early maternal expression of Crb and Sdt in the Baz_{5xA} mutant embryos with *baz*$^{815-8}$ background is able to rescue to some degree the localization of aPKC and GFP-tagged Baz_{5xA} to the apical junctions (Chapter 5.7; Figure 22). Additionally the *baz*$^{815-8}$, *sdt*^{K85}*;* GFP-Baz_{5xA} mutant embryos displayed strong polarity defects with severely disrupted epithelial morphology. As the adaptor protein Sdt is missing in these embryos, Crb is destabilized and thereby also aPKC becomes cytoplasmic mislocalized in later embryonic stages (stage 9) (Figure 22b, c). Moreover GFP-Baz_{5xA} and aPKC did not accumulate in aggregates in the *baz*$^{815-8}$, *sdt*^{K85}*;* GFP-Baz_{5xA} mutant embryos as observed during stage 9 in the Baz_{5xA} mutant embryos (Figure 19c). These observations further strengthen the hypothesis that Crb is able to rescue the Baz_{5xA} mutant phenotype and functions thereby from embryonic stage 9 onwards redundantly with Baz_{PDZ2-3} phosphorylation to recruit aPKC to the cortex in order to establish apical-basal polarity in the embryonic epithelia.

Moreover we had a closer look on the third member of the Par complex, PAR-6. As PAR-6 has a supposed type II PDZ-binding motif (PBM), a short peptide at the very C-terminus, *in vivo* experiments were performed to answer the question, if this postulated motif has a biological significance (Chapter 5.10). The provided lethality test in this study demonstrated an over twofold increased embryonic lethality in *par-6; PAR-6ΔPBM* rescued flies in comparison to the wild type PAR-6 rescued flies (Figure 28). These findings are a first hint that the found PBM sequence of PAR-6 seems to have an *in vivo* impact on the *Drosophila* embryonic development. However the wild type rescued control *par-6; PAR-6* flies already showed an increased lethality in comparison to the dag::GAL4 control fly strain. Therefore the observed results might also be influenced by an artificial over- or missexpression of the mutated protein rather than from the loss of the PBM.

Moreover in the *in vivo* immunostaining analysis comparing flies lacking the PBM or PDZ domain of PAR-6 the observation was made, that in PAR-6ΔPDZ embryos with *par-6* mutant background Baz displayed a cytosolic accumulation whereas in PAR-6ΔPBM embryos with *par-6* mutant background Baz was still able to locate at the apical junctions, whereas aPKC localization was not affected (Figure 30a, b). Corresponding to that also the analysis of embryonic neuroblasts revealed for GFP-PAR-6ΔPBM only very slight abnormalities, as it was still detectable at the cortex

together with aPKC although in a non-homogenous distribution (Figure 30c-f). In contrast to that GFP- PAR-6ΔPDZ was not able to locate correctly together with aPKC in these mutants anymore. Moreover the double mutant embryos for PAR-6ΔPBM and PAR-6ΔPDZ showed a complete loss of cortical localization, which could give a first hint that these two domains cooperate to some extent. These findings showed that the PBM seems to be not responsible for Baz and aPKC localization to the apical junctions but may have an alternative influence in the embryonic development which is also indicated by the increased lethality of flies lacking this motif. Further analyses have to be done to identify the function of the found PB motif.

To gain more realistic insights into the role of the PAR-6 PBM we started to generate a PAR-6 mutant using the CRISPR/Cas9 technique at the end of this work. These new method may give more reliable results about the functionality of the found PB motif of PAR-6.

6.3 The impact of kinase activity on the establishment of early epithelial polarity

As kinases play an important role in the epithelial development, in the third part of this work firstly the basolateral kinase PAR-1 and its influence on Baz function in connection with the Baz PDZ phosphorylation of aPKC was analyzed. It was shown, that the PAR-1 mediated phosphorylation at serine 151 (pS151) of Baz_{5xA} in *baz*-mutant embryos in comparison to wild type Baz in *baz*-mutant embryos displayed a decreased total Baz protein level of Baz_{5xA} but a more than twofold increase in phosphorylation at S151 in Baz_{5xA} (Chapter 5.8, Figure 23), which suggests an excessive PAR-1 activity in these mutant embryos. This hypothesis could be further confirmed by the *in vivo* studies showing that downregulation of PAR-1 activity in Baz_{5xA} mutant embryos rescued aPKC and PAR-6 and to a certain degree also Baz_{5xA} cortical localization during late cellularization/early gastrulation (embryonic stage 6) (Figure 24a). With the decrease of basolateral PAR-1 activity in these embryos, the aPKC and also to some extent the PAR-6 localization was shifted more laterally

compared to wild type situation (Figure 18). Additionally also the second experiment in this context coincided with this hypothesis using Baz_{7xA} mutant embryos, where additionally to the five found phosphorylation sites of aPKC in Baz_{PDZ2-3} the two phosphorylation targets of PAR-1 in Baz (serine 151 and 1085) were mutated. Here a clear membrane targeting of the GFP-tagged Baz_{7xA}, which extended over the entire lateral plasma membrane, was observed (Figure 24b). Because Baz_{7xA} cannot be phosphorylated by PAR-1 anymore, it cannot be excluded from the basolateral membrane through binding to 14-3-3 proteins and membrane detachment as in wild type situation (Benton and St. Johnston, 2003b; Hurd et al., 2003). Moreover the cytoplasmic accumulation of aPKC in these embryos (Figure 24b) showed substantially similarities to the staining in Baz_{5xA} mutant embryos (Figure 19a, d), which should be caused by the deficient ability of Baz_{7xA} to recruit aPKC to the cortex as the five phosphorylation targets of aPKC are severely impaired in these embryos.

The findings in this work confirmed previous studies that PAR-1 restricts the formation of the mature PAR complex to the apical membrane (Benton and St. Johnston, 2003a; Hurd et al., 2003; Krahn et al., 2009; McKinley and Harris, 2012) and moreover demonstrated that the Baz PDZ phosphorylation plays an important role for apical aPKC activity and consequently for basolateral PAR-1 activity. The impaired recruitment and thereby activity of aPKC in the Baz_{5xA} mutant embryos during late cellularization and early gastrulation therefore results in a decreased PAR-1 inhibition at the apical domain and consequently failure in AJ formation (Hurov et al., 2004).

This relationship was further elucidated by the analysis of the influence of the aPKC activity in connection with the findings in the Baz_{5xA} mutant embryos. The z-stack projection analysis of Baz_{5xA} mutant embryos in the baz^{815-8} background, which exhibited a maternal expression of $aPKC^{CAAX}$, showed a rescue of the localization of aPKC and PAR-6 and to a certain degree Baz_{5xA}, although the cell morphology and the cell size were severely disturbed in these embryos (Chapter 5.9, Figure 25a). This rescue experiment showed that indeed the Baz PDZ phosphorylation in early embryonic epithelia is fundamentally important for aPKC recruitment and function.

Nevertheless it was observed that the localization of Baz was rescued to a slight degree in embryos which were maternally and zygotically mutant for *apkc*

(*aPKC*^{k06403}) (Figure 25b), although Baz possessed mostly cytosolic accumulation. In order to explain this observation, we asked wether some of the serines/threonines of Baz_{PDZ2-3} which are phosphorylated by aPKC can be phosphorylated by another kinase, too. And indeed the data in this work show, that PKA is able to phosphorylate the threonine on position 741 in the Baz_{PDZ2-3} region.

This finding suggests that PKA can somehow rescue the observed phenotype of the aPKC mutant embryos by phosphorylating the threonine 741 of Baz. Baz_{PDZ1-3} lacks a canonical PKA phosphorylation motif (R-R-X-S/T). However some aPKC-phosphorylation motifs (R/K-X-X-S/T) display a similarity to the PKA-motif. Therefore aPKC and PKA could work redundantly together to recruit Baz to the apical junctions. In an experimental setup we tried to knockdown both kinases, aPKC and PKA, in the fly to get closer insights into the assumed connection. However, these flies were sterile and not able to produce offspring. Therefore no final result could be received. Therefore further experiments have to be done in order to answer the question how Baz is recruited to the apical junctions more precisely.

The data in this study indicate that the Baz PDZ phosphorylation of aPKC is chronologically very important in epithelial development to recruit aPKC during early embryogenesis in the absence of Crb in order to compensate the PAR-1 activity. After Crb expression later in development PDZ-phosphorylation of Baz acts in concert with Crb-mediated recruitment of aPKC in epithelial cells of the embryonic epidermis. Both aPKC binding domains of Baz, the PDZ2-3 domain and the CR3, are necessary to provide robust aPKC-binding. Moreover experiments made in this study give a first hint to a certain role of the PDZ binding motif in the correct function of PAR-6. Furthermore the data in this study suggest aPKC and PKA to work redundantly together to recruit Baz to the apical junctions. Nevertheless it could be possible, that there are more kinases that are able to phosphorylate Baz/PAR-3 also in a certain timepoint during development of polarity, which needs to be investigated intensively in the future to gain a detailed knowledge about the mechanisms working in establishing cellular polarity.

7 References

Atwood, S.X., Chabu, C., Penkert, R.R., Doe, C.Q., Prehoda, K.E. (2007). Cdc42 acts downstream of Bazooka to regulate neuroblast polarity through Par-6 aPKC. *J Cell Sci* 120(Pt 18):3200-6.

Bachmann, A., Schneider, M., Theilenberg, E., Grawe, F., Knust, E. (2001). Drosophila Stardust is a partner of Crumbs in the control of epithelial cell polarity. *Nature* 414(6864):638-43.

Bachmann, A., Timmer, M., Sierralta, J., Pietrini, G., Gundelfinger, E.D., Knust, E., Thomas, U. (2004). Cell type-specific recruitment of Drosophila Lin-7 to distinct MAGUK-based protein complexes defines novel roles for Sdt and Dlg-S97. *J Cell Sci* 117(Pt 10):1899-909.

Benton, R., St Johnston, D. (2003a). A conserved oligomerization domain in Drosophila Bazooka/PAR-3 is important for apical localization and epithelial polarity. *Curr Biol* 3(15):1330-4.

Benton, R., St Johnston, D. (2003b). Drosophila PAR-1 and 14-3-3 inhibit Bazooka/PAR-3 to establish complementary cortical domains in polarized cells. *Cell* 115(6):691-704.

Berger, S., Bulgakova, N.A., Grawe, F., Johnson, K., Knust, E. (2007). Unraveling the genetic complexity of Drosophila stardust during photoreceptor morphogenesis and prevention of light-induced degeneration. *Genetics* 176(4):2189-200

Betschinger, J., Mechtler, K., Knoblich, J.A. (2003). The Par complex directs asymmetric cell division by phosphorylating the cytoskeletal protein Lgl. *Nature* 422(6929):326-30.

Bopp, D., Bell, L.R., Cline, T.W., Schedl, P. (1991). Developmental distribution of female-specific Sex-lethal proteins in Drosophila melanogaster. *Genes Dev*. 5(3):403-15.

Brand, A.H., Perrimon, N. (1993). Targeted gene expression as a means of altering cell fates and generating dominant phenotypes. *Developmen*t 118(2):401-15

Brownes, M. (1975). A photographic study of development in the living embryo of Drosophila melanogaster. *J Embryol Exp Morphol* 33:789-801.

Bulgakova, N.A., Kempkens, O., Knust, E. (2008). Multiple domains of Stardust differentially mediate localisation of the Crumbs-Stardust complex during photoreceptor development in Drosophila. *J Cell Sci* 121(Pt 12):2018-26.

Bulgakova, N.A., Knust, E. (2009). The Crumbs complex: from epithelial-cell

polarity to retinal degeneration. *J Cell Sci* 122(Pt 15):2587-96.

Bulgakova, N.A., Rentsch, M., Knust, E. (2010). Antagonistic functions of two stardust isoforms in Drosophila photoreceptor cells. *Mol Biol Cell* 21(22):3915-25.

Burbelo, P.D., Drechsel, D., Hall, A. (1995). A conserved binding motif defines numerous candidate target proteins for both Cdc42 and Rac GTPases. *J Biol Chem* 270(49):29071-4.

Campos-Ortega, J.A., Hartenstein, V. (1997). The embryonic Development of Drosophila melanogaster. *Springer Verlag, Berlin.*

Chakraborty, A.; Bandyopadhyay, S. (2013). FOGSAA: Fast Optimal Global Sequence Alignment Algorithm. *Sci Rep* 3:1746

Chan, J.R., Jolicoeur, C., Yamauchi, J., Elliott, J., Fawcett, J.P., Ng, B.K., Cayouette, M. (2006). The polarity protein Par-3 directly interacts with p75NTR to regulate myelination. *Science* 314(5800):832-6

Chartier, F.J., Hardy, É.J., Laprise, P. (2011). Crumbs controls epithelial integrity by inhibiting Rac1 and PI3K. *J Cell Sci* 124(Pt 20):3393-8

Chen, J., Zhang, M. (2013). The PAR-3/PAR-6/aPKC complex and epithelial cell polarity. *Exp Cell Res* 319(10):1357-64

Chou, T.B., Noll, E., Perrimon, N. (1993). Autosomal P[ovoD1] dominant female-sterile insertions in Drosophila and their use in generating germ-line chimeras. *Development* 119(4):1359-69

David, D.J., Tishkina, A., Harris, T.J. (2010). The PAR complex regulates pulsed actomyosin contractions during amnioserosa apical constriction in Drosophila. *Development* 137(10):1645-55

David, D.J., Wang, Q., Feng, J.J., Harris, T.J. (2013). Bazooka inhibits aPKC to limit antagonism of actomyosin networks during amnioserosa apical constriction. *Development*. 140(23):4719-29

Drubin, D.G., Nelson, W.J. (1996). Origins of cell polarity. *Cell* 84(3):335-44.

Ebnet, K. Suzuki, A, Horikoshi, Y., Hirose, T., Meyer Zu Brickwedde, M.K., Ohno, S., Vestweber, D. (2001). The cell polarity protein ASIP/PAR-3 directly associates with junctional adhesion molecule (JAM). *The EMBO journal* 20(14):3738-48.

Ebnet, K., Aurrand-Lions, M., Kuhn, A., Kiefer, F., Butz, S., Zander, K., Meyer zu Brickwedde, M.K., Suzuki, A.,. Imhof, B.A, Vestweber D. (2003). The junctional adhesion molecule (JAM) family members JAM-2 and JAM-3 associate with the cell polarity protein PAR-3: a possible role for JAMs in endothelial cell

polarity. *J. Cell Sci* 116(Pt 19):3879-91.

Fan, S., Fogg, V., Wang, Q., Chen, X.W., Liu, C.J., Margolis, B. (2007). A novel Crumbs3 isoform regulates cell division and ciliogenesis via importin β interactions. *J Cell Biol* 178(3):387-98.

Feigin, M.E., Muthuswamy, S.K. (2009). Polarity proteins regulate mammalian cell-cell junctions and cancer pathogenesis. *Curr Opin Biol* 21(5):694-700.

Feng, W., Wu, H., Chan, L.N., Zhang, M. (2007). The Par-3 NTD adopts a PB1-like structure required for Par-3 oligomerization and membrane localization. *EMBO J* 26(11):2786-96

Flores-Benitez, D., Knust, E. (2016). Dynamics of epithelial cell polarity in Drosophila: how to regulate the regulators? *Curr Opin Cell Biol* 42:13-21.

Garrard, S.M., Capaldo, C.T., Gao, L., Rosen, M.K., Macara, I.G., Tomchick, D.R. (2003). Structure of Cdc42 in a complex with the GTPase-binding domain of the cell polarity protein, PAR-6. *Embo J* 22(5): 1125-33.

Giancotti, F.G. Ruoslahti, E. (1999). Integrin signaling. *Science* 285(5430):1028-32.

Graybill, C., Wee, B., Atwood, S.X., Prehoda, K.E. (2012). Partitioning-defective protein 6 (Par-6) activates atypical protein kinase C (aPKC) by pseudosubstrate displacement. *J Biol Chem* 287(25):21003-11.

Harris, T.J., Pfeifer, M. (2004). Adherens junction-dependent and -independent steps in the establishment of epithelial cell polarity in *Drosophila*. *J Cell Biol* 167(1):135-47.

Harris, T.J., Pfeifer, M. (2005). The positioning and segregation of apical cues during epithelial polarity establishment in Drosophila. *J Cell Biol* 170(5):813-23

Hong, Y., Stronach, B., Perrimon, N., Jan, L.Y., Jan, Y.N. (2001). Drosophila Stardust interacts with Crumbs to control polarity of epithelia but not neuroblasts. *Nature* 414(6864):634-8.

Horikoshi, Y., Suzuki, A., Yamanaka, T., Sasaki, K., Mizuno, K., Sawada, H., Yonemura, S., Ohno, S. (2009). Interaction between PAR-3 and the aPKC-PAR-6 complex is indispensable for apical domain development of epithelial cells. *J Cell Sci* 122(Pt 10):1595-606.

Hung, T.J., Kemphues, K.J. (1999). PAR-6 is a conserved PDZ domain-containing protein that colocalizes with PAR-3 in Caenorhabditis elegans embryos. Development 126(1):127-35.

Hurd, T.W., Gao, L., Roh, M.H., Macara, I.G., Margolis, B. (2003). Direct interaction of two polarity complexes implicated in epithelial tight junction

assembly. *Nat Cell Biol* 5(2):137-42.

Hurov, J.B., Watkins, J.L., Piwnica-Worms, H. (2004). Atypical PKC phosphorylates PAR-1 kinases to regulate localization and activity. *Curr Biol* 14(8):736-41.

Itoh, M., Sasaki, H., Furuse, M., Ozaki, H., Kita, T., Tsukita, S. (2001). Junctional adhesion molecule (JAM) binds to PAR-3: a possible mechanism for the recruitment of PAR-3 to tight junctions. *J Cell Biol* 154(3):491-7.

Izumi, Y., Hirose, T., Tamai, Y., Hirai, S., Nagashima, Y., Fujimoto, T., Tabuse, Y., Kemphues, K.J., Ohno, S. (1998). An atypical PKC directly associates and colocalizes at the epithelial tight junction with ASIP, a mammalian homologue of Caenorhabditis elegans polarity protein PAR-3. *J Cell Biol* 143(1):95-106.

Javier, R.T., Rice, A.P. (2011). Emerging theme: cellular PDZ proteins as common targets of pathogenic viruses. *J Virol* 85(22):11544-56.

Joberty, G., Petersen, C., Gao, L., Macara, I.G. (2000). The cell-polarity protein PAR-6 links PAR-3 and atypical protein kinase C to Cdc42. *Nat Cell Biol* 2(8): 531-9.

Johnson, K., Wodarz, A. (2003). A genetic hierarchy controlling cell polarity. *Nat Ce Biol* 5(1):12-4.

Kemphues, K.J., Priess, J.R., Morton, D.G., Cheng, N.S. (1988). Identification of genes required for cytoplasmic localization in early C. elegans embryos. *Cell* 52(3):311-20.

Kim, S., Gailite, I., Moussian, B., Luschnig, S., Goette, M., Fricke, K., Honemann-Capito, M., Grubmuller, H., Wodarz, A. (2009). Kinase-activity-independent functions of atypical protein kinase C in Drosophila. *J Cell Sci* 122(Pt 20):3759-71

Knust, E., Bossinger, O. (2002). Composition and formation of intercellular junctions in epithelial cells. *Science* 298(5600):1955-9.

Krahn, M.P., Bückers, J., Kastrup, L., Wodarz, A. (2010a). Formation of a Bazooka-Stardust complex is essential for plasma membrane polarity in epithelia. *J Cell Biol* 190(5):751-60

Krahn, M.P., Egger-Adam, D., Wodarz, A. (2009). PP2A antagonizes phosphorylation of Bazooka by PAR-1 to control apical-basal polarity in dividing embryonic neuroblasts *Dev Cell* 16(6):901-8.

Krahn, M.P., Klopfenstein, D.R., Fischer, N., Wodarz, A. (2010b). Membrane targeting of Bazooka/PAR-3 is mediated by direct binding to phosphoinositide lipids. *Curr Biol* 20(7):636-42

Kuchinke, U., Grawe, F., Knust, E. (1998). Control of spindle orientation in Drosophila by the Par-3-related PDZ- domain protein Bazooka. *Curr Biol* 8(25):1357-65.

Kusakabe, M., Nishida, E. (2004). The polarity-inducing kinase Par-1 controls Xenopus gastrulation in cooperation with 14-3-3 and aPKC. *EMBO J* 23(21):4190-201.

Lecuit, T. (2004). Junctions and vesicular trafficking during Drosophila cellularization. *J Cell Sci* 117(Pt 16):3427-33.

Lee, H.J., Zheng, J.J. (2010). PDZ domains and their binding partners: structure, specificity, and modification. *Cell Commun Signal* 8:8.

Lin, D., Edwards, A.S., Fawcett, J.P., Mbamalu, G., Scott, J.D., Pawson, T. (2000). A mammalian PAR-3-PAR-6 complex implicated in Cdc42/Rac1 and aPKC signalling and cell polarity. *Nat Cell Biol* 2(8):540-7.

Martin-Belmonte, F., Gassama, A., Datta, A., Yu, W., Rescher, U., Gerke, V., Mostov, K. (2007). PTEN-mediated apical segregation of phosphoinositides controls epithelial morphogenesis through Cdc42. *Cell* 128(2):383-97.

McKim, K.S., Dahmus, J.B., Hawley, R.S. (1996). Cloning of the Drosophila melanogaster meiotic recombination gene mei-218: a genetic and molecular analysis of interval 15E. *Genetics* 144(1):215-28

McKinley, R.F., Harris, T.J. (2012). Displacement of basolateral Bazooka/PAR-3 by regulated transport and dispersion during epithelial polarization in Drosophila. *Mol Biol Cell* 23(22):4465-71

McKinley, R.F., Yu, C.G., Harris, T.J. (2012). Assembly of Bazooka polarity landmarks through a multifaceted membrane-association mechanism. *J Cell Sci* 125(Pt 5):1177-90

Mizuno, K., Suzuki, A., Hirose, T., Kitamura, K., Kutsuzawa, K., Futaki, M., Amano, Y., Ohno, S. (2003). Self-association of PAR-3-mediated by the conserved N-terminal domain contributes to the development of epithelial tight junctions. *J Biol Chem* 278(33):31240-50

Morais-de-Sá, E., Mirouse, V., St Johnston, D. (2010). aPKC phosphorylation of Bazooka defines the apical/lateral border in Drosophila epithelial cells. *Cell* 141(3):509-23.

Mullis, K., Faloona, F., Scharf, S., Saiki, R., Horn, G., Erlich, H. (1986). Specific enzymatic amplification of DNA in vitro: the polymerase chain reaction. *Biotechnology* 24:17-27

Nagai-Tamai, Y., Mizuno, K., Hirose, T., Suzuki, A., Ohno, S. (2002). Regulated protein-protein interaction between aPKC and PAR-3 plays an essential role in the

polarization of epithelial cells. *Genes Cells* 7(11):1161-71.

Nam, S.C., Choi, K.W. (2003). Interaction of Par-6 and Crumbs complexes is essential for photoreceptor morphogenesis in Drosophila. *Development* 130(18):4363-72.

Nelson, W.J. (2003). Adaptation of core mechanisms to generate cell polarity. *Nature* 422(6933):766-74.

Nourry, C., Grant, S.G., Borg, J.P. (2003). PDZ domain proteins: plug and play! *Sci STKE* 2003(179) :RE7.

Oda, H., Uemura, T., Harada, Y., Iwai, Y., Takeichi, M. (1994). A Drosophila homolog of cadherin associated with armadillo and essential for embryonic cell-cell adhesion. *Dev Biol* 165(2):716-26.

Parnas, D., Haghighi, A.P., Fetter, R.D., Kim, S.W., Goodman, C.S. (2001). Regulation of postsynaptic structure and protein localization by the Rho-type guanine nucleotide exchange factor dPix. *Neuron* 32(3):415-24.

Pearsin, R.B., Kemp, B.E. (1991). Protein kinase phosphorylation site sequences and consensus specificity motifs: tabulations. *Methods Enzymol* 200:62-81.

Peterson, F.C., Penkert, R.R., Volkman, B.F., Prehoda, K E. (2004). Cdc42 regulates the Par-6 PDZ domain through an allosteric CRIB-PDZ transition. *Mol Cell* 13(5): 665-76.

Plant, P.J., Fawcett, J.P., Lin, D.C., Holdorf, A.D., Binns, K., Kulkarni, S., Pawson, T. (2003). A polarity complex of mPar-6 and atypical PKC binds, phosphorylates and regulates mammalian Lgl. *Nat Cell Biol* 5(4):301-8

Rodriguez-Boulan, E., Nelson, W.J. (1989). Morphogenesis of the polarized epithelial cell phenotype. *Science* 245(4919):718-25.

Rolls, M.M., Albertson, R., Shih, H.P., Lee, C.Y., Doe, C.Q. (2003). Drosophila aPKC regulates cell polarity and cell proliferation in neuroblasts and epithelia. *J Cell Biol* 163(5):1089-98.

Shahab, J., Tiwari, M.D., Honemann-Capito, M., Krahn, M.P., Wodarz, A. (2015). Bazooka/PAR3 is dispensable for polarity in *Drosophila* follicular epithelial cells. *Biol Open* 4(4): 528–541.

Shin, K., Fogg, V.C., Margolis, B. (2006). Tight junctions and cell polarity. *Annu Rev Cell Dev Biol* 22:207-35.

Simões, Sde, M., Blankenship, J.T., Weitz, O., Farrell, D.L., Tamada, M., Fernandez-Gonzalez, R., Zallen, J.A. (2010). Rho-kinase directs Bazooka/Par-3 planar polarity during Drosophila axis elongation. *Dev Cell* 19(3):377-88.

Soriano, E.V., Ivanova, M.E., Fletcher, G., Riou, P., Knowles, P.P., Barnouin, K., Purkiss, A., Kostelecky, B., Saiu, P., Linch, M., Elbediwy, A., Kjær, S., O´Reilly, N., Snijders, A.P., Parker, P.J., Thompson, B.J., McDonald, N.Q. (2016). aPKC Inhibition by Par3 CR3 Flanking Regions Controls Substrate Access and Underpins Apical-Junctional Polarization. *Dev Cell* 38(4):384-98.

Sotillos, S., Diaz-Meco, M.T., Caminero, E., Moscat, J., Campuzano, S. (2004). DaPKC-dependent phosphorylation of Crumbs is required for epithelial cell polarity in Drosophila. *J Cell Biol* 166(4):549-57

St Johnston, D. (2002). The art and design of genetic screens: Drosophila melanogaster. *Nat Rev Genet* 3(3):176-88

Suzuki, A. and Ohno, S. (2006). The PAR-aPKC system: lessons in polarity. *J Cell Sci* 119, 979-87

Suzuki, A., Akimoto, K., Ohno, S. (2003). Protein kinase C lambda/iota (PKClambda/iota): a PKC isotype essential for the development of multicellular organisms. *J Biochem* 133(1):9-16.

Suzuki, A., Hirata, M., Kamimura, K., Maniwa, R., Yamanaka, T., Mizuno, K., Kishikawa, M., Hirose, H., Amano, Y., Izumi, N., Miwa, Y., Ohno, S. (2004). aPKC acts upstream of PAR-1b in both the establishment and maintenance of mammalian epithelial polarity. *Curr Biol* 14(16):1425-35.

Suzuki, A., Yamanaka, T., Hirose, T., Manabe, N., Mizuno, K., Shimizu, M., Akimoto, K., Izumi, Y., Ohnishi, T., Ohno, S. (2001). Atypical protein kinase C is involved in the evolutionarily conserved par protein complex and plays a critical role in establishing epithelia-specific junctional structures. *J Cell Biol* 152(6):1183-96.

Tabuse, Y., Izumi, Y., Piano, F., Kemphues, K.J., Miwa, J., Ohno, S. (1998). Atypical protein kinase C cooperates with PAR-3 to establish embryonic polarity in Caenorhabditis elegans. *Development* 125(18):3607-14

Tanentzapf, G., Tepass, U. (2003). Interactions between the crumbs, lethal giant larvae and bazooka pathways in epithelial polarization. *Nat Cell Biol* 5(1):46-52.

Tepass, U. (2012). The apical polarity protein network in Drosophila epithelial cells: regulation of polarity, junctions, morphogenesis, cell growth, and survival. *Annu Rev Cell Dev Biol* 28:655-85.

Tepass, U., Hartenstein, V. (1994). The development of cellular junctions in the Drosophila embryo. *Dev Biol* 161(2):563-96.

Tepass, U., Knust, E. (1993). Crumbs and Stardust act in a genetic pathway that controls the organization of epithelia in Drosophila melanogaster. *Dev Biol* 159(1):311-26.

Tepass, U., Tanentzapf, G., Ward, R., Fehon, R. (2001). Epithelial cell polarity

and cell junctions in Drosophila. *Annu Rev Genet* 35:747-84.

Tepass, U., Theres, C., Knust, E. (1990). *crumbs* encodes an EGF-like protein expressed on apical membranes of Drosophila epithelial cells and required for organization of epithelia. *Cell* 61(5):787-99.

Tepass, U., Truong, K., Godt, D., Ikura, M. Peifer, M. (2000). Cadherins in embryonic and neural morphogenesis. Nat Rev Mol Cell Biol 1(2):91-100.

Terasawa, H., Noda, Y., Ito, T., Hatanaka, H., Ichikawa, S., Oqura, K., Sumimoto, H., Inagaki, F. (2001). Structure and ligand recognition of the PB1 domain: a novel protein module binding to the PC motif. *EMBO J* 20(15):3947-56.

Theodosiou, N.A., Xu, T. (1998). Use of FLP/FRT system to study Drosophila development. *Methods* 14(4):355-65

Thorpe, H.M., Wilson, S.E., Smith, M.C. (2000). Control of directionality in the site-specific recombination system of the Streptomyces phage phiC31. *Mol Microbiol* 38(2):232-41

Tsukita, S., Furuse, M., Itoh, M. (2001). Multifunctional strands in tight junctions. *Nat Rev Mol Cell Biol* 2(4):285-93**.**

Walther, R.F., Pichaud, F. (2010). Crumbs/DaPKC-dependent apical exclusion of Bazooka promotes photoreceptor polarity remodeling. *Curr Bio* 20(12):1065-74.

Wang, C., Shang, Y., Yu, J., Zhang, M. (2012). Substrate recognition mechanism of atypical protein kinase Cs revealed by the structure of PKCiota in complex with a substrate peptide from Par-3. *Structure*. 20(5):791-801

Wang, Q., Hurd, T.W., Margolis, B. (2004). Tight junction protein PAR-6 interacts with an evolutionarily conserved region in the amino terminus of PALS1/Stardust. *J Biol Chem* 279(29):30715-21.

Wie, S.Y., Escudero, L.M., Yu, F., Chang, L.H., Chen, L.Y., Ho, Y.H., Lin, C.M., Chou, C.S., Chia, W., Modolell, J., Hsu, J.C. (2005). Echinoid is a component of adherens junctionsthat cooperates with DE-Cadherin to mediate cell adhesion. *Dev Cell* 8(4):493-504.

Wieschaus, E., Niisslein-Volhard, C., Jiirgens, G. (1984). Mutations affecting the pattern of the larval cuticle in Drosophila melanogaster III. Zygotic loci on the X-chromosome and fourth chromosome. *Roux's Arch Dev Biol* 193:296-307

Wirtz-Peitz, F., Nishimura, T., Knoblich, J.A. (2008). Linking cell cycle to asymmetric division: Aurora-A phosphorylates the Par complex to regulate Numb localization. *Cell*. 135(1):161-73

Wodarz, A. (2002). Establishing cell polarity in development. *Nat Cell Biol*

4(2):E39-44

Wodarz, A., Grawe, F., Knust, E. (1993). CRUMBS is involved in the control of apical protein targeting during Drosophila epithelial development. *Mech Dev* 44(2-3):175-87.

Wodarz, A., Ramrath, A., Grimm, A., Knust, E. (2000). Drosophila atypical protein kinase C associates with Bazooka and controls polarity of epithelia and neuroblasts. *J Cell Biol* 150(6):1361-74

Wodarz, A., Ramrath, A., Kuchinke, U., Knust, E. (1999). Bazooka provides an apical cue for Inscuteable localization in Drosophila neuroblasts. *Nature* 402(6761):544-7.

Wu, H., Feng, W., Chen, J., Chan, L.N., Huang, S., Zhang, M. (2007). PDZ domains of Par-3 as potential phosphoinositide signaling integrators. *Mol Cell* 28(5):886-98.

Yamanaka, T., Horikoshi, Y., Sugiyama, Y., Ishiyama, C., Suzuki, A., Hirose, T., Iwamatsu, A., Shinohara, A., Ohno, S. (2003). Mammalian Lgl forms a protein complex with PAR-6 and aPKC independently of PAR-3 to regulate epithelial cell polarity. *Curr Biol* 13(9):734-43.

Yeaman, C., Grindstaff, K.K., Nelson, W.J. (1999). New perspectives on mechanisms involved in generating epithelial cell polarity. *Physiol Rev* 79(1):73-98.

Yu, C.G., Harris, T.J. (2012). Interactions between the PDZ domains of Bazooka (Par-3) and phosphatidic acid: in vitro characterization and role in epithelial development. *Mol Biol Cell* 23(18):3743-53.

8 Appendix

8.1 List of Figures

8.2 List of Tables

8.3 Abbreviations

AA	amino acid
AJ	adherens junction
Amp	ampicillin
aPKC	atypical protein kinase C
aPKC-B	aPKC-binding motif
APS	Ammonium peroxodisulfate
Arm	Armadillo
ATP	adenosine triphosphate
ATPγS	Adenosine-5'-(γ-thio)-triphosphate
Baz	Bazooka
bp	base pair
BSA	Bovine Serumalbumin
C. elegans	Caenorhabditis elegans
CBB	coomassie brilliant blue
Cdc42	Cell division control protein 42
Co-IP	co-immunoprecipitation
CR	conserved region
Crb	Crumbs
CRIB	Cdc42/Rac interactive binding
CTP	Cytidine triphosphate
DAPI	4', 6-diamide-2'-phenylindole dihydrochloride
DE-Cad	DE-Cadherin
Dlg	Discs large
DNA	deoxyribonucleic acid
dNTP	deoxynucleotide triphsophate
DTT	dithiothreitol
E	embryonic
E. coli	Escherichia coli
ECM	extracellular matrix
Ed	Echinoid
F	Forward
FBS	fetal bovine Serumalbumin
FLP	Flipase
FRT	Flipase recognition target sequence
GAL4	GAL4 transcription factor
GFP	green fluorescent protein
GSK-3ß	Glycogen synthase kinase 3ß
GST	Gluthathione-S-transferase
GTP	Guanosine triphosphate
HRP	Horseradish peroxidase
IP	immunoprecipitation
IPTG	Isopropyl-β-D-thiogalactopyranosid
JAM	junctional adhesion molecule
Kan	Kanamycin
kb	kilo bases
kD	kilodalton
L	larval
L27	Lin-2-Lin-7
LB	Lysogeny broth
LEW	lysis, equilibration, wash
Lgl	lethal giant larvae
LKB1	liver kinase B1
MAGUK	membrane –associated guanylate kinase
MARCKS	Myristoylated alanine-rich C-kinase substrate
MARK1/2	MAP/microtubule affinity-regulating kinases 1/2 (PAR-1)
min	minutes

Mir	Miranda
n.t.s.	not to scale
NBs	Neuroblasts
NTD	N-terminal domain
OD	Optical density
ORF	Open-reading frame
P	pupal
PAGE	polyacrylamide gel electrophoresis
PALS-1	protein associated with Lin-7
PAR	partitioning-defective
PATJ	PALS-1 associated TJ protein
PB1	Phox and Bem1 domain
PBM	PDZ binding motif
PBS	Phosphate-buffered saline
PCR	Polymerase chain reaction
PDZ	Postsynaptic-density protein95 Dlg-Zonula Occludentes1
PKA	protein kinase A
PMSF	Phyenylmethylsulfonylfluoride
PNBM	*p*-Nitrobenzyl mesylate
PTEN	Phosphatase and tensin homolog
R	Reverse
rpm	rounds per minute
S2R	Schneider cells
SAR	sub-apical region
Scrib	Scribble
SDS	sodium dodecyl sulfate
Sdt	Stardust
SJ	Septate junction
SXL	sex lethal
TEMED	N,N,N’,N’-tetramethylethylenediamine
TJ	tight junction
Tris	Trishydroxymethyl-aminomethane
TTP	Thymidine triphosphate
TUNEL	TdT-mediated dUTP-biotin nick end labeling
UAS	upstream activating sequence
V	Volt
ZA	*zonula adherens*
ZO-1	zonula occludens 1

9 Acknowledgements

Mein herzlicher Dank gilt Herrn Prof. Dr. Dr. Krahn für die Möglichkeit, diese Doktorarbeit in seiner Arbeitsgruppe anfertigen zu können sowie die engagierte Unterstützung und die vielen Ratschläge und Tipps im Verlauf der gesamten Arbeit. Auch möchte ich mich herzlich bei Herrn Prof Dr. Kerkhoff und Herrn Prof. Dr. Sprenger für die Übernahme der Mentorenschaft und die vielen hilfreichen Anregungen bedanken.

Weiterhin danke ich Herrn Prof. Dr. Witzgall für die Möglichkeit diese Promotion an seinem Institut durchführen zu können.

Mein Dank geht auch an alle Mitarbeiter des Instituts für Molekulare und Zelluläre Anatomie für die immerwährende Hilfsbereitschaft und Freundlichkeit.

Besonders möchte ich mich auch bei allen Mitgliedern der AG Krahn bedanken, bei Olga, Lars, Rui, Ina, Barbara, Daniela, Giada, Vroni, Flo, Gudrun und Lucia, die nicht nur alle Kollegen für mich waren, sondern auch zu Freunden in diesen drei Jahren geworden sind. Danke für die tolle Zeit im und außerhalb des Labors und die angenehme Atmosphäre während der Arbeit.

Ich möchte mich herzlich bei meinen Eltern, Gisela und Peter, meiner Schwester Christine und meiner ganzen Familie bedanken, die mir es erst ermöglicht haben, diesen Weg zu gehen und die schon mein ganzes Leben immer für mich da sind und mich unterstützen. Ohne Euch hätte ich das alles nie geschafft!

Zu guter letzt möchte ich mich ganz besonders bei meinem Mann Tobias bedanken, der immer hinter mir steht und für mich da ist, mir unendlich viel Kraft und Mut gibt und immer an mich glaubt!

Danke.